2020

Perivascular fibroblast activation states in human skin diseases

BOSTON UNIVERSITY

SCHOOL OF MEDICINE

Dissertation

PERIVASCULAR FIBROBLAST ACTIVATION STATES IN HUMAN SKIN DISEASES

by

ALEXANDER MICHAEL SHUFORD BARRON

B.A., Reed College, 2005

Submitted in partial fulfillment of the

requirements for the degree of

Doctor of Philosophy

2020

Approved by

First Reader _____

Jeffrey L. Browning, Ph.D.
Research Professor of Microbiology

Second Reader _____

Matthew D. Layne, Ph.D.
Associate Professor of Biochemistry

In going on with these Experiments how many pretty Systems do we build which we soon find ourselves oblig'd to destroy…it may help to make a vain man humble.

BENJAMIN FRANKLIN

(1706-1790)

Illness is the night side of life, a more onerous citizenship. Everyone who is born holds dual citizenship, in the kingdom of the well and in the kingdom of the sick. Although we all prefer to use the good passport, sooner or later each of us is obliged, at least for a spell, to identify ourselves as citizens of that other place.

SUSAN SONTAG, *Illness as Metaphor*

(1933-2004)

DEDICATION

To my parents, who taught me what is important, and my wife, who reminds me of the order.

ACKNOWLEDGMENTS

I chose to pursue my doctoral research in the Program in Biomedical Sciences largely because of the collegiality I saw when I visited. This decision paid off handsomely, and there are many colleagues, both mentors and friends, to whom I owe much.

My advisor, Jeffrey Browning, had a deft hand on the tiller. His touch was light and patient enough that I had the freedom to pursue many of my own (often failing) scientific directions without letting me stray wildly off-course. With perpetual creativity and enthusiasm, Jeff has helped to reshape the way I think about science at the molecular, microscopic and macroscopic levels. Thank you, Jeff, for sharing the depth and breadth of your knowledge, and unfailing curiosity with me.

To the members of my committee, Barbara Nikolajczyk, Greg Viglianti, Rahm Gummuluru, Ian Rifkin, Matthew Layne, Hans Dooms and Chris Gabel, I am immensely grateful. Your insightful critiques and support have been especially helpful to my figuring out how to clearly present both raw data and a quantified summary of that data. Matt, I am especially indebted to you for your critiques of my writing and scientific reasoning both in committee meetings and one-on-one. Jennifer Snyder-Cappione and John Connor, thank you for your generosity and advice about matters of both the head and heart. Thank you to David Sherr and Thomas Kepler for awarding me a place on the T32 training grant, which funded me during much of my research. Kathy Marinelli, Linda Parlee, Becky Washburn, and Lena Rybak: you kept the cogs whirring with nary a peep, I am forever

indebted. Ron Corley, Greg Viglianti and Rachel Fearns, I very much appreciate the consideration you gave to the opinions voiced by the students.

Friends, there are too many of you to list here; hopefully you will forgive me. I am especially grateful to Michelle Fleury, Julio Mantero, Ian Francis, Mehraj Awal, Tina Lisk, Gaby , Kim, Fumi, Emily, Lisa, Aleks and Tim. You have fed my love of science, but also reminded me to come up for air. I cherish our scientific sparring as much as the climbing, Dungeons and Dragons, board games, good meals and good company.

Katy, you know me better than I know myself. My parents, Dianne and Terry, thank you for giving equal thought and care to the lessons you have taught me and your methods of instruction. My gratitude for the three of you is beyond words.

PERIVASCULAR FIBROBLAST ACTIVATION STATES IN HUMAN SKIN DISEASES

ALEXANDER MICHAEL SHUFORD BARRON

Boston University School of Medicine, 2020

Major Professor: Jeffrey L. Browning, Ph.D., Research Professor of Microbiology

ABSTRACT

The perivascular adventitia (PA) senses and responds to injuries in blood vessels and the tissues they feed. Cells in the PA form the outermost vascular layer, joining the circulatory system to other organs. Housing hematopoietic, mesenchymal and neuronal cells allows flexible adventitial responses to diverse perturbations. However, the PA response can also be pathogenic. Thickening of the adventitia may drive ischemia and hypertension. It can also be a niche for local lymphocyte priming in diseases such as idiopathic pulmonary arterial hypertension. Despite their importance, PA contributions to skin diseases were understudied.

The hypothesis that contrasting two cutaneous diseases, scleroderma and discoid lupus erythematosus (DLE), would illuminate discrete PA alterations was explored. Vascular changes are prominent, but distinct, in both diseases. Studying perivascular adventitial changes in these diseases may yield insights into both dermal and vascular pathologies. PA fibroblasts in healthy human skin were phenotypically distinct from the surrounding dermal fibroblasts. In both scleroderma and DLE, PA fibroblasts expanded and expressed surface markers

not observed in healthy skin including vascular cell adhesion molecule 1 (VCAM1), podoplanin (PDPN) and the p75 low affinity nerve growth factor receptor (NGFR). Elaborated networks of PA fibroblasts in DLE expressed VCAM1 and enmeshed dense, T cell-rich infiltrates. Transcriptional analyses indicated positive correlations between VCAM1, T cell chemoattractants and interleukin (IL)-15, which promotes their survival. Activated PA fibroblasts in DLE likely create a supportive niche for T cells infiltrating the skin.

In contrast, enlarged PA fibroblast networks in scleroderma expressed NGFR in the absence of leukocyte infiltrates. This PA fibroblast phenotype was shared among reparative and pathologic scarring, and four dermal tumors. NGFR is a mesenchymal stem cell (MSC) marker, and expanded NGFR+ mesenchymal cells were immediately adjacent to cluster of differentiation (CD)34+ and CD73+ PA MSC. Expression of NGFR by PA fibroblasts is likely associated with reparative responses. Different stimuli induced VCAM1 and NGFR on cultured human dermal fibroblasts, supporting these as discrete activation states. In conclusion, these studies demonstrated the responsive and plastic nature of human dermal PA mesenchymal cells, and pointed to connections with vascular alterations in skin diseases.

TABLE OF CONTENTS

DEDICATION v

ACKNOWLEDGMENTS vi

ABSTRACT viii

TABLE OF CONTENTS x

LIST OF TABLES xiv

LIST OF FIGURES xv

LIST OF ABBREVIATIONS xvii

CHAPTER ONE: INTRODUCTION 1

Scleroderma and Discoid Lupus Erythematosus Skin Diseases 1

Scleroderma and Systemic Sclerosis 3

Discoid Lupus Erythematosus 5

Vascular Pathology in SSc and DLE 7

Adventitial Thickening in SSc 9

Perivascular Cuffing in DLE 11

PA Mesenchymal Cells in SSc and DLE 13

Potential Roles for PA Mesenchymal Cells in SSc 14

PA Fibroblast Support of Leukocytes in DLE 15

Central Hypothesis and Summary of Results 16

CHAPTER TWO: MATERIALS AND METHODS 18

Tissue Samples 18
Histology 22
Gene Expression Data and Analysis 25
Cell Culture 27
Flow Cytometry 27
Statistics 28
CHAPTER THREE: PERIVASCULAR ADVENTITIAL FIBROBLAST SPECIALIZATION ACCOMPANIES T CELL RETENTION IN THE INFLAMED HUMAN DERMIS 30
Abstract 30
Introduction 31
Results 34
Defining the Perivascular Adventitial Compartment in Normal, SSc and DLE Skin 34
VCAM1 Display on Activated Perivascular Adventitial Fibroblasts 38
Dermal Perivascular T Cell Infiltrates Localize to VCAM1+ Vascular Adventitia 41
VCAM1 RNA Levels Correlate with T Cell Accumulation 44
Perivascular T Cell Accumulation Can Occur in the Absence of PDPN+ PA Fibroblasts 48
Do VCAM1+ PA Fibroblasts Resemble FRC? 51

Is the PA Compartment a “Perivascular Cuff” or a Tertiary Lymphoid Structure? 53
Comparison of Murine and Human PA Compartments 56
Discussion 61
CHAPTER FOUR: NERVE GROWTH FACTOR RECEPTOR EXPRESSION IDENTIFIES AN EXPANDED DERMAL PERIVASCULAR STROMAL CELL IN SYSTEMIC SCLEROSIS AND WOUND HEALING 67
Abstract 67
Introduction 68
Results 71
Rare Perivascular Cells Expressing NGFR in Healthy Human Skin are More Frequent and Cover Greater Area in SSc 71
Human Dermal PA Cells Expressing NGFR are Mesenchymal 75
Relationships Between NGFR+ PA Cells and Adventitial MSC 77
Perivascular NGFR-Expressing Cells are More Frequent and Occupy Larger Areas in Human Reparative and Pathologic Dermal Scarring than Healthy Skin 79
NGFR Expression in the Hypodermis During Early Wound Healing in Mice 81
Perivascular NGFR Expression is Common in Four Types of Dermal Tumors 83
Expanded PA Fibroblasts in SSc and DLE Distinguished by NGFR and VCAM1 Expression 85

Polar Solvents Induce NGFR, While the Combination of TNF and IFNγ Stimulates VCAM1 Expression by Cultured Primary Human Dermal Fibroblasts 87
Discussion 91
CHAPTER FIVE: CONCLUDING REMARKS 97
Summary of Results and Integration with the Literature 97
Mesenchymal Cell Heterogeneity and PA Fibroblast Functions in Healthy Skin 100
Expansion and Activation of PA Fibroblasts in DLE and Dermatitis 103
Expansion of NGFR+ PA Mesenchymal Cells in SSc, Wound Healing and Fibromas 107
Limitations 111
APPENDIX: COPYRIGHT PERMISSION 113
BIBLIOGRAPHY 117
CURRICULUM VITAE 171

LIST OF TABLES

Table 1. Characteristics of healthy, SSc, CSD, AD and DLE patients whose biopsies were studied in Chapter Three. 20

Table 2. Characteristics of healthy, SSc, DLE and reparative and pathologic scar patients whose biopsies were studied in Chapter Four. 21

Table 3. Antibodies used for histology. 25

Table 4. Antibodies used for flow cytometry. 29

Table 5. VCAM1 RNA is positively correlated with CD3G, IL-15 and CCL19 RNA in SSc, AD and DLE. 46

LIST OF FIGURES

Figure 1. Layers of the vascular unit wall. 8

Figure 2. Perivascular adventitial fibroblasts express CD90. 36

Figure 3. PA CD90+, VCAM1+ and PDPN+ cells are PDGFRβ+ fibroblasts. 37

Figure 4. VCAM1 expression defined a different state of the perivascular adventitia. 41

Figure 5. Dense perivascular T cell infiltrates are found within VCAM1+ PA fibroblast networks. 43

Figure 6. VCAM1 RNA correlates with T cell infiltration, ITGA4, and IL15, but not IL7 RNA. 45

Figure 7. Perivascular T cell infiltrates occur regardless of PA fibroblast PDPN expression. 50

Figure 8. VCAM+SMA- PA fibroblasts associated with MFAP5+ fibers. 52

Figure 9. Perivascular structures in SSc, CSD, and DLE are not mature TLS. .. 54

Figure 10. PA compartment in mouse skin. 57

Figure 11. T cells co-localized with VCAM+ perivascular stromal cells in the diabetic NOD pancreas and the livers of *gld.ApoE* mice. 60

Figure 12. NGFR expression in healthy human skin. 72

Figure 13. Perivascular cells expressing NGFR are more frequent and cover larger areas in the skin of SSc patients. 74

Figure 14. Perivascular adventitial NGFR+ cells are mesenchymal. 76

Figure 15. Relationship between NGFR+ PA cells and PA MSC. 78

Figure 16. Expansion of perivascular cells expressing NGFR in reparative and pathologic scars. 80
Figure 17. NGFR+ cells appear in the murine hypodermis 4 days post-incisional wound in skin adjacent to the wound. 82
Figure 18. Patterns of NGFR expression in four dermal tumors. 84
Figure 19. PA fibroblasts expressing NGFR in SSc and VCAM1 in DLE are in distinct states. 86
Figure 20. Polar solvents induce NGFR expression by primary human dermal fibroblasts, whereas the combination of TNF and IFNγ stimulates VCAM1 and ICAM1 production without altering CD90. 90
Figure 21. Model of PA mesenchymal cell phenotypes and layers observed in affected SSc skin. 93
Figure 22. Proposed model of PA fibroblast activation states in DLE and SSc. . 99

LIST OF ABBREVIATIONS

AD ..... atopic dermatitis

AFX ..... atypical fibroxanthoma

AP.....alkaline phosphatase

BMP.....bone morphogenic protein

CCL2 .....CC motif chemokine ligand 2

CCL17 .....CC motif chemokine ligand 17

CCL19 .....CC motif chemokine ligand 19

CCL21 .....CC motif chemokine ligand 21

CCR2..... CC motif chemokine receptor 2

CCR7..... CC motif chemokine receptor 7

CXCL9..... CXC motif chemokine ligand 9

CXCL10..... CXC motif chemokine ligand 10

CXCL11..... CXC motif chemokine ligand 11

CXCL12..... CXC motif chemokine ligand 12

CXCL13..... CXC motif chemokine ligand 13

CXCR3 .....CXC motif chemokine receptor 3

CSD..... chronic spongiotic dermatitis

DC ..... dendritic cell

DF..... dermatofibroma

DFSP..... dermatofibrosarcoma protuberans

DLE ..... discoid lupus erythematosus

DMF ..... dimethylformamide

DMSO ..... dimethyl sulfoxide

dpw ..... days post-wound

dSSc ..... diffuse systemic sclerosis

ECM ..... extracellular matrix

EGF ..... epidermal growth factor

FACS ..... fluorescence activated cell sorting

FDC ..... follicular dendritic cell

FGF2 ..... fibroblast growth factor 2

FRC ..... fibroblastic reticular cell

GEO ..... gene expression omnibus

gld.ApoE ..... $Fasl^{gld}.apoE^{-/-}$

HEV ..... high endothelial venule

HRP ..... horseradish peroxidase

HS ..... hypertrophic scar

ICAM1 ..... Intercellular adhesion molecule 1

IFNγ ..... interferon γ

IL-4 ..... interleukin-4

IL-7 ..... interleukin-7

IL-13 ..... interleukin-13

IL-15 ..... interleukin-15

IL-17A interleukin-17A

ILC ..... innate lymphoid cell

ITGA4 ..... integrin α4

KS ..... keloid scar

LFA1 ..... leukocyte function-associated antigen 1

lSSc ..... limited systemic sclerosis

LTβR ..... lymphotoxin-β receptor

MCAM ..... melanoma cell adhesion molecule

MFAP5 ..... Microfibrillar-associated protein 5

MFI ..... median fluorescence intensity

MMP ..... matrix metalloproteinase

MRL/lpr ..... MRL/MpJ-*Fas*^{lpr}/J

MRSS ..... modified Rodnan skin score

MSC ..... mesenchymal stem cell

NGF ..... nerve growth factor

NGFR ..... p75 low affinity nerve growth factor receptor

NOD ..... non-obese diabetic (NOD/ShiLtJ)

PA ..... perivascular adventitia

PAH ..... pulmonary arterial hypertension

PBS ..... phosphate-buffered saline

PDGF ..... platelet-derived growth factor

PDGFRβ ..... platelet-derived growth factor receptor β

PDPN ..... Podoplanin

PNAd ..... peripheral lymph node addressin

RP .....Raynaud's phenomenon

RS .....reparative scar

SELE .....E-selectin

SELP .....P-selectin

SMA..... α-smooth muscle actin

SSc..... systemic sclerosis

TBS .....tris-buffered saline

TBST ..... TBS with 0.05% tween-20

TGFβ .....transforming growth factor β

T_H1 .....type 1 T helper cel

TLS.....Tertiary lymphoid structure

TNF .....tumor necrosis factor α

Treg .....regulatory T cell

TrkA..... neurotrophic receptor tyrosine kinase 1

UCHL1..... ubiquitin carboxyl-terminal esterase L1

VCAM1 ..... Vascular cell adhesion molecule 1

VLA4.....very late antigen 4

VSMC .....vascular smooth muscle cell

CHAPTER ONE: INTRODUCTION

Scleroderma and Discoid Lupus Erythematosus Skin Diseases

Every year approximately 85 million Americans (25% of the US population) seek treatment for skin diseases costing $75 billion (1). The resulting shame and social stigma frequently cause depression in these patients (2). Effective treatments for skin diseases have outsized benefits for patients' quality of life. Cutaneous disorders may be restricted to the skin or associated with systemic disease (3–6). Morbidities associated with skin diseases are frequently less severe than those for systemic diseases; correspondingly, the safety demanded of therapies is higher than for more physically severe diseases, such as multiple sclerosis. Developing effective drugs that meet this rigorous safety profile requires a detailed understanding of the contributing cells and their disease-specific changes.

Understanding the cellular and molecular drivers of disease has led to the development of powerful and safe therapies for some skin diseases, such as interleukin-17A (IL-17A) blockade for psoriasis (7). Other skin diseases still await such treatments. Scleroderma and discoid lupus erythematosus (DLE) are two such diseases. Targeted treatments, such as blocking IL-17A, and microenvironment-modifying drugs, which deactivate the niche that supports pathogenic cells, may circumvent the adverse effects of the generalized immunosuppressants and chemotherapeutics currently prescribed for scleroderma and DLE patients (8–10). Although the end-stage skin lesions of both

scleroderma and DLE can be called scars, the cutaneous presentations are clinically and microscopically distinct (11, 12). Scleroderma scars are likely caused by ischemia and fibrosis, while DLE scars are thought to result from autoimmune attack upon cells of the epidermis and dermis. Contrasting diseases with such distinct pathologies is one method of identifying discrete microenvironments and potential therapeutic targets.

Comparing scleroderma and DLE can illuminate both conditions. Disease-associated cutaneous alterations can be identified by contrasting healthy and affected skin. Similarly, distinctions between clinically divergent diseases can discriminate between changes related to a specific manifestation and those common to many forms of sickness. For example, large T cell infiltrates are common in DLE, but not SSc, skin lesions leading to the hypothesis that autoimmune attack by T cells against cutaneous cells causes the atrophy seen in end-stage DLE scars (13–17). Conversely, increased levels of the chemokine CC motif chemokine ligand (CCL)2, are shared between the two diseases (13, 18) suggesting that CCL2 may be a general signal of sickness unrelated to disease pathogenesis. Indeed, several clinical trials of antibodies blocking CCL2 or its receptor, CCR2, in cancer and inflammatory diseases have either had little success or demonstrated enhanced metastasis upon withdrawal (19–22). Contrasting scleroderma, DLE and healthy skin may identify cutaneous changes specifically associated with fibrosis or inflammatory destruction that point to safer

drug targets than those manipulated by immunosuppressants and cytotoxic therapies.

Scleroderma and Systemic Sclerosis

Scleroderma is a heterogeneous disease with the ultimate shared features of vascular pathology, immunological dysfunction and skin hardening (i.e. sclerosis) (11). Although scleroderma specifically refers to skin fibrosis, it occurs in over 90% of patients with the broader disease systemic sclerosis (SSc) (23). All of the patients studied herein had both systemic and cutaneous disease, so I will use SSc. SSc patients can be further subdivided into those with limited (lSSc) or diffuse (dSSc) cutaneous sclerosis. Estimates indicate that lSSc represents 60-80% of cases (24). Patients with limited disease have skin fibrosis restricted to their extremities, whereas diffuse disease also occurs on the trunk (25).

Prevalence data for SSc in the United States estimate 276 cases occur per million adults. Five women are affected for every man. Most female SSc patients are diagnosed in middle age (24, 26). While SSc is rare, the associated internal organ fibrosis and lack of effective treatments make it one of the deadliest rheumatic diseases (27). The median survival for SSc patients is 11 years after diagnosis (28).

The etiology of SSc is unclear. Given the clinical heterogeneity of SSc, it is likely that there are several pathologic paths that end in similar manifestations (23, 29, 30). Clinically, vascular dysfunction precedes cutaneous fibrosis in most patients (11, 23). One hypothesis is that vascular injury leads to perivascular

infiltration by monocytes or macrophages that activate surrounding fibroblasts (31). Activated fibroblasts thicken the skin by depositing and crosslinking extracellular matrix (ECM) proteins. As a result, affected areas adopt a plump and shiny or waxy appearance (11). Skin thickening in SSc is measured using the modified Rodnan skin score (MRSS), where a physician pinches 17 areas on a patient's body and records a score from zero to three, with three being the most severe thickening (32).

Apoptotic endothelial cells are frequently detected in the skin of SSc patients prior to fibrosis (17, 33, 34). Anti-endothelial cell autoantibodies, ischemia, reperfusion-induced reactive oxygen species and environmental toxins have all been proposed to trigger endothelial cell apoptosis, although there is scant data for most of these hypotheses (27, 35–38). Leukocyte infiltrates in SSc skin are generally dominated by macrophages, which may activate fibroblasts by secreting transforming growth factor-β (TGFβ) and platelet-derived growth factors (PDGFs) (16, 17, 39, 40). Fibroblasts in SSc may also be activated by other cytokines, such as IL-4 and IL-13, but the sources of these molecules remain controversial (41–44). Collectively, these observations signify the complex pathogenesis of SSc and likely represent one of many potential routes.

The complexity and relatively short median survival time for SSc patients are reflected in the lack of US Food and Drug Administration-approved treatments (45). Calcium channel blockers, phosphodiesterase type 5 inhibitors and intravenous prostanoids all moderately reduce symptoms of vascular constriction,

but only in subsets of patients (6, 46). For patients not aided by these drugs, the only other option is radical sympathectomy (47–49). Much is known about changes in endothelial and vascular smooth muscle cells, but fewer studies have examined other blood vessel-associated cells. A better understanding of changes in blood vessels may aid the development of treatments for SSc vascular disease that also improve ischemic injuries and fibrosis.

Discoid Lupus Erythematosus

Unlike SSc, active DLE lesions are overtly inflamed. These lesions are frequently covered by a crust and, over time, become sunken and atrophic. DLE is more clinically uniform than SSc. This is due, in part, to discrete definitions of three types of cutaneous lupus. Chronic cutaneous lupus erythematosus is one of these, and DLE is its most common subtype (12).

Prevalence estimates for DLE range from 280 to 780 per million adults, (50, 51). Similar to SSc, DLE has a female:male ratio of approximately 2:1, and the average onset of DLE is in the early 30's, a decade earlier than SSc (3, 51). While DLE patients are at slightly higher risk for squamous cell carcinoma, direct mortality is less of a concern than psychological distress (52). Data on the median survival time from diagnosis is unavailable for these patients, but appears to be longer than 25 years (3).

Relatively few DLE patients develop systemic disease. About 75% of patients present with localized DLE, where lesions are restricted to the head and neck. The remaining patients develop lesions anywhere on their skin (generalized

DLE). Only 5% of localized and 20% of generalized DLE patients manifest systemic involvement (4, 53, 54). Low risk of internal organ complications in DLE patients also sets this disease apart from SSc.

The etiology of DLE is unclear. Studies indicate that the epithelial cells of some DLE patients produce high levels of inflammatory cytokines in response to UV light (55–58) (reviewed by (59)). Inflammation induces adhesion molecules on endothelial cells and the production of chemokines throughout the skin (60, 61). These changes allow lymphocytes, such as cytotoxic CD8 and type 1 helper CD4 T (T_H1) cells, to extravasate into the skin (13–15). Within DLE lesions, leukocytes are highly concentrated at the dermo-epidermal junction, and around hair follicles and blood vessels (12, 62). Epithelial cells produce the chemokines CXC motif chemokine ligand 9-11 (CXCL9-11) and CC motif chemokine ligand 17 (CCL17) to attract invading leukocytes, but why these cells accumulate around blood vessels is unknown (63, 64).

There are no US Food and Drug Administration-approved treatments for any variation of cutaneous lupus (65). Treatments for DLE, primarily steroids and immunosuppressants, reflect our lack of understanding of the etiology. Few clinical studies of DLE treatments have been published, and even fewer of these were well-powered, randomized and placebo-controlled trials (66). The available data suggest that even the best of these treatments, oral hydroxychloroquine, completely resolves only ~50% of lesions (67). These medications work by blocking leukocyte activation and proliferation. However, given the risks of

generalized immunosuppression, DLE patients need drugs that are both more effective and targeted.

An alternative approach is modifying the microenvironment that promotes leukocyte accumulation in the skin. Several layers of regulation govern leukocyte numbers in inflamed tissues: extravasation out of the blood, survival within the inflamed skin and signals that promote or prevent retention or egress (68, 69). Therapies that block leukocyte entry, reduce survival or promote exit from the inflamed skin by targeting non-leukocytes may halt damage.

Vascular Pathology in SSc and DLE

Vessels carrying both blood and lymph are critically important to maintaining dermal homeostasis. Blood vessels can have up to three layers: the intima, media and adventitia (Figure 1). Endothelial cells line the blood vessel lumen, and together with abluminal pericytes, to which they are joined by peg-socket contacts, comprise the vascular intima (70). Wrapping the intima are vascular smooth muscle cells (VSMC), which constitute the medial layer. The outer-most vascular layer is the adventitia. Several cell types, including fibroblasts, leukocytes, nerves and MSC cohabitate in this ECM-rich compartment (71–73). Although the blood vasculature in human skin, especially capillaries, can appear as individual vessels it is more common to find at least two (and often more) vessels bundled together into a plexus (74). Due to the complex vascular layers and frequent clustering of blood vessels, I will use the term “vascular unit” to refer to these structures.

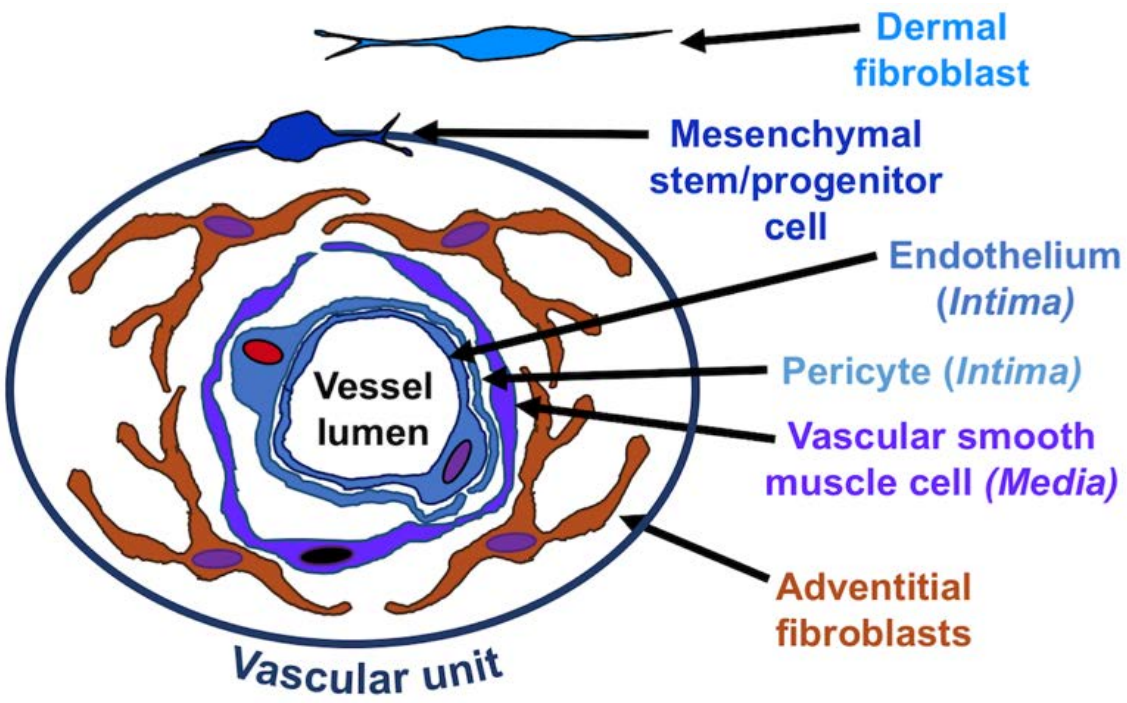

Figure 1. Layers of the vascular unit wall.
Blood vessels can have up to three layers: the intima, media and adventitia. Endothelial cells create the vascular lumen and adhere to a basement membrane interwoven with pericytes. This innermost layer is the *tunica intima*. Vascular smooth muscle cells in the *tunica media* wrap the intima, provide structural support and control vascular tone. The outermost layer, the *tunica adventitia*, is a complex, connective tissue-rich layer that anchors the blood vessel to the surrounding tissue. Fibroblasts, MSC, leukocytes and the tips of neuronal axons are all found in the adventitia. Here, the border between the vascular unit and surrounding dermis is indicated by the oval with surrounding dermal fibroblasts shown outside of the adventitia. Cells are drawn to show their relative positions within the vessel wall, but are not shown to scale.

For SSc patients, the transport of oxygen and nutrients to the skin are both important functions of blood vessels. Ischemia, or starvation of the skin by vascular constriction or other blockage of flow, occurs in approximately 95% of SSc patients (23, 75). Blood vessels also facilitate immunological surveillance of the skin by transporting leukocytes from lymphoid tissues to sites of inflammation (69). The perivascular space may also serve as a niche for local priming of infiltrating leukocytes in the skin. Both of these are likely important for the pathogenesis of DLE. Although the immune system may also contribute to SSc, the large disparity in cutaneous leukocyte infiltration between SSc and DLE patients suggests a more central role in DLE. Perhaps the distinct vascular pathologies in SSc and DLE influence the disparate dermal manifestations of these diseases and provide clues for treatments.

Adventitial Thickening in SSc

Raynaud's phenomenon (RP), where the fingers become blanched and numb due to reduced blood flow followed by pain upon reperfusion, occurs in ≥90% of SSc patients (23). It often precedes the onset of fibrosis by months or years, suggesting a causal link between RP and fibrosis (23). This frequency and timing of vascular pathology in SSc patients led LeRoy to propose his vascular hypothesis in 1975: macrophage activation or monocyte infiltration into the adventitia induces proliferation and ECM production by perivascular fibroblasts, intimal occlusion and microvascular destruction (31). Fibroblast activation leads to perivascular adventitial expansion, interstitial fibrosis and may contribute to neointima formation

(31). Together, these vascular changes increase the severity of Raynaud's vasospasms and the risk of complete vascular blockage in SSc patients (46, 76, 77). If this occurs in areas fed by few blood vessels, it can cause critical ischemia and necrosis. Critical ischemia leads to digital ulceration in 40% and amputation in approximately 20% of these patients (76). Even resolution of ischemia is fraught, as vascular reperfusion can generate reactive oxygen species that further damage tissues (78).

Adventitial thickening is suspected to constrict vessels and increase the risk of critical ischemia in SSc (23, 79, 80). However, there are few primary studies of the PA in SSc skin disease. Early histopathology studies were the first step in identifying that adventitial thickening may contribute to SSc vasculopathy (79, 81–83). Only two SSc-related studies have remarked on the PA. One demonstrated elevated levels of leukotriene B_4 in the serum of patients with pulmonary arterial hypertension (PAH) (84). Blocking leukotriene B_4 signaling in a rat model of PAH curtailed adventitial enlargement and the development of hypertension (84). Using a mouse model of activated TGFβ1 receptor signaling in fibroblasts, the second study showed that this was sufficient to drive adventitial fibrosis (85). This study did not establish the relative contributions of intimal, medial and adventitial changes to vascular dysfunction (85).

More is known about pathologic vascular constriction by the adventitia in cardiovascular diseases than in SSc. Signals such as angiotensin II drive production of endothelin 1 and reactive oxygen species by the adventitia (86–88).

This molecular combination acts as a potent vasoconstrictor. Reactive oxygen species counteracted nitric oxide-mediated dilation, and endothelin 1 strongly induced vasoconstriction by vascular smooth muscle cells (87, 89, 90). In models of hypertension, post-angioplasty restenosis and transplant vasculopathy the adventitia is often the first vascular layer where proliferation occurs (84, 91–96). T cells that are activated in the PA during hypertension exacerbate vascular dysfunction by producing IL-17A, which drives fibrosis and further contraction (97). Collectively, these data support studying adventitial changes to gain a better understanding of SSc pathogenesis.

Perivascular Cuffing in DLE

Inflammation and large leukocyte infiltrates are a feature of all DLE lesions (12, 98). These infiltrates are likely responsible for the tissue destruction and resulting sunken, atrophied scars (5). Activated blood endothelial cells promote leukocyte infiltration by expressing E-selectin, intercellular adhesion molecule 1 (ICAM1), vascular cell adhesion molecule 1 (VCAM1) and peripheral lymph node addressin (PNAd) (60, 61, 99). Expression of several leukocyte chemoattractants including the CXC motif chemokine receptor 3 (CXCR3) ligands CXCL9, 10 and 11 is increased in DLE lesions (13, 14, 63). Vascular dilation, which reduces the speed of blood flow and increases the frequency of rolling and firm adhesion by leukocytes, is part of inflammation such as occurs in DLE (100, 101). Collectively, these observations point to blood vessels being central to DLE pathology.

Once in the skin, leukocytes receive signals directing them to the dermo-epidermal junction and hair follicles (13, 14, 63, 64). Perivascular cuffing, or the dense accumulation of leukocytes around blood vessels, is also common (12, 98). Belying this, perivascular cuffing was recently included in updated diagnostic criteria for DLE (98). Little is known about perivascular cuffing in DLE. Only one study has examined differences in leukocyte infiltrate composition between the dermo-epidermal junction and perivascular space (102). These investigators found comparable levels of CD4 and CD8 T cells, CD20+ B cells, CD68+ macrophages and cells expressing CXCR3 and one of its ligands, CXCL10 in the two locations (102). Accumulation of leukocytes in the PA is better studied in other diseases, the best known of which is atherosclerosis.

Leukocytes infiltrating the aortic adventitia were observed as early as 1962 (103). More recently, organized structures (called tertiary lymphoid structures or TLS) resembling secondary lymphoid organs were identified in the adventitia of both humans and mice (104, 105). Aortic TLS are a site of local immunological priming, likely generating both protective and pathological responses (104, 106, 107). TLS are supported by networks of specialized fibroblasts similar to those found in lymphoid organs (108–111). These fibroblasts produce pro-survival cytokines and retentive chemokines, and generate a microenvironment conducive to lymphocyte priming (108–111). Current evidence suggests that priming of regulatory T cells (Treg) in TLS delays vascular occlusion in a murine model of atherosclerosis (104). Later in the disease, it is postulated that Tregs lose control

of the TLS and leukocytes appear to enter the media heading for intimal plaques (112). This model of the aortic TLS suggested that similarly specialized networks of adventitial fibroblasts may contribute to the perivascular cuffing common to DLE lesions.

PA Mesenchymal Cells in SSc and DLE

Endothelial cells are the most famous constituents of vascular units, but many vessels are dominated by mesenchymal cells (71–73, 113). Vascular units wrapped by all three layers are surrounded by at least four types: pericytes, vascular smooth muscle cells, fibroblasts and MSC (Fig. 1) (114–118). Two of these, fibroblasts and MSC, are found in the PA (115–118). These normally sessile adult mesenchymal cells derive from motile, ECM-producing embryonic precursors (119, 120). In this dissertation, “MSC” refers to cells thought to be capable of self-renewal and multi-lineage differentiation. “Fibroblast” will refer to cells thought of as being more differentiated. Neither of these definitions is set in stone, as the abilities of both fibroblasts and MSC to proliferate and differentiate are under investigation. When the precise identity of the cell is unclear, “mesenchymal cell” encompasses multiple cell types within this lineage.

Because of their developmental heritage, adult mesenchymal cells are commonly conflated with fibroblasts. However, over the past two decades, differences among fibroblasts from distinct organs and within the same tissue have been discovered (40, 121–129). For example, in lymph nodes there are at least seven phenotypically and functionally distinct fibroblast subsets (130–139). Many

of these are specialized to support the survival and functions of specific types of leukocytes (130–139). Within the skin, many populations of fibroblasts exist including papillary and reticular dermal fibroblasts, as well as fibroblasts of the hair follicle papilla and hair follicle sheath (40, 74, 125–129, 140). Recent evidence has implicated fibroblasts in functions beyond ECM production, such as fighting infections, and the pathogenesis of inflammatory diseases and cancers (118, 123, 141–151). Increasing recognition of mesenchymal cell heterogeneity has sparked interest in associating specialized fibroblast states with disease pathologies, and therapeutically targeting these cells.

Potential Roles for PA Mesenchymal Cells in SSc

Little is known about the PA in SSc skin disease, so there is much to be gained from studying changes to its resident mesenchymal cells. Although vascular injury is thought to be one of the first triggers of SSc, this has not been definitively proven (78, 80, 152, 153). In lSSc patients, vascular dysfunction usually long precedes skin fibrosis, but in dSSc patients the two can occur almost simultaneously (27). Several animal models of vascular and hypoxic diseases PA demonstrated that fibroblasts proliferate and become activated prior to other vascular or interstitial cells (91, 92, 94). Regardless of whether the primary injury in an SSc patient is vascular or interstitial, PA fibroblasts may sense and respond to both cases (113). Consistent with this concept, we previously observed expansion of a discrete set of CD90+ PA fibroblasts in the skin of SSc and DLE patients (154).

In line with the idea of the PA as a site of first responders to injury, reports have identified MSC in the adventitia (115, 116, 155). A local niche of precursor cells is likely important for repairing injuries (156–160). In humans, these adventitial MSC have been described using several markers including CD34+ (115, 161). Adventitial CD34+ MSC have been observed in and isolated from human skin (117, 154, 162). Murine dermal perivascular MSC have also been identified, and these contributed to dermal fibrosis after inflammatory injury (163). A deeper understanding of PA fibroblast and MSC activation in SSc may yield insights into how this compartment contributes to vascular pathology and fibrosis.

PA Fibroblast Support of Leukocytes in DLE

Leukocyte accumulation in the skin is regulated at several levels, including survival and retention (69). Within lymphoid organs, mesenchymal lineage cells fill both roles. For example, lymph node fibroblastic reticular cells (FRC) form a specialized niche to give succor to T cells. FRC produce the chemokines CCL19 and CCL21 to attract CC motif chemokine receptor 7 (CCR7)+ T cells and dendritic cell (DC)s (143, 164–167). Adhesion molecules, including VCAM1 and ICAM1, may be important during the early steps of forming a lymphocyte-supporting niche but their role in T cell retention *in vivo* is unclear (168). *In vitro*, both ICAM1 and VCAM1 contribute to fibroblast-T cell adherence. T cell pro-survival cytokines, such as IL-7 and IL-15 round out the care that FRC provide (169, 170). Fibroblasts in the skin of DLE patients also produce IL-15, likely thanks to tumor necrosis factor α (TNF) from infiltrating T cells or other activated leukocytes (13, 171).

Requirements for signaling through the TNF receptors vary among FRC in different secondary lymphoid organs; splenic FRC require TNF receptor ligands, while lymph node FRC do not (172–175). If the perivascular cuffs observed in DLE lesions occur in the PA, these activated fibroblasts may form a supportive niche for the leukocytes.

This notion is supported by evidence that lymphoid organ fibroblasts develop from perivascular precursors during both embryonic development and inflammation (150, 176–183). Leukocytes extravasate specifically through post-capillary venules, which lack vascular smooth muscle cells (72, 101, 184). Once infiltrating leukocytes pass the endothelial cells and pericytes of the intima, they come into direct contact with the post-capillary venule PA (72) making this a potential hub for local lymphocyte priming. Local priming of T cells by perivascular macrophages and dendritic cells in murine contact hypersensitivity is consistent with this idea (185). Examining PA fibroblast activation in DLE may shed light on how leukocytes accumulate in the inflamed skin of these patients.

Central Hypothesis and Summary of Results

The central hypothesis of this study was that human dermal PA fibroblasts are distinct from dermal fibroblasts, and adopt unique activation states associated with fibrosis in SSc and leukocyte infiltration in DLE. Dermal PA fibroblasts were distinguished from surrounding dermal fibroblasts, leukocytes, endothelial cells, VSMC and pericytes by expression of CD90 and platelet-derived growth factor receptor β (PDGFRβ), lack of CD34, α-smooth muscle actin (SMA), CD45 and

CD31, location adjacent to VSMC marked by SMA and morphology of wrapping vascular units in healthy skin (186). Expansion of PA fibroblasts was observed in the affected skin of both SSc and DLE patients (186). In DLE, activated PA fibroblasts expressed VCAM1, which was associated with dense perivascular T cell infiltrates (186). VCAM1 transcript levels were positively correlated with CCL19, a chemokine that attracts CCR7+ T cells, and IL-15, a cytokine that promotes the survival and activation of T cells (164, 169, 171, 184, 186–188). PA fibroblasts in SSc skin adopted a distinct NGFR+VCAM1- activation state, which was not observed on dermal fibroblasts. NGFR is commonly used to identify MSC (189–191), and NGFR+ PA fibroblasts were observed in close proximity to and demonstrated phenotypic overlaps with cells previously identified as MSC (115–117, 180). Expansion of NGFR-expressing PA fibroblasts was also detected in reparative and pathologic scarring, as well as four dermal tumors. Together, these data indicate divergence between PA and dermal fibroblasts, and identify discrete PA fibroblast activation states associated with inflammation and ECM deposition.

CHAPTER TWO: MATERIALS AND METHODS

Data and portions of the text in this chapter were originally published as: Barron, A. M. S., Mantero, J. C., Ho, J. D., Nazari, B., Horback, K. L., Bhawan, J., Lafyatis, R., Lam, C., and Browning, J. L. (2019) Perivascular Adventitial Fibroblast Specialization Accompanies T Cell Retention in the Inflamed Human Dermis. *Journal of immunology (Baltimore, Md.: 1950)*. **202**, 56–68.

Tissue Samples

Diffuse SSc and DLE biopsies were collected and processed as previously defined (154). DLE and chronic spongiform dermatitis biopsies for histology were selected by pathologists (JB and JDH) based on histological and clinical assessment. DLE samples for RNA analysis were paired biopsies of lesioned and non-lesioned skin obtained from 7 patients. All biopsies were collected under patient consent and approval of the Boston University Medical Campus Institutional Review Board. Demographics and clinical characteristics of the patient cohorts from Chapter Three are defined in Table 1, and those for Chapter Four are in Table 2. Control human tonsil samples were obtained from Boston University Medical Center Pathology and lymph nodes were provided by the Renal Section from an unused donor kidney (courtesy of Dr. Ramon Bonegio).

Skin tissue was obtained from four female MRL/MpJ-*Fas*^{lpr}/J (MRL/lpr) mice with inflamed skin lesions, and from two C57BL/6 mice at one, two and four days post-incisional wounding (dpw) as described previously (154). Approximately full-thickness, 1-cm long incisions were made in the shaved mid-dorsal skin using a

scalpel, and the wounds were sealed with Liquid Bandaid. Similar wounds have grown over the first two dpw followed by contraction over days 3-10, and are fully closed by approximately 9-10 dpw (192). Healthy skin adjacent to the incisional wounds was also collected from the mice. Liver tissue was collected from one *Fasl*^{gld}*.apoE*$^{-/-}$ (*gld.ApoE*) mouse as previously described (193) and two C57BL/6 control mice. Pancreatic tissue was obtained from four female NOD/ShiLtJ (NOD) and two control C57BL/6 mice. All mice were originally from The Jackson Laboratory (Bar Harbor, ME), and none of the controls were co-caged or littermates of the experimental animals. Histological analyses were conducted on all of the tissues described above. All murine tissues were collected with approval by the Boston University Medical Campus Institutional Animal Care and Use Committee.

	RNA analysis						Histology			
Indication	H	H	SSc	DLE	DLE	AD	H	SSc	CSD	DLE
Source	BU	GEO	BU	BU	GEO	GEO	BU	BU	BU	BU
N	15	21	65	7	7	13	15	60	17	19
Age (years)										
Mean (SD)	46 (14)	ND	50 (11)	42 (10)	ND	40 (15)	39 (16)	49 (10)	54 (14)	51 (20)
Range	23-63	ND	22-83	24-55	ND	16-81	20-63	22-76	19-73	22-84
Sex										
% female	67%	ND	63%	71%	71%	ND	31%	65%	41%	89%
Disease duration (months)										
Mean (SD)	ND	ND	19 (33)	83 (64)	ND	ND	ND	26 (39)	ND	ND
Range	ND	ND	1-252	25-185	ND	ND	ND	0-252	ND	ND
Systemic sclerosis characteristics										
Diffuse SSc (%)	0%	0%	100 %	0%	0%	0%	0%	100 %	0%	0%
Modified Rodnan Skin Score										
Mean MRSS (SD)	ND	ND	27 (9)	ND	ND	ND	ND	22 (11)	ND	ND
MRSS range	ND	ND	5-43	ND	ND	ND	ND	0-48	ND	ND
Mean local pinch score (SD)	ND	ND	2.2 (0.7)	ND	ND	ND	ND	1.8 (0.8)	ND	ND
Local pinch score range	ND	ND	1-3	ND	ND	ND	ND	0-3	ND	ND

Table 1. Characteristics of healthy, SSc, CSD, AD and DLE patients whose biopsies were studied in Chapter Three.

Samples collected over the past 13 years were included in this study. Due to limited material remaining from older biopsies, subsets of patients were used for each staining analysis. H, healthy; SSc, systemic sclerosis; DLE, discoid lupus erythematosus; AD, atopic dermatitis; CSD, chronic spongiotic dermatitis. ND, not determined.

	Histology								
Indication	H	H	lSSc	dSSc	SSc	RS	HS	KS	DLE
Source	BU	PRESS	BU	BU	PRESS	BU	BU	BU	BU
N	11	12	10	18	13	12	8	8	10
Age (years)						ND	ND	ND	
Mean (SD)	45 (17)	44 (13)	51 (14)	50 (10)	47 (16)	ND	ND	ND	53 (20)
Range	23-62	30-71	31-69	34-66	25-78	ND	ND	ND	27-84
Sex						ND	ND	ND	
% female	65%	42%	80%	65%	46%	ND	ND	ND	65%
Disease duration (months)									
Mean (SD)	ND	ND	63 (58)	27 (38)	ND	ND	ND	ND	ND
Range	ND	ND	2-192	6-156	ND	ND	ND	ND	ND
Systemic sclerosis characteristics									
Diffuse SSC (%)	0%	0%	0%	100%	100%	0%	0%	0%	0%
Modified Rodnan Skin Score									
Mean MRSS (SD)	ND	ND	4 (3)	20 (11)	26 (11)	ND	ND	ND	ND
MRSS range	ND	ND	2-12	0-48	6-43	ND	ND	ND	ND
Mean local pinch score (SD)	ND	ND	0 (0)	2 (1)	1.9 (0.9)	ND	ND	ND	ND
Local pinch score range	ND	ND	0-1	0-3	0-3	ND	ND	ND	ND

Table 2. Characteristics of healthy, SSc, DLE and reparative and pathologic scar patients whose biopsies were studied in Chapter Four.

Samples collected over the past 13 years were included in this study. Due to limited material remaining from older biopsies, subsets of patients were used for each staining analysis. H, healthy; SSc, systemic sclerosis; DLE, discoid lupus erythematosus; RS, reparative scar; HS, hypertrophic scar; KS, keloid scar. ND, not determined.

Histology

All analyses utilized conventional formalin fixed paraffin embedded sections. Two-color immunohistochemistry and three-color immunofluorescence was performed as described previously (154). Slides were baked at 60°C for 30 minutes, followed by dewaxing in histoclear for 6 minutes, and rehydration through graded ethanol/water baths (100% ethanol, 95% ethanol, 75% ethanol, 50% ethanol) and tris-buffered saline, pH 7.4 (TBS: 50 mM Tris base, 150 mM sodium chloride, pH to 7.4 with hydrochloric acid). Heat-induced epitope retrieval was performed in boiling tris-EDTA buffer, pH 9 (0.1 mM EDTA, 1 mM Tris base) for 20 minutes using an electric steamer followed by cooling at room temperature for 20 minutes. Sections were ringed with a pap pen. Endogenous peroxidases and phosphatases were blocked with Bloxall (Vector Laboratories) for 20 minutes at room temperature. After a brief rinse in TBS with 0.05% Tween-20 (TBST), sections were blocked with 2.5% normal horse or goat serum (Vector Laboratories). Another brief rinse in TBST was followed by incubation with the primary antibody diluted in phosphate-buffered saline, pH 7.4 (PBS: 2.68 mM potassium chloride, 0.14 M sodium chloride, 10.14 mM disodium phosphate, 1.76 mM monopotassium phosphate, pH to 7.4 with hydrochloric acid) with 1% bovine serum albumin, heat shock fraction V (Fisher Scientific) for either at 4°C overnight or at room temperature for 1-2 hours. Sections were washed in TBST on a rotating shaker for 10 minutes at room temperature, followed by incubation with enzyme-labeled secondary antibody (Vector Laboratories ImmPress horseradish

peroxidase (HRP) or alkaline phosphatase (AP) polymer secondary antibodies) for 30 minutes at room temperature. Following another wash in TBST for 10 minutes at room temperature, slides were incubated with the appropriate substrate for between 1-10 minutes. For immunohistochemistry, the HRP substrate used was AMEC red (Vector Laboratories) and the AP substrate was Hi-Def Blue AP (Enzo Life Sciences). Immunofluorescence substrates were tyramide-conjugated CF488, CF594 and CF405S (Biotium) diluted to a final concentration of 10 μM in borate buffer (100 mM boric acid, pH to 8.5 with sodium hydroxide) with hydrogen peroxide added to a final concentration of 0.003% immediately before use. A brief TBST rinse was followed by Bloxall quenching of the remaining enzymatic activity as before. Additional antigens were detected by repeating the above procedure. Slides developed with chromogens were mounted in VectaMount AQ (Vector Laboratories), covered and sealed with nail polish; fluorescent slides were mounted with either Vectashield Hard Mount, Vectashield Hard Mount with DAPI (both from Vector Laboratories) or Fluoroshiled Mounting Medium with DAPI (Abcam).

Antibodies were separately titered for the two modalities. For immunofluorescence, an isotype control section was included in each experiment. Confocal microscope laser power and photodiode gain were set so that no fluorescence was detected from the isotype control. Primary antibodies were rat anti-human CD3 (CD3-12; ThermoFisher Scientific, Waltham, MA); rabbit anti-mouse/human CD3 (polyclonal; Abcam, Cambridge, MA); rabbit anti-human CD20

(EP459Y; Abcam); mouse anti-human CD20 (L26; ThermoFisher Scientific); rabbit anti-human CD21 (EP3093; Abcam); mouse anti-human CD31 (mAbs C31.3+JC/70A; Novus Biologicals, Littleton, CO); rat anti-mouse CD31 (SZ31; Dianova, Hamburg, Germany); mouse anti-human CD34 (QBend10; Dako, Carpinteria, CA); rabbit anti-human/mouse CD34 (EP373Y; Abcam); mouse anti-human CD45RA/RO (mAbs 2B11+PD7/26; Dako); rabbit anti-human CD90 (EPR3132; Abcam); rat anti-mouse CD90 (IBL-6/23; Abcam); mouse anti-human CD90 (7E1B11; Promab, Richmond, CA); mouse anti-human SMA (1A4; Dako); rabbit anti-mouse/human SMA (E184; Abcam); goat anti-human VCAM1 (polyclonal; R&D Systems, Minneapolis, MN); rabbit anti- mouse/human VCAM1 (EPR5047; Abcam); mouse anti-human PDPN (D2-40; Dako); rat anti-human PNAd (MECA79; Santa Cruz Biotechnology, Dallas, TX); rabbit anti-mouse/human NGFR (EP1039Y; Abcam); mouse anti-human FDC (CNA.42; Dako); rabbit anti-mouse/human PDGFRβ (28E1; Cell Signaling Technology, Danvers, MA); mouse anti-human NGFR (NGFR5+NTR/912; Novus); rabbit anti-human CD73 (EPR6114; Abcam); mouse anti-UCHL1 (13C4; Abcam).

Morphometrics were performed using the FIJI distribution of ImageJ2 (194, 195). Regions of interest were drawn around distinct vascular units. For measuring perivascular areas covered by PA fibroblasts expressing VCAM1 or NGFR in immunohistochemically-stained samples, the brown and blue were separated using the Color Deconvolution plugin (196). Custom color vectors were created using images of single stained slides developed with only brown or blue and

imaged under the same conditions as the slides to be analyzed. Positive controls were used to set threshold values, and binary images were created. Staining above the threshold value within each region of interest was measured. Images used in each morphometric analysis were captured at the same time using the same microscope and camera settings.

Antibody	Clone	Dilution
Rat anti-human CD3	CD3-12	1:4000
Rabbit anti-mouse/human CD3	polyclonal	0.2 μg/mL
Rabbit anti-human CD20	EP459Y	0.6 μg/mL
Mouse anti-human CD20	L26	Neat
Rabbit anti-human CD21	EP3093	0.1 μg/mL
Biotinylated mouse anti-human CD31	C31.3+JC/70A	8.0 μg/mL
Rat anti-mouse CD31	SZ31	2.0 μg/mL
Mouse anti-human CD34	QBend10	0.1 μg/mL
Rabbit anti-mouse/human CD34	EP373Y	5.0 μg/mL
Mouse anti-human CD45RO/RA	2B11+PD7/26	0.8 μg/mL
Rabbit anti-human CD90	EPR3132	0.2 μg/mL
Rat anti-mouse CD90	IBL-6/23	5.0 μg/mL
Mouse anti-human CD90	7E1B11	1:500
Mouse anti-human SMA	1A4	2.0 μg/mL
Rabbit anti-mouse/human SMA	E184	2.0 μg/mL
Goat anti-human VCAM1	Polyclonal	1:1500
Rabbit anti-mouse/human VCAM1	EPR5047	0.2 μg/mL
Mouse anti-human PDPN	D2-40	Neat
Rat anti-human PNAd	MECA79	1:1000
Rabbit anti-human/mouse NGFR	EP1039Y	2.0 μg/mL
Mouse anti-human FDC	CNA.42	0.5 μg/mL
Rabbit anti-mouse/human PDGFRβ	28E1	1:200
Mouse anti-human NGFR	NGFR5+NTR/912	0.2 μg/mL
Rabbit anti-human CD73	EPR6114	1:2000
Mouse anti-human UCHL1	13C4	1:50000

Table 3. Antibodies used for histology.

Gene Expression Data and Analysis

All microarray data used in this paper is available from the GEO database (https://www.ncbi.nlm.nih.gov/geo/). GEO accession numbers for each data set are listed below. The microarray gene expression data in this study was obtained as either internal or from public GEO databases as follows (n=129): Normal

controls in house (n=14) and GEO (n=21, GSE52471, GSE32407, and GSE32924), SSc internal (n=65, GSE94340, GSE95065, GSE55036), DLE internal (n=7, GSE120809) and GEO (n=7, GSE52471), and atopic dermatitis (AD) GEO (n=15, GSE32924) and all used either the Affymetrix array U133A 2.0 or U133A Plus 2.0 chips (197–201). Raw array CEL files were processed with the "affy" package from the statistical software R studio (version 3.3.2) and normalized using the RMA algorithm. Microarray probe sets were mapped using Brainarray, version 21.0.0, Entrez mapping (http://brainarray.mbni.med.umich.edu/Brainarray/Database/CustomCDF).

Correction for batch effects was performed by using the COMBAT algorithm part of the SVA package (version 3.22.0) (202). Low variation genes were then filtered out by selecting genes with a standard deviation greater than 0.3 from the median expression across all samples, resulting in 8,575 genes for further analysis. To determine the composition of infiltrating immune cells in the tissues of the different diseases, we utilized the CIBERSORT algorithm (http://cibersort.stanford.edu/) as described by Newman et al (203). CIBERSORT returns the percentage of the RNA that can be accounted for by the various subsets and this percentage was normalized using the ratio of a pan leukocytic marker (CD45/PTPRC) to GAPDH. The final fraction is proportional to the absolute numbers of leukocytic subsets. All T and B cell subsets were summed to create total T and B values reflective of the biopsy content.

Cell Culture

Primary human neonatal foreskin fibroblasts were derived as previously described (204) and grown in Advanced Modified Eagle's Medium with 5% fetal bovine serum, 10 mM HEPES, 2 mM GlutaMAX, 100 U/mL penicillin and 100 U/mL streptomycin (all from ThermoFisher Scientific). Cells were used for experiments before passage 13. For experiments, 40,000 fibroblasts were plated in 6-well plates and equilibrated overnight. Fibroblasts were treated by adding fresh complete Advanced Modified Eagle's Medium (described above) with the combination of 10 ng/mL TNFα (R&D Systems, Minneapolis, MN) and 200 U/mL IFNγ (Stemcell Technologies, Vancouver, BC, Canada), dimethyl sulfoxide (DMSO, Sigma-Millipore, Burlington, MA) to a final concentration of 2 or 4%, dimethylformamide (DMF, Sigma-Millipore) to a final concentration of 2% or 1 μm retinoic acid (RA, Sigma-Millipore).

Flow Cytometry

Cells were harvested for flow cytometry after three days of stimulation. Accutase (Biolegend) was used to detach the cells, which were transferred to 96-well, round-bottom plates (Corning, Corning, NY) for staining. Zombie UV viability dye (Biolegend) diluted in PBS or Hank's Balanced Salt Solution (ThermoFisher Scientific) was used to exclude dead cells, followed by staining with the following primary labeled antibodies (also see Table 4): anti-NGFR PE-Cy7 (clone ME20.4), anti-VCAM APC (clone STA), anti-CD90 APC-Cy7 (clone 5E10), anti-PDPN PE (clone NC-08), anti-ICAM1 FITC (clone HA58) and anti-PD-L1 Brilliant Violet 421

(clone 29E.2A3) all from Biolegend. Fluorescence-minus-one controls were included for the NGFR and VCAM stains. An isotype control sample was also included in all experiments. Antibodies were diluted in FACS buffer (1x PBS or 1x Hank's balanced salt solution (no phenol red, calcium or magnesium), 1% bovine serum albumin heat shock fraction V and 0.1% sodium azide). All samples were run on a BD LSRII (Becton, Dickinson and Company, Franklin Lakes, NJ) using 450/50 nm filters to collect Brilliant Violet 421 and Zombie UV from the 355 nm and 405 nm lasers, respectively; 505 nm long-pass and 530/30 nm filters to collect FITC from the 488 nm laser; 735 nm long-pass and 780/60 nm filters to collect PE-Cy7 and a 590/35 nm filter to collect PE from the 561 nm laser; and 735 nm long-pass and 780/60 nm filters to collect APC-Cy7 and a 670/30 nm filter to collect APC from the 633 nm laser. Software compensation and data analysis was performed using FlowJo (Becton, Dickinson and Company).

Statistics

Analyses were performed using Prism software. Group comparisons used Kruskal-Wallis tests followed by post-hoc pairwise Dunn's multiple comparison tests unless noted. Correlations are Spearman analyses with Holm-Sidak adjusted P values. In all cases P values <0.05 were considered significant.

Antibody	Clone	Dilution
Mouse anti-human CD90 APC/Cy7	5E10	0.40 μg/mL
Rat anti-human Pdpn PE	NC-08	0.25 μg/mL
Mouse anti-human VCAM1 APC	STA	0.5 μg/mL
Mouse anti-human ICAM1 FITC	HA58	0.5 μg/mL
Mouse anti-human NGFR PE/Cy7	ME20.4	0.5 μg/mL
Mouse anti-human PD-L1 BV421	29E.2A3	0.25 μg/mL
Mouse IgG1, κ isotype control APC/Cy7	MOPC-21	0.4 μg/mL
Rat IgG2a, λ isotype control PE	B39-4	0.25 μg/mL
Mouse IgG1, κ isotype control APC	MOPC-21	0.5 μg/mL
Mouse IgG1, κ isotype control FITC	MOPC-21	0.5 μg/mL
Mouse IgG1, κ isotype control PE/Cy7	MOPC-21	0.5 μg/mL
Mouse IgG2b, κ isotype control BV421	MPC-11	0.25 μg/mL

Table 4. Antibodies used for flow cytometry.

CHAPTER THREE: PERIVASCULAR ADVENTITIAL FIBROBLAST SPECIALIZATION ACCOMPANIES T CELL RETENTION IN THE INFLAMED HUMAN DERMIS

Data and portions of the text in this chapter were originally published as: Barron, A. M. S., Mantero, J. C., Ho, J. D., Nazari, B., Horback, K. L., Bhawan, J., Lafyatis, R., Lam, C., and Browning, J. L. (2019) Perivascular Adventitial Fibroblast Specialization Accompanies T Cell Retention in the Inflamed Human Dermis. *Journal of immunology (Baltimore, Md.: 1950)*. **202**, 56–68.

Abstract

Perivascular accumulation of lymphocytes can be a prominent histopathologic feature of various human inflammatory skin diseases. Select examples include SSc, spongiotic dermatitis and cutaneous lupus. While a large body of work has described various aspects of the endothelial and vascular smooth muscle layers in these diseases, the outer adventitial compartment is poorly explored. The goal of the present study was to characterize perivascular adventitial fibroblast states in inflammatory human skin diseases and relate these states to perivascular lymphocyte accumulation. In normal skin, adventitial fibroblasts are distinguished by CD90 expression and dense perivascular lymphocytic infiltrates are uncommon. In SSc, this compartment expands, but lymphocyte infiltrates remain sparse. In contrast, perivascular adventitial fibroblast expression of VCAM1 is upregulated in spongiotic dermatitis and lupus and is associated with a dense perivascular T cell infiltrate. VCAM1 expression marks transitioned fibroblasts that

show some resemblance to the reticular stromal cells in secondary lymphoid organs. Expanded adventitial compartments with perivascular infiltrates similar to the human settings were not seen in the inflamed murine dermis. This species difference may hinder the dissection of aspects of perivascular adventitial pathology. The altered perivascular adventitial compartment and its associated reticular network form a niche for lymphocytes and appear to be fundamental in the development of an inflammatory pattern.

Introduction

Leukocytic infiltrates occur in various patterns in inflammatory skin disease, ranging from diffuse collections at the dermoepidermal junction, such as in lichenoid interface dermatitis, to densely packed and highly organized perivascular structures (205–207). On one end of this spectrum lies classical inflammation-induced activation of the endothelium and the display of ICAM1 and E/P-selectins which especially facilitate leukocyte entry (208). At the other end, chronic inflammation results in the emergence of lymphocytic aggregates that organize into lymphoid-tissue-like structures called tertiary lymphoid structures (TLS). Generally, TLS possess high endothelial venules (HEV) that allow naïve and certain memory lymphocyte subsets to emigrate from the blood, segregated T and B cell regions and germinal center reactions (209). Within TLS, the reticular stroma begins to resemble the fibroblastic reticular cells (FRC) and follicular dendritic cells (FDC) in secondary lymphoid organs, presumably facilitating T and B cell segregation and function (210). While TLS have been intensely studied, the

reticular stromal underpinnings of the more common unorganized perivascular infiltrates, originally termed “perivascular cuffs”, remain poorly explored (211).

The presence of localized infiltrates can be dissected into entrance, retention and egress stages. Decades of work has revealed the mechanisms by which inflammation triggers increased leukocytic trafficking through post-capillary venules. However, in contrast to secondary lymphoid organs, the questions of whether retention and egress are active processes in perivascular infiltrates remain ill-defined. We have focused on the perivascular adventitia (PA) or *tunica adventitia* compartment in dermal autoimmune disease. The PA is a fibroblast and collagen fiber-rich region external to the vascular smooth muscle layer (*tunica media*). Originally designated veiled cells, such adventitial fibroblasts are observed surrounding arterioles and terminal arterioles as well as in post-capillary, collecting and larger venules (71, 72). Of late the PA has received increasing notice as a reservoir of resident progenitor cells; as such, this region is well-poised to sense perturbations and initiate repair programs, but can also be a source of pathogenic fibroblasts (212–215). PA fibroblasts, as well as resident macrophages/dendritic cells and mast cells, are involved in immune surveillance and an active supportive vasculature, the *vasa vasorum*, could serve as a portal for cellular entry into the inflamed compartment (216). This may be the case in atherosclerosis, where TLS arise within the arterial adventitial compartment (105, 217).

Stenmark and colleagues have defined a VCAM1+ (vascular cell adhesion molecule-1) fibroblast in the PA of hypoxic rat and calf lungs (218, 219). VCAM1

is widely known as an inflammation-induced adhesion molecule on endothelial cells mediating integrin $\alpha4\beta1$ (very late antigen-4, VLA4) and $\alpha9\beta1$ positive leukocyte trafficking at both the attachment and transmigration levels (220). This trafficking system can be utilized by T cells, monocytes, neutrophils and eosinophils (221, 222). However, there is substantial expression on non-endothelial cells (223), including activated fibroblasts (219, 224–226), synoviocytes (227, 228), smooth muscle cells (229, 230), pericytes (231), astrocytes (232) and epithelial cells (233, 234). In several instances, the non-endothelial cell expression dominates (235–237). In secondary lymphoid organs from both mouse and human, the reticular stromal networks, i.e. FRC and FDC, display VCAM1 (238–241). VCAM1+ reticular networks were described in murine models of experimentally induced TLS in the thyroid gland and pancreas (242, 243). The functional relevance of VCAM1-VLA4 interactions *in vivo* in these non-endothelial settings remains poorly explored, although roles for lymphocyte retention were demonstrated in Peyer's patch development (244), the spleen (245–247), bone marrow (248, 249) and the fibrotic heart (250). VCAM1 expression in the vasculature has been explored histologically in SSc and DLE skin, albeit with limited resolution (251–253). Despite this long history, the questions of whether PA fibroblasts express VCAM1 in human inflammatory skin diseases, and whether this correlates with perivascular lymphocyte infiltration, remain open.

In healthy human skin, lymphocytes are described as occupying primarily a perivascular region, although few leukocytes are present relative to inflamed skin (254). The skin of chronic cutaneous or discoid lupus (DLE) and many chronic spongiotic dermatitis (CSD) patients is characterized by substantial perivascular and adnexal inflammation (62, 199, 255–257). In contrast to CSD and DLE, expanded perivascular regions are accompanied by only a limited monocytic infiltrate in the skin of most SSc patients (16). Only in a small subset of SSc patients are substantial perivascular lymphocytic infiltrates present. We hypothesized that the differing nature of the perivascular infiltrates in SSc, DLE and dermatitis reflects the activation state of the reticular stroma in the PA. A picture emerges where the perivascular adventitial compartment expands, engulfing the entire infiltrated region with lymphocytes being retained within a VCAM1+ reticular network.

Results

Defining the Perivascular Adventitial Compartment in Normal, SSc and DLE Skin

We will use the term “vascular unit” to refer to the entire region encompassed by the PA compartment including the vascular media and intima. In cases where multiple vessels are surrounded by a single PA compartment, all of the vessels are defined as being part of one vascular unit. Earlier work indicated that dermal PA fibroblasts are CD90+ (Thy1) and CD34- (154, 258–260). We combined CD90 with CD34 and SMA staining to reveal CD90+ cells with fibroblastic morphology external to both the CD34+ endothelial and the SMA+

medial layers around blood vessels larger than capillaries (diameter ≥8 μm). These CD90+ cells form a layer between the media/intima and the CD34+ dermal fibroblasts in sections from healthy skin, where the term “dermal fibroblast” is used here to designate non-adnexal fibroblasts external to the perivascular layer (Fig. 2A-B). We define these CD90+SMA-CD34- cells as perivascular adventitial fibroblasts. Extensive co-localization of CD90 and the mesenchymal lineage marker PDGFRβ validated these cells as fibroblasts (Fig. 3A). Pericytes are distinguished from PA fibroblasts by location, within the basement membrane and attached to endothelial cells by peg-socket contacts, and by expression of SMA in addition to CD90 and PDGFRβ (70, 261). CD34+ bright cells at the edge of the vascular unit were also observed and these are potentially MSC (259). Despite potential lineage overlaps between adventitial fibroblasts, MSC, smooth muscle cells and pericytes, the PA fibroblasts are readily recognized with this staining system.

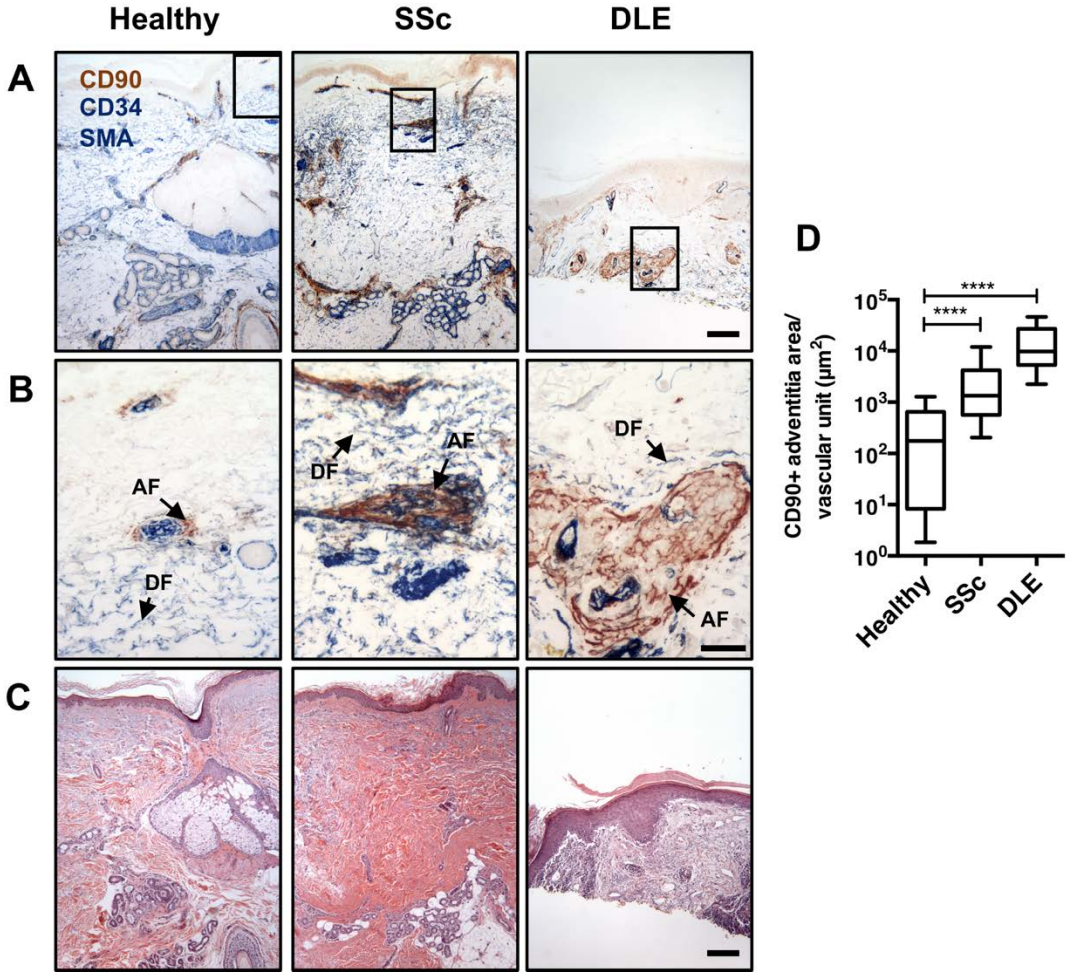

Figure 2. Perivascular adventitial fibroblasts express CD90.
(**A**) Immunohistochemical staining of human skin biopsies for CD90 (brown) and a combination of CD34 and SMA (both blue) to define the vascular media and intimal layers. CD90 staining highlights the PA layer. Scale bar is 200 μm. (**B**) A higher magnification view of the boxed vessels in (**A**) with adventitial (AF) and dermal (DF) fibroblasts indicated. Scale bar is 50 μm. (**C**) H&E stain of a serial section showing the equivalent region in (**A**) with the region shown in (**B**) boxed. Scale bar is 200 μm. (**D**) Morphometric analysis of the area of CD90 staining in the PA in healthy skin (107 vascular units, 5 volunteers), skin from SSc patients (107 vascular units, 5 patients), and DLE skin lesions (80 vascular units, 5 patients). Area refers to the μm^2 of CD90+ pixels per vascular unit. ****, $p<0.0001$; Kruskal-Wallis followed by post-hoc pairwise Dunn's multiple comparison tests.

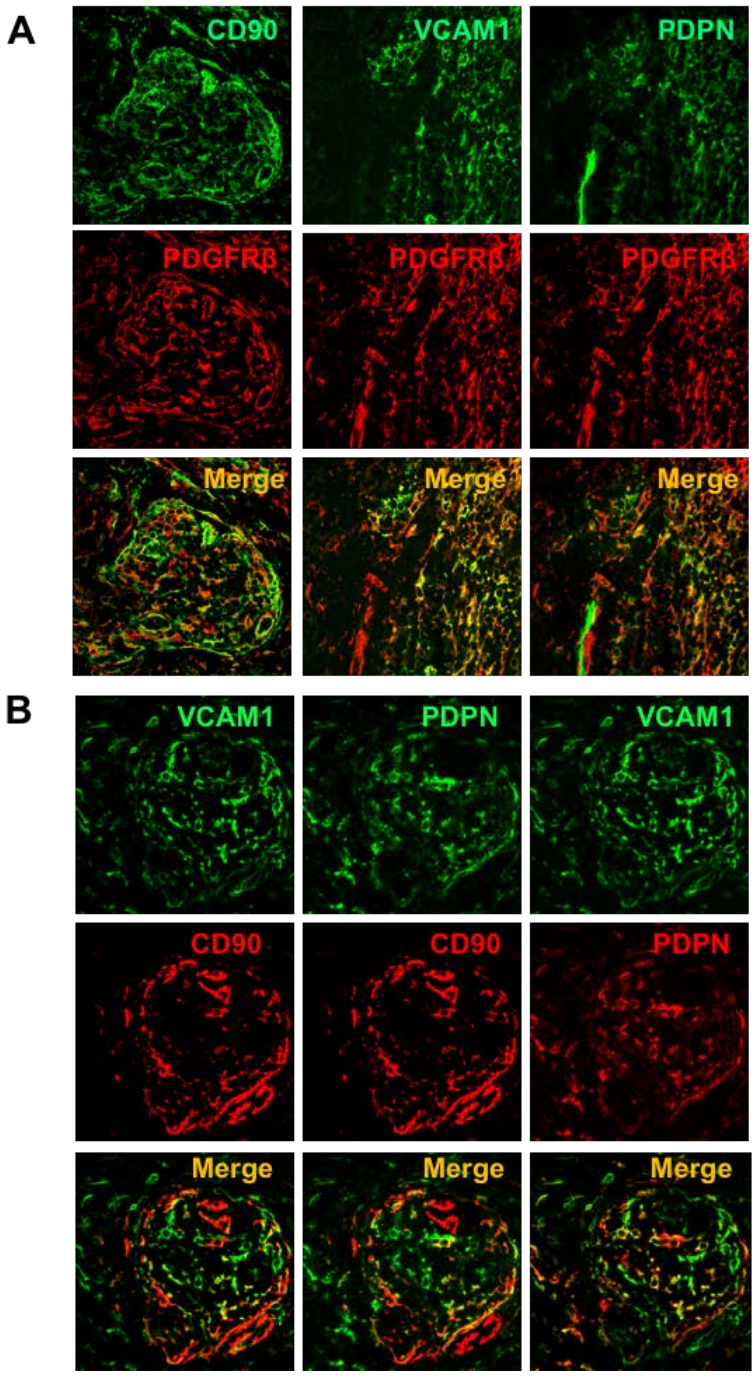

Figure 3. PA CD90+, VCAM1+ and PDPN+ cells are PDGFRβ+ fibroblasts. (**A**) Single channel and merged false color images of a DLE lesion biopsy stained as indicated with co-localization in the merge in yellow. (**B**) DLE lesion biopsy co-stained for VCAM1 PDPN and CD90 showing the extent of co-localization.

In the dermis of SSc patients, the CD90+ PA fibroblast layer was expanded relative to healthy controls (Fig. 2A-B, D). CD90 expression appeared more intense, but we did not attempt to discriminate between increased expression and simply a denser packing of fibroblast processes. The outer edge of the PA abuts the CD34+CD90- dermal fibroblasts which were readily distinguished in the normal dermis, yet in SSc skin, these cells often convert to a CD34-CD90+ cells (154). Notably, we found some examples of PA pathology in the absence of this dermal CD34-to-CD90 fibroblast transition (Fig. 2A) suggesting that this aspect of the perivascular disease can precede the fibroblast activation. In DLE biopsies, PA fibroblasts covered more area than in either healthy controls or SSc patients and displayed a morphology similar to that seen in the FRC in lymphoid tissues (Fig. 2A-B, D). We examined CD90 expression in PA compartments in biopsies from 17 healthy, 61 diffuse SSc and 11 DLE subjects, and the sections chosen for morphometric analysis in Fig. 3D were representative. PA fibroblasts were seen around vessels with large perivascular leukocytic infiltrates (Fig. 2A-C). We conclude that PA fibroblasts expand in SSc and DLE patients, and in DLE the expansion was accompanied by dense leukocytic infiltrates.

VCAM1 Display on Activated Perivascular Adventitial Fibroblasts

Since VCAM1 is expressed by activated PA fibroblasts in pulmonary hypertension, by normal FRC in lymphoid organs and by lymphoid tissue organizer cells during lymph node anlage nucleation (210, 218, 219), we hypothesized that PA fibroblasts in DLE patients may express this adhesion molecule. Sections co-

stained for both antibodies and visualized by immunofluorescence showed complete overlap (Fig. 4D). No or very limited VCAM1 expression was observed in the PA of dermal blood vessels in healthy individuals (8 donors). The healthy patient in Fig. 4A exemplified the high end of PA VCAM1 expression and, when present, these positive cells cover a small area. VCAM1-expressing PA fibroblasts were infrequent and small in SSc biopsies (3/23), and examples of typical VCAM1-negative and VCAM1+ SSc PA are shown in Fig. 4A. In contrast to SSc, extensive reticular networks of VCAM1+ adventitial cells were detected around vessels in the skin of all (14/14) DLE patients examined. Morphometric analysis of representative sections supported the conclusion that VCAM1+ PA areas were greater in DLE patients than in SSc and healthy skin (Fig. 4B). Co-localization of VCAM1 with the mesenchymal marker PDGFRβ confirmed that these cells are fibroblastic (Fig. 3A). Moreover, many of the VCAM1+ reticular cells also expressed CD90 (Fig. 3B).

VCAM1 is also expressed by a narrow subset of macrophages, e.g. murine and human splenic red pulp macrophages and Kupffer cells in the liver sinusoids and therefore we searched for VCAM1+ leukocytes in the human skin samples. Although fibroblasts were the most frequent VCAM1-expressing cells in DLE, the expected endothelial VCAM1 expression was also detected. CD31+ vasculature expressing VCAM1 and vessels lacking VCAM1 surrounded by an extensive VCAM1+ reticular network were apparent (Fig. 4C). The VCAM1+ cells as revealed with either the rabbit or the goat anti-VCAM1 antibodies were distinct from

the pan-leukocyte staining using a CD45RO/RA antibody combination, indicating that reticular VCAM1+ cells are not hematopoietic (Fig. 4D). Roughly half of the DLE biopsies possessed VCAM1+ endothelium. Therefore, VCAM1 display identifies a phenotypic change in the dermal PA fibroblasts in DLE.

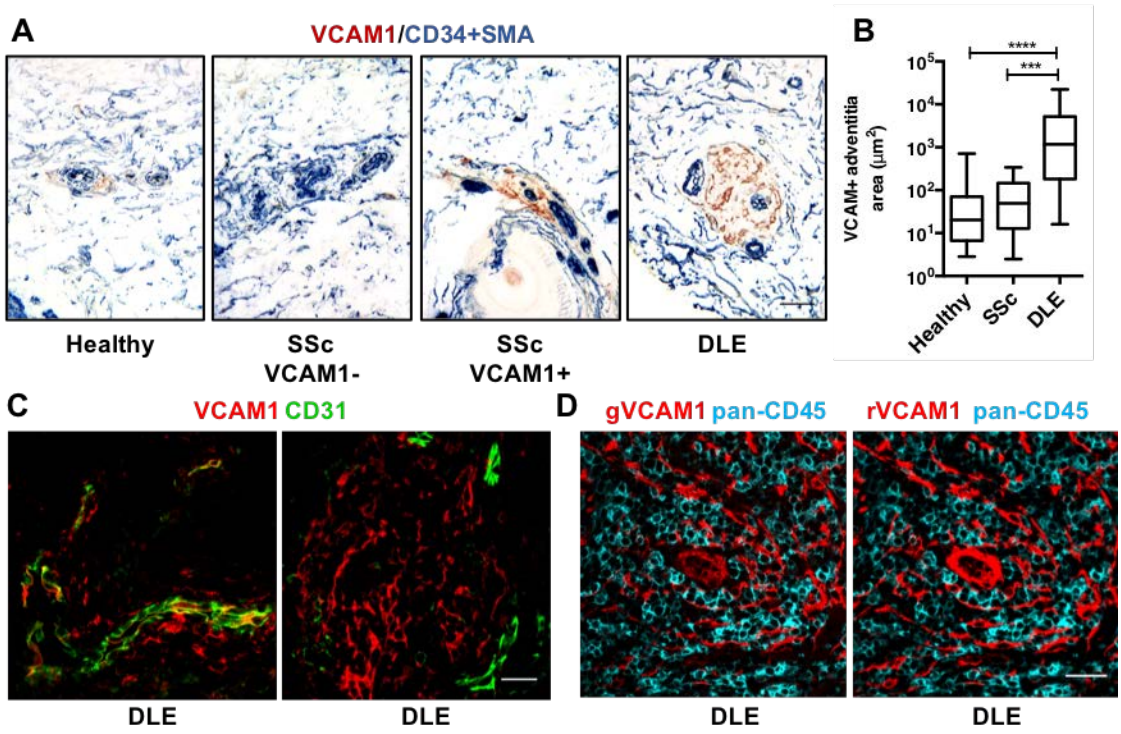

Figure 4. VCAM1 expression defined a different state of the perivascular adventitia.
(**A**) Typical VCAM1 expression (brown) in the PA compartments in healthy, SSc and DLE biopsies with a combination of CD34 and SMA (blue). The SSc VCAM1- and VCAM1+ panels represent the full range of patterns observed in SSc. Scale bar is 50 μm. (**B**) Morphometric analysis of the area of VCAM1+ vascular adventitia in healthy skin (56 vascular units, 3 volunteers), skin from SSc patients (260 vascular units, 4 patients), and DLE skin lesions (194 vascular units, 3 patients). Area refers to the μm^2 of VCAM1+ pixels per vascular unit. ****, $p<0.0001$; Kruskal-Wallis followed by post-hoc pairwise Dunn's multiple comparison tests. (**C**) Examples of VCAM1+ (left) and VCAM1- (right) vessels in DLE, VCAM1 (red), CD31 (green). (**D**) Immunofluorescent staining of a human DLE skin lesion for VCAM1 (red; left, goat polyclonal, right, rabbit monoclonal antibodies) and a combination of CD45RO and RA (cyan). (**C-D**) Scale bars are 25μm.

Dermal Perivascular T Cell Infiltrates Localize to VCAM1+ Vascular Adventitia

We examined the relationship between the presence of an activated PA fibroblast, as defined by VCAM1 expression, and perivascular lymphocytic

infiltrates. In general, densely packed perivascular infiltrates were rare in healthy and SSc biopsies. Typical VCAM1+ SSc PA regions contained some (~5-15) CD3+ T cells while such infiltrates were not seen in VCAM1- compartments. In DLE, dense infiltrates were found in adventitial regions containing VCAM1+ fibroblasts outside of the CD31+ and SMA+ vascular intima and media (Fig. 5A-B). We suspected that infiltrating T cells would co-localize with VCAM1+ PA fibroblasts. For this and subsequent analyses, we included patients with the histologic diagnosis of CSD to determine whether our findings extended to other inflammatory diseases with perivascular infiltrates. Immunofluorescent staining for VCAM1 and CD3 showed that PA T cell infiltrates were moderate to dense and common in all examined (6/6) CSD and (14/14) DLE patients (Fig. 5C). Enumeration of the leukocytes in the vascular media and adventitia of all infiltrated vessels using hematoxylin and eosin-stained DLE skin sections confirmed that the majority of perivascular leukocytes accumulate in the adventitia (Fig. 5D). Morphometric analysis confirmed the influx of CD3+ cells in CSD and DLE skin with a 10-50 fold increase over healthy and SSc samples (Fig. 5E). T cell infiltrates could require a VCAM1+ vessel to gain access, and hence PA reticular VCAM1 could simply track with endothelial VCAM1. However, as noted above, many examples were found of T cell infiltrated PA without VCAM1+ vessels consistent with the notion of PA VCAM1 expression tracking with T cell clusters.

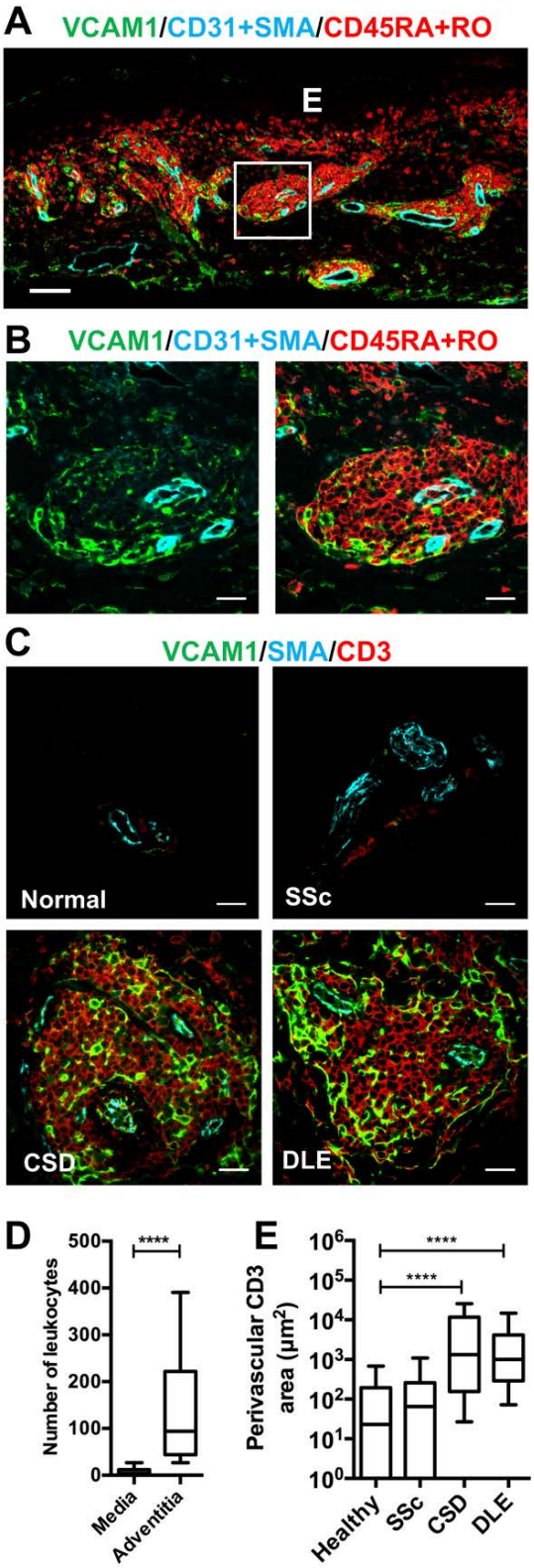

Figure 5. Dense perivascular T cell infiltrates are found within VCAM1+ PA fibroblast networks.
(**A**) Low power immunofluorescence image of DLE skin showing VCAM1+ structures (green), CD31/SMA+ blood vessels (cyan) and CD45RA+RO positive leukocytes (red), "E" marks the epidermis. Scale bar is 100 μm. (**B**) Higher magnification of the white boxed area from (**A**). (**C**) Immunofluorescent staining for VCAM1 (green), CD3 (red), and SMA (cyan) in representative healthy, SSc, CSD and DLE biopsies. Scale bars are 25 μm in (**B**) and (**C**). (**D**) Counts of perivascular leukocytes in the vascular adventitia and media from hematoxylin and eosin stained skin sections (101 vascular units, 8 DLE patients). (**E**) Morphometric analysis of the area of CD3+ T cells in the PA compartment in healthy skin (35 vascular units, 4 volunteers), SSc (57 vascular units, 5 patients), CSD (47 vascular units, 5 patients) and DLE skin lesions (57 vascular units, 5 patients). Area refers to the μm^2 of CD3+ pixels per vascular unit. (**D**-**E**) ****, $p<0.0001$. (**D**) Wilcoxon test. (**E**) Kruskal-Wallis followed by post-hoc pairwise Dunn's multiple comparison tests.

VCAM1 RNA Levels Correlate with T Cell Accumulation

To independently query the relationship between VCAM1 expression and cellular infiltration, we utilized whole skin RNA expression datasets. Since PA fibroblasts dominated dermal VCAM1 expression in the histological views, we considered VCAM1 RNA levels as a surrogate for activated PA fibroblasts. Using publicly available and in-house microarray data from healthy, SSc, atopic dermatitis (AD, a subset of spongiotic dermatitis patients) and DLE patient skin biopsies, we created a dataset normalized for batch effects. When compared to healthy skin and matched non-lesioned DLE skin, VCAM1 RNA levels were elevated in biopsies taken from AD, DLE and a subset of SSc samples (Fig. 6A). The CIBERSORT algorithm was used to probe the nature of the cellular infiltrates in the various settings (203). CIBERSORT returns proportions of various leukocyte subsets, but does not reflect changes in the total number of leukocytes in a biopsy. Assuming that CD45 expression was proportional to the total leukocyte content while GAPDH reflected the total number of cells, we used the CD45/GAPDH ratio to normalize the subset fraction into a value that reflected the relative levels of the cell subset in the whole tissue. All CIBERSORT T or B cell subsets were summed to represent total dermal T and B cells. T cell RNA signatures were higher in lesioned tissue from AD and DLE biopsies compared to matched, non-lesioned biopsies (Fig. 6B). Although a subset (8%) of SSc patients had elevated T cell signals, the overall distribution was similar to the healthy controls.

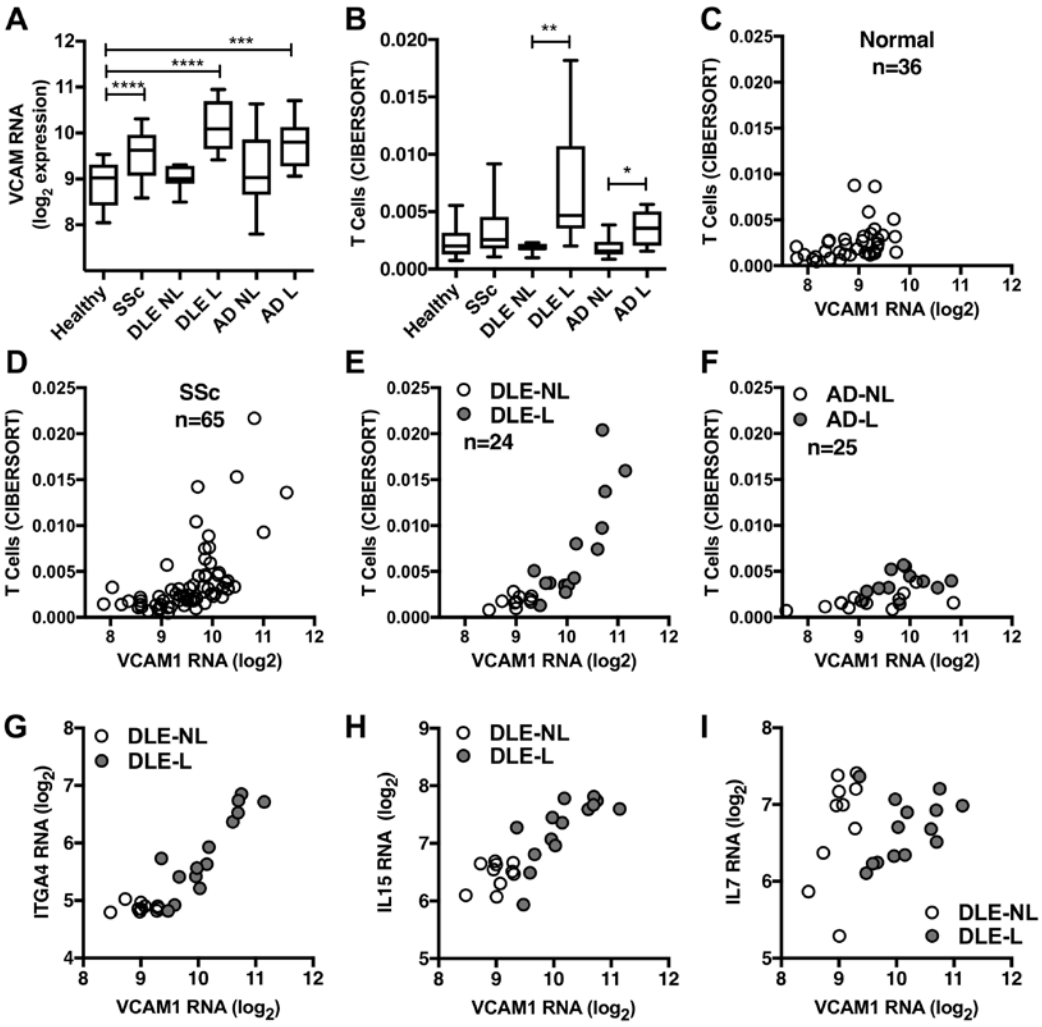

Figure 6. VCAM1 RNA correlates with T cell infiltration, ITGA4, and IL15, but not IL7 RNA.

(**A**) Relative VCAM1 RNA expression from microarray analyses of whole skin biopsies (NL non-lesioned skin, L lesioned skin). (**B**) Relative total T cell levels as determined by CIBERSORT analysis of the whole biopsy transcriptome. (**C-F**) Relationship between the levels of VCAM1 RNA and total T cells as determined by CIBERSORT. (**G-I**) Relationship between the levels of VCAM1 RNA and ITGA4, IL15 and IL7 RNA as assessed by microarray. (**A**-**B**) *, p<0.05; **, p<0.01; ***, p<0.001; ****, p<0.0001; Kruskal-Wallis followed by post-hoc pairwise Dunn's multiple comparison tests.

Gene	Patients	VCAM1		CIBERSORT T		CIBERSORT B	
		rho	Adj. p	rho	Adj. p	rho	Adj. p
VCAM1	Control	-	-	0.49	0.0798	0.22	0.8805
	SSc	-	-	0.69	0.0000	0.44	0.0053
	AD	-	-	0.49	0.4320	0.03	0.9983
	DLE	-	-	**0.88**	**0.0000**	0.60	0.0512
CD3G	Control	0.43	0.1724	**0.71**	**0.0001**	0.55	0.0243
	SSc	0.68	0.0000	**0.85**	**0.0000**	0.47	0.0026
	AD	**0.79**	**0.0000**	**0.68**	**0.0166**	0.23	0.9847
	DLE	**0.81**	**0.0000**	**0.90**	**0.0000**	0.69	0.0102
ITGA4	Control	0.53	0.0228	0.66	0.0009	0.42	0.2467
	SSc	0.60	0.0000	0.63	0.0000	0.44	0.0059
	AD	**0.71**	**0.0020**	**0.71**	**0.0092**	0.16	0.9899
	DLE	**0.85**	**0.0000**	**0.89**	**0.0000**	**0.71**	**0.0056**
ICAM1	Control	0.39	0.2836	0.31	0.6894	0.35	0.5377
	SSc	0.63	0.0000	0.60	0.0000	0.39	0.0256
	AD	**0.82**	**0.0000**	0.38	0.7805	-0.06	0.9983
	DLE	**0.73**	**0.0010**	**0.76**	**0.0016**	0.42	0.5087
SELP	Control	-0.14	0.9651	0.06	0.9730	0.12	0.9730
	SSc	0.39	0.0166	0.25	0.3341	0.17	0.7810
	AD	0.35	0.7805	0.08	0.9958	0.19	0.9872
	DLE	**0.71**	**0.0018**	0.68	0.0102	0.50	0.1817
IL-7	Control	0.19	0.8949	0.55	0.0225	0.29	0.7411
	SSc	0.11	0.9562	0.16	0.8491	0.12	0.9562
	AD	0.37	0.7493	0.53	0.2641	0.04	0.9983
	DLE	0.02	0.9938	0.11	0.9938	-0.03	0.9938
IL-15	Control	0.37	0.4056	0.34	0.5583	0.29	0.7407
	SSc	0.65	0.0000	0.64	0.0000	0.50	0.0006
	AD	**0.79**	**0.0001**	0.61	0.0874	0.23	0.9847
	DLE	**0.79**	**0.0001**	**0.85**	**0.0000**	0.61	0.0502
CCL19	Control	0.48	0.0640	0.25	0.8406	0.22	0.8805
	SSc	0.60	0.0000	**0.71**	**0.0000**	0.52	0.0003
	AD	**0.76**	**0.0003**	0.53	0.2641	0.18	0.9899
	DLE	**0.79**	**0.0001**	**0.70**	**0.0079**	0.42	0.5087
CCL21	Control	0.24	0.8406	0.10	0.9681	0.10	0.9681
	SSc	0.29	0.1955	0.48	0.0015	0.29	0.2282
	AD	0.45	0.4320	0.34	0.8820	0.23	0.9847
	DLE	0.50	0.1487	0.61	0.0502	0.26	0.9129
CXCL12	Control	0.60	0.0029	0.16	0.9174	0.04	0.9681
	SSc	0.04	0.9727	-0.05	0.9727	-0.11	0.9562
	AD	0.36	0.7704	-0.10	0.9983	0.38	0.7805
	DLE	0.09	0.9938	-0.24	0.9129	-0.19	0.9566
CXCL13	Control	0.44	0.1555	0.65	0.0011	0.67	0.0005
	SSc	0.63	0.0000	0.66	0.0000	0.44	0.0059
	AD	0.26	0.9378	0.41	0.7493	-0.33	0.8960
	DLE	**0.79**	**0.0001**	**0.87**	**0.0000**	**0.73**	**0.0036**

Table 5. VCAM1 RNA is positively correlated with CD3G, IL-15 and CCL19 RNA in SSc, AD and DLE.

Rho values higher than 0.7 are bolded.

We found VCAM1 and CD3G RNA correlated strongly in all patient groups, and this relationship was largely paralleled with the CIBERSORT T cell data (Fig. 6C-F, Table 5). These data are consistent with the hypothesis that the presence of perivascular T cells tracks with PA reticular VCAM1 expression. The T cell levels in AD returned by the CIBERSORT algorithm suggested a less pronounced infiltrate than we observed histologically in CSD, and this discrepancy probably reflects patient heterogeneity in the AD vs CSD cohorts.

We queried the datasets for genes that tracked with VCAM1 expression and found that expression of Integrin-α4 (ITGA4), i.e. a component of the VLA4 ligand for VCAM1, correlated well with that of VCAM1 (Fig. 6G, Table 5). Additionally, genes potentially related to FRC function, e.g. homeostatic chemokines or T cell survival/growth factors, were also elevated. IL-15, a survival factor for effector T cells, tracked well with VCAM1 expression whereas IL-7, a survival factor for naïve and memory T cells, did not (Fig. 6H-I, Table 5) (238, 262). Homeostatic chemokine levels, i.e. CXCL13 and CCL19, also correlated well with the maturation of the reticulum to the VCAM1+ state and presence of T and B cells (Table 5). The combination of Intercellular adhesion molecule 1 (ICAM1) and VCAM1 expression has been used to track mesenchymal lymphoid tissue organizer cell differentiation during development and repair (210). VCAM1 and ICAM1 RNA were highly correlated in SSc, AD, and DLE; moreover, the correlation of VCAM1 or ICAM1 with T and B cell signatures was similar across diseases, consistent with the hypothesis of VCAM1+ PA fibroblasts adopting an FRC-like

program (Table 5). It is likely that the VCAM1 and ICAM1 correlations are specifically related to lymphocyte infiltration, rather than non-specific sequelae of inflammation, as another adhesion molecule, P-selectin (SELP), tracked with VCAM1 and T and B cell signatures only in DLE and not in AD (Table 5). Together our histological and transcriptomic data support the hypothesis that VCAM1+ PA fibroblasts specialize to promote perivascular lymphocyte accumulation.

Perivascular T Cell Accumulation Can Occur in the Absence of PDPN+ PA Fibroblasts

Podoplanin (PDPN) is another molecule commonly used to characterize reticular elements and, like VCAM1, PDPN is expressed by FRC in both secondary and tertiary lymphoid organs in mice and humans (210) as well as by FDC in humans (263). Using either conventional or immunofluorescence methods, stromal PDPN was rarely detected in the PA compartment in healthy and SSc biopsies, in roughly a third of the CSD and in all DLE biopsies (Fig. 7A). Stromal PA PDPN co-localized with PDGFRβ, CD90, and VCAM1, indicating overlap with the VCAM1+ PA fibroblast population; although, the expression pattern of these four proteins varied per cell which is consistent with recently published single cell RNA-Seq data demonstrating considerable heterogeneity among fibroblasts (127, 264–266) (Fig. 3A-B). All DLE patients had large networks of PA fibroblasts expressing both VCAM1 and PDPN, but VCAM1+PDPN- cells were also seen (Fig. 7B). Thus, at least three cell types or stages are exemplified here: homeostatic

CD90+VCAM1-PDPN-, as well as activated CD90+VCAM1+PDPN- and CD90+ VCAM1+PDPN+ PA fibroblasts.

We determined the relationship between PA fibroblast expression of VCAM1 or PDPN and the size of the T cell infiltrates. Importantly, VCAM1+PDPN- PA regions with dense T cell infiltrates were found in CSD, indicating that PDPN expression was not obligatory for the infiltration (Fig. 7C). By morphometric analysis, there was a strong positive relationship between the area covered by VCAM1+ PA fibroblasts and the size of PA T cell infiltrates, with relatively few T cells in the VCAM1- PA in healthy and SSc skin, and increasingly large T cell infiltrates in VCAM1+ PA from CSD and DLE patients. The equivalent correlation with PDPN area was poor, although vascular units with very high VCAM1 also expressed PDPN (Fig. 7D). Because we detected PDPN on many activated keratinocytes in addition to fibroblasts and lymphatics in SSc, CSD, and DLE lesions, we were unable to use our whole skin biopsy microarray data to analyze fibroblast PDPN correlations with lymphocyte signatures. These data indicate that perivascular T cells can accumulate regardless of PA fibroblast PDPN expression.

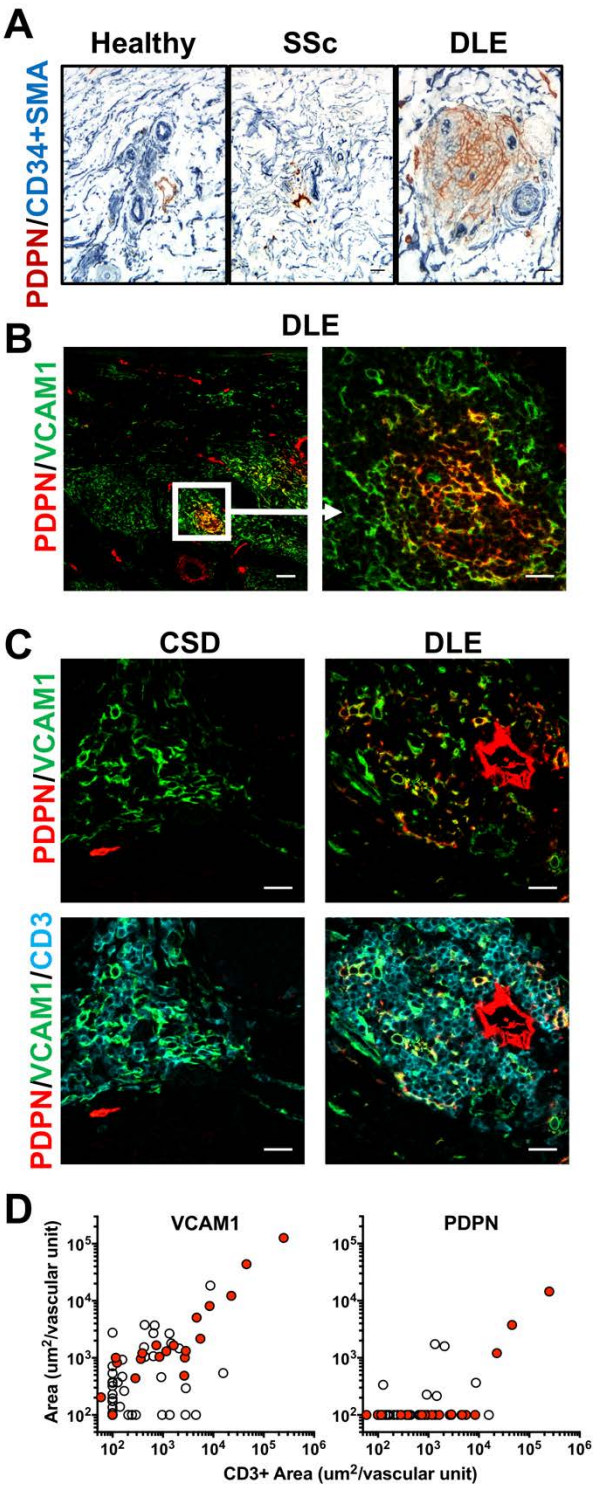

Figure 7. Perivascular T cell infiltrates occur regardless of PA fibroblast PDPN expression. (**A**) Representative examples of PDPN staining (brown) in the PA compartment in healthy, SSc and DLE biopsies with CD34 and SMA (both blue). (**B**) Low- and high-power images of a PDPN+ reticular network (red) that co-stained with VCAM1 (green). (**C**) Contrast between CSD and DLE biopsies showing PDPN (red), CD3 (cyan), and VCAM1 (green). In the CSD panels a PDPN+ lymphatic vessel is seen below the VCAM1+ network. The DLE panels have a dilated PDPN+ lymphatic on the right side. (**D**) Correlation of the CD3+ area and the corresponding VCAM1+ or PDPN+ areas within individual vascular units. Red dots are both non-lesioned and lesioned DLE biopsies while the remainder are healthy, SSc and CSD samples. (**A-C**) Low-power scale bar in (**B**) is 100 μm, all other scale bars are 25 μm.

Do VCAM1+ PA Fibroblasts Resemble FRC?

One defining characteristic of FRC in secondary lymphoid organs is the formation and wrapping of collagen matrix-containing fibers called conduits (210). We investigated whether VCAM1+ PA fibroblasts ensheath conduits similar to FRC. Rodent conduits contain fibrillins 1 and 2, and even elastin fibers (241, 267, 268). As elastin fibers are coated with microfibrils, we looked for microfibril-associated proteins in human conduits that can be identified by immunohistochemistry in formalin-fixed, paraffin-embedded tissues. We identified microfibrillar-associated protein 5 (MFAP5) as a conduit component in human spleen, lymph node, and tonsil, and VCAM1+ FRC were found to wrap the MFAP5+ conduits (Fig. 8A-C). We postulated that MPAF5 could potentially identify fibrils associated with an FRC-like stroma. In the PA, a subset of VCAM1+ fibroblasts in both CSD and DLE were frequently in contact with MFAP5+ structures, yet the extent of wrapping was incomplete (Fig. 8D-F). FRC in secondary lymphoid organs also express SMA and resemble myofibroblasts (238, 269). In contrast to lymphoid organ FRC, PA fibroblasts in DLE were SMA-, indicating a partial transition to FRC status (compare Fig. 8A-C with 8D-F). On this basis we conclude that PA fibroblasts may form incomplete conduit-like structures, but lack full FRC differentiation status.

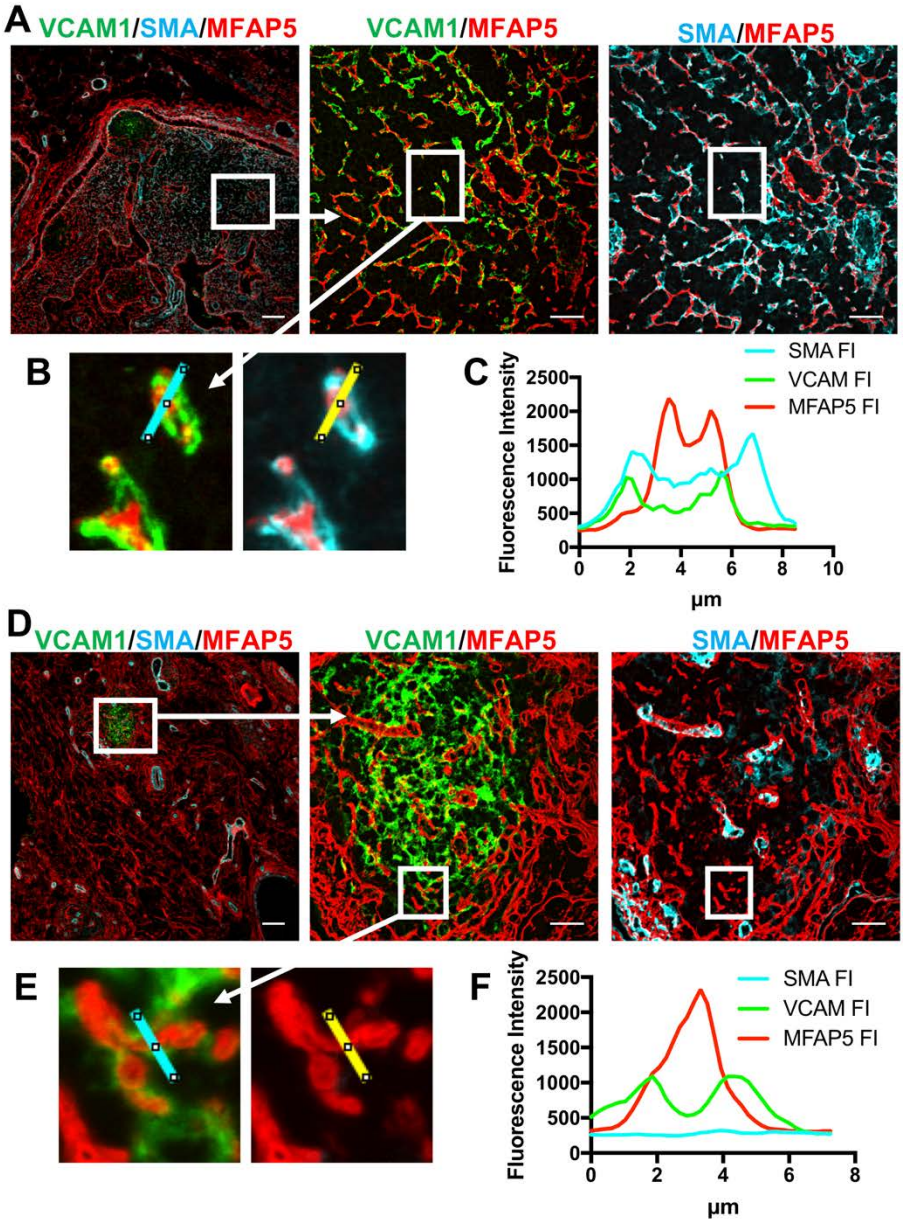

Figure 8. VCAM+SMA- PA fibroblasts associated with MFAP5+ fibers.
(**A**) Immunofluorescence images of a human lymph node stained for VCAM (green), MFAP5 (red), and SMA (cyan). A low-power view is magnified showing the approximate co-localization of VCAM1 and MFAP5 as well as MFAP5 and SMA. (**B-C**) High magnification image of VCAM1+ or SMA+ cells with a cross-sectional intensity analysis of an individual fiber/reticular cell complex. (**D-F**) Identical analysis of a VCAM1+ network in the PA from a DLE biopsy. Cross-sectional analysis was consistent with fiber wrapping, but SMA was not present. (**A**, **D**) Low power scale bars are 100 μm, high power scale bars are 25 μm.

Is the PA Compartment a "Perivascular Cuff" or a Tertiary Lymphoid Structure?

It is reasonable to postulate that there is a continuum of events between early unorganized perivascular infiltrates and mature TLS with their high endothelial venules (HEV), spatially segregated T and B cells and germinal center reactions. Peripheral lymph node addressin (PNAd) expression marks the transition from flat to high endothelium, i.e. HEV formation. PNAd+ vessels were present in all (11/11) DLE biopsies and were rarer in CSD and SSc biopsies (Fig. 9A). Dense B cell infiltrates were detected in DLE by both histology (11/12 biopsies) and RNA (Fig. 9B-C). B cells were rare and sparse in most CSD patients (5/6 biopsies), although one patient had a single large, dense B cell infiltrate similar to DLE lesions. DLE-like B cell infiltrates were also very rare in SSc (Fig. 9C). Since PA PDPN staining appeared to track with B cell presence, we sought to determine the presence of PDPN+ FDC networks by staining for CD21. In DLE, 7/11 biopsies had CD21+ FDC-like networks present (Fig. 9B), and therefore VCAM1+ PDPN+ reticular cells may resemble nascent FDC. The presence of CD21+ PA fibroblasts correlated with dense B cell infiltrates; however, B cell infiltrates did not precisely co-localize with the CD21 staining (Fig 9B). Likewise, many DLE infiltrates lacked the segregated T cell zones and B cell follicles characteristic of mature TLS (Fig. 9D). We conclude that DLE PA compartments are immature TLS structures.

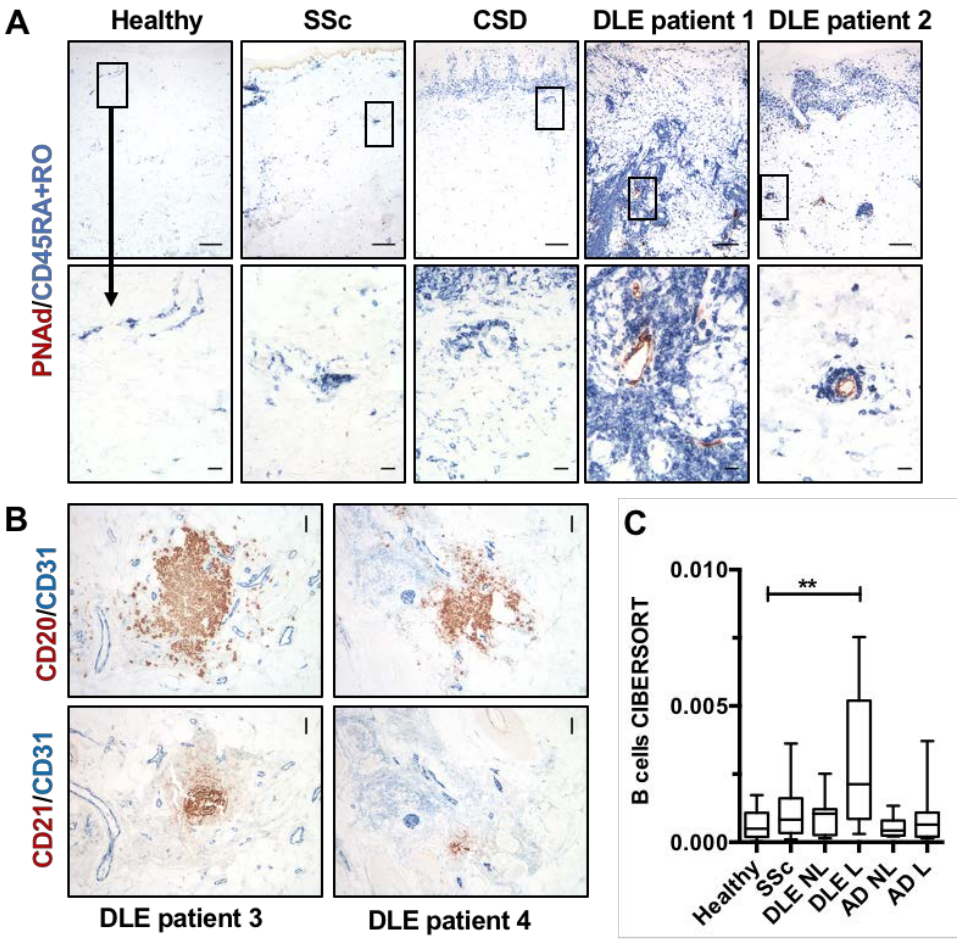

Figure 9. Perivascular structures in SSc, CSD, and DLE are not mature TLS. (**A**) Immunohistochemical staining for Peripheral lymph node addressin (PNAd, brown) and both CD45RA and RO (blue) in healthy (7 volunteers), SSc (7 patients), CSD (6 patients), and DLE (11 patients). Boxed regions from the low-magnification images in the top row are shown in the bottom row. Two distinct DLE patients demonstrate PNAd conversion of many vessels throughout the dermis. Top row scale bar 200 μm, bottom row scale bar 25 μm. (**B**) Staining of serial sections from two unique DLE patient biopsies for CD31 (blue) and CD20 (brown, top) or CD21 (brown, bottom). Scale bars are 50 μm. (**C**) Relative total B cell levels as determined by CIBERSORT analysis of the whole biopsy transcriptome. **, $p<0.01$. ****, $p<0.0001$; Kruskal-Wallis followed by post-hoc pairwise Dunn's multiple comparison tests. (**D**) A DLE lesion biopsy stained for CD20 (red) and CD3 (green). The boxed area in the low power image (left) is shown at higher

magnification (right). Low-power image scale bar 100 μm, high-power scale bar 25 μm.

Comparison of Murine and Human PA Compartments

The question of how closely the murine dermal PA compartment resembles the human counterpart remains poorly explored. Stenmark and colleagues found an expanded PA compartment in hypertensive lungs in humans and calves, but only a slight expansion in rats and none in mice (270)**.** We examined whether the changes in the vascular units in the human inflamed dermis were mimicked in three settings: normal mouse skin, an incisional wound and the lesioned skin of lupus-prone MRL/lpr mice. Thin PDGFRβ+ fibroblastic cell layers were observed surrounding vessels in the hypodermis (the sub-dermal fat layer) or fascial layers with no evidence of any dermal vessels having an adventitial layer (Fig. 10A-C). More pronounced rings were observed in the hypodermis in the incisional wound setting at day 4 and in lesioned MRL/lpr skin (Fig. 10A, C). The vessel in Fig. 11C in the MRL/lpr hypodermis was the largest example found. The combined staining for CD90 and CD31 revealed the lack of CD90+ rings in both the normal murine dermis and hypodermis (Fig. 10D). Thin rings of CD90 staining were visible around large hypodermal vessels in healing skin four days after an incisional wound, yet similar rims were lacking in active MRL/lpr lesions (Fig. 10D). None of the murine injured skin sections contained infiltrated CD90+ vascular adventitial networks resembling those in the active human DLE lesions.

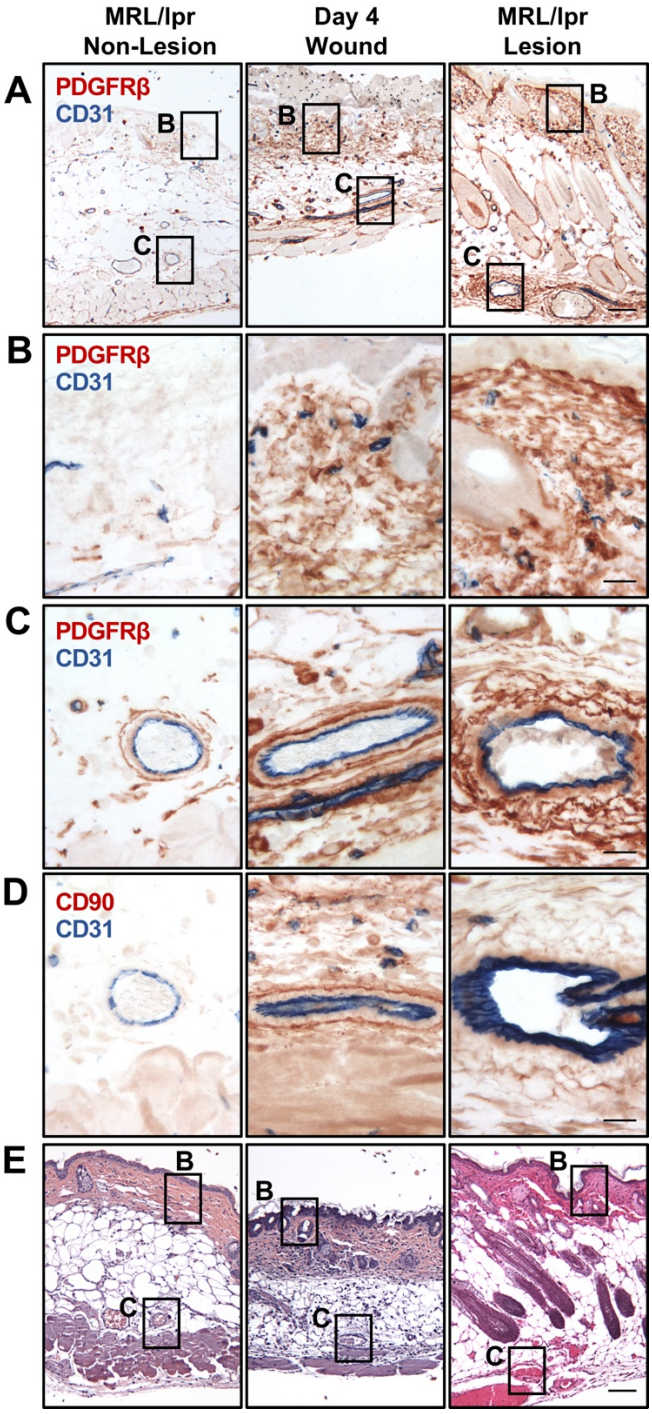

Figure 10. PA compartment in mouse skin.
(**A**) Low power images of skin sections from non-lesioned MRL/lpr skin, C57BL/6 skin 4 days post-incisional wound (Day 4 Wound), and an MRL/lpr skin lesion stained for PDGFRβ (brown) and CD31 (blue). (**B-C**) Higher magnification images of the indicated regions in (**A**) showing blood vessels in the dermis (**B**) and hypodermis (**C**). (**D**) A serial section with the PA regions from the vessels in (**C**) were stained with CD90 (brown) and CD31 (blue). (**E**) Serial skin sections to those in (**A**) stained for H&E. Epidermis is at the top of the pictures. Images were representative of 4 MRL/lpr mice with lesioned skin, two mice 4 days post-wounding, and two healthy mice. (**A, E**) Scale bars are 100 μm. (**B-D**) Scale bars are 25 μm.

Perivascular infiltrates resembling human CSD and DLE were not found in the murine dermis as ascertained by H&E staining of the tissues (Fig. 10E). Skin from C57BL/6 incisional wounds, as well as the non-lesioned and lesioned regions of MRL/lpr mice, lacked VCAM1+ adventitial fibroblasts around dermal and hypodermal vessels. The rabbit antibody used to detect murine VCAM1 also detected human VCAM1, and there the staining patterns overlapped those of a second goat anti-human VCAM1 antibody. Murine keratinocytes, hair follicle epithelial cells and lymphoid organ FRC were VCAM1 positive and hence we consider the antibody staining validated. We conclude that murine dermal blood vessels lack PA fibroblasts, while activated murine hypodermal PA fibroblasts, unlike human PA fibroblasts, neither express VCAM1 nor retain infiltrating leukocytes.

We examined murine settings where perivascular leukocyte infiltrates have previously been described, e.g. TLS in the liver and pancreas (210). Perivascular fibroblastic VCAM1+ networks were observed in the pancreas of NOD mice and in the livers of *gld.ApoE* mice (Fig. 11). Serial sections stained for CD3 and CD31 indicated that T cell infiltrates in the NOD pancreas and *gld.ApoE* liver are dense in areas of perivascular VCAM1+ fibroblasts and much sparser in parenchymal areas lacking VCAM1+ fibroblasts. Subsets of murine FRC have been shown by FACS analysis to display CD90 (271). Normal vessels in the mouse liver and pancreas also lacked a CD90+ PA ring; however, given that murine T cells express CD90, we could not determine if these VCAM1+ TLS networks are also CD90+.

The caliber of vessels surrounded by perivascular infiltrates in the murine pancreas and liver were larger (≥50 μm diameter lumen) than the vessels seen in the murine dermis (≤8 μm) or hypodermis (≤50 μm). However, these vessels were also of larger caliber than the human dermal vessels around which perivascular infiltrates were seen. These data reveal some basic differences in the stromal architecture of the perivascular compartment of mouse and human dermal blood vessels.

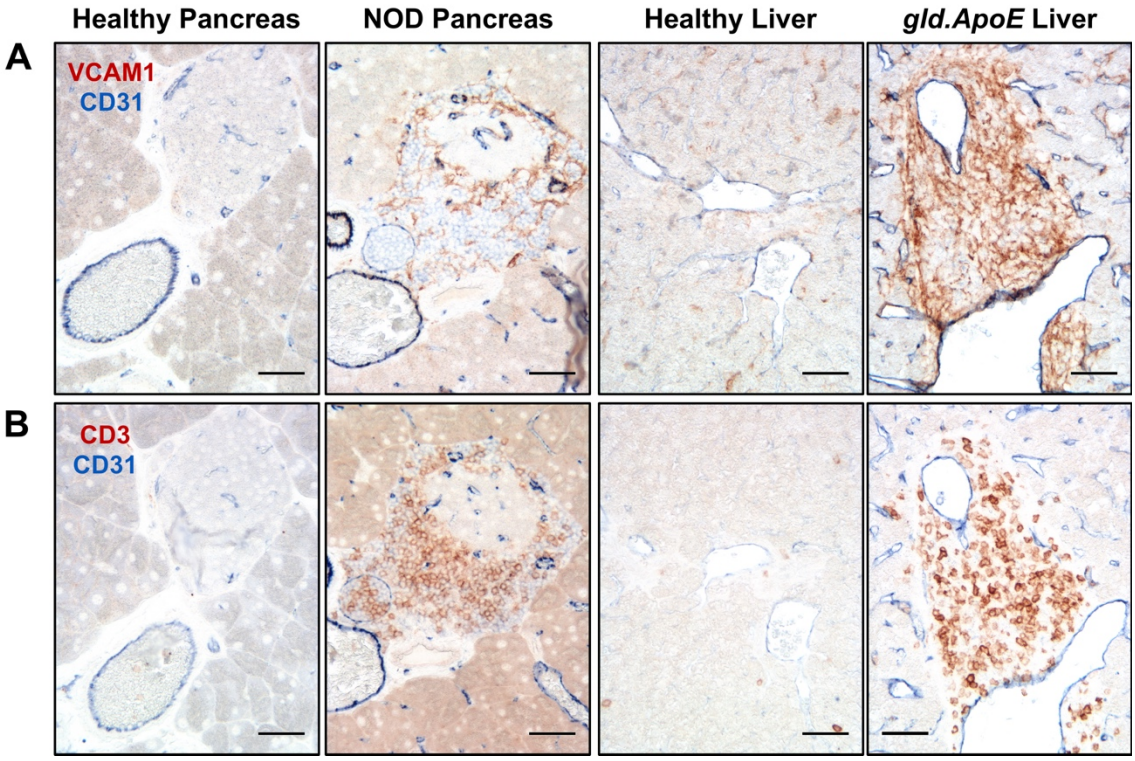

Figure 11. T cells co-localized with VCAM+ perivascular stromal cells in the diabetic NOD pancreas and the livers of *gld.ApoE* mice.

(**A**) Immunohistochemical staining for VCAM (brown) and CD31 (blue) in the indicated organs. VCAM1+ Kupffer cells are visible in the liver sinusoids. (**B**) Serial sections to those in (**A**) stained for CD3 (brown) and CD31 (blue). Healthy organs were from C57BL/6 mice. All scale bars are 50 μm.

Discussion

We have exploited the varying degrees of dermal leukocytic infiltration in SSc, CSD, and DLE to query changes in fibroblast status within the human dermal PA compartment. We found multiple fibroblast states based on the protein expression of CD90, VCAM1 and PDPN. Normal PA fibroblasts expressed CD90 with no or very little VCAM1 or PDPN, and the presence of CD90 distinguishes these cells from resting non-PA dermal fibroblasts. PA fibroblasts are likely some of the CD90-expressing cells detected by FACS and RNA-Seq in normal human skin, adipose tissue and the rheumatoid arthritis synovium (259, 265, 266, 272). Display of VCAM1 and/or PDPN further identified cells in inflamed PA settings. VCAM1+ networks were prominent in CSD and DLE, whereas its display in SSc was less frequent and confined to a smaller region. Nonetheless, when present in SSc, the VCAM1+ PA compartment had more T cells present. PDPN expression represented another level and was prominent in DLE but relatively rare in SSc and CSD. Overlaid upon these states was expansion of the PA compartment which occurred in all disease settings. SSc was notable in that the CD90+ PA compartment was expanded even though the VCAM1 and PDPN activation markers were not present. CD90+ and PDPN- reticular structures were also noted in the human spleen (269).

VCAM1 expression by presumably activated PA fibroblasts correlated with dense perivascular T cell infiltration across the skin conditions we studied. The association between T cell infiltrates and VCAM1 expression was seen both

histologically and transcriptionally. RNA for VCAM1 was positively correlated with ITGA4, which, along with ITGB1, comprises the VCAM1 binding VLA4 ligand. The use of the CIBERSORT algorithm to quantitate relative levels of T cell infiltration supported the relationship between VCAM1 expression and T cell presence. PA fibroblast VCAM1 may be sufficient to tether T cells, or it could be part of a coordinated program necessary for optimal T cell retention. VCAM1 and T cell RNA signatures correlated with CCL19 and IL15, which are produced by FRC to attract T cells and to promote their survival, suggesting that VCAM1 acts in concert with these molecules (262). In agreement, IL-15 is expressed by VCAM1+ stromal cells in mouse bone marrow, lymph nodes and spleen (273, 274). While consistent with our hypothesis, it needs to be noted that CCL19 and IL-15 can be produced by both non-hematopoietic and hematopoietic cells (169, 275). Alternatively, VCAM1 could simply be a surrogate for a fibroblast differentiation state wherein other molecular entities control retention, or it is linked to the presence of activated endothelial cells that are gating lymphocyte entry. PDPN display in DLE but not CSD indicated that it was not essential for T cell accumulation. ICAM1 and VCAM1 RNA expression tracked closely, and we cannot exclude ICAM1 involvement. Indeed, a combination of VLA4 and LFA1 inhibition is often employed to efficiently block cell adhesion, yet non-endothelial VCAM1 alone can support lymphocyte adherence in multiple settings *in vitro*, e.g. (225, 227, 228, 231). VCAM1 was also more important than ICAM1 *in vivo* for the development of murine models of atherosclerosis and dermatitis (276, 277). Since we observed perivascular T cell

infiltrates around VCAM1-negative endothelial cells, we favor the view that the VCAM1+ PA reticulum is actively supporting retention. We note that it is also possible that vascular VCAM1 expression was limited to specific post-capillary caliber venules and some sections simply missed these vessels.

Expansion of the PA compartment appears to be a common pathological event. Almost all SSc biopsies had expanded CD90 positive PA compartments; yet, this change rarely supported an enhanced lymphocytic infiltrate. While not quantitated in this study, these expanded PA compartments in SSc and DLE appeared to encompass multiple small blood vessels at a density not seen in normal tissue, perhaps suggestive of neoangiogenesis. It has been suggested that angiogenesis occurs early in the disease course in SSc (278). A similar expansion of perivascular CD90+ fibroblasts was previously described in human invasive melanoma biopsies (279). Unlike in SSc, cancer-associated fibroblasts in metastatic melanoma and other tumors frequently express VCAM1 and can promote leukocyte infiltration (150, 279–284). Expansion of the CD90+ PA networks suggests simple growth of preexisting PA fibroblasts, primarily since activation markers were not usually present in expanded SSc regions. In support of this idea, FRC networks can expand by direct proliferation during reactive events (210). Alternatively, expanded PA reticular networks could derive from local perivascular MSC, vascular smooth muscle cells or pericytes. Lymphoid FRC and FDC cells have been described as originating from various perivascular cells, e.g. pericytes or local adipose associated MSC (181, 285, 286).

PA fibroblast VCAM1 expression fits with the theme of inflammation recapitulating ontogeny as articulated previously (287, 288). In lymphoid organ development VCAM1 display on stromal lymphoid tissue organizer cells represents an early differentiation event and is maintained on mature FRC (210). The ability to secrete, assemble and completely wrap collagen containing conduits is a hallmark of mature lymphoid fibroblasts (177, 242, 289); however, full conduit structures have not been described in human TLS (242). Conduits are largely wrapped by VCAM1+SMA+ fibroblasts that produce IL-7 in lymphoid tissues. We describe here a novel marker for human lymphoid conduits, MFAP5, and in contrast to lymphoid FRC, the MFAP5 expression in the PA compartment in CSD and DLE was patchy and incompletely wrapped by VCAM1+SMA- fibroblasts. Additionally, VCAM1 RNA did not correlate with IL7 RNA. Therefore, the PA fibroblasts in CSD and DLE appear to be in a nascent FRC stage.

To dissect functional roles for the PA compartment, we sought a murine system that could mimic the human vascular DLE lesions. However, we could not find evidence of an analogous PA compartment in the mouse dermis. Large vessels in the mouse hypodermis have a PA fibroblast ring, but these PA fibroblasts neither expressed VCAM1 nor scaffolded perivascular leukocyte infiltrates in healing wounds and in MRL/lpr lupus-like skin lesions. When present, infiltrates were more akin to the scattered cells seen in human interface dermatitis. Our results were limited to an autoimmune model and wound healing, and it is possible models more similar to human skin can yet be found. For example,

Natsuaki and colleagues observed perivascular dendritic cell-T cell clusters in a mouse model of contact hypersensitivity that were essential for the activation of T effector cells (185); however, these clusters are rather small by comparison with the human setting. Where substantial T cell infiltrates were observed in the NOD mouse pancreatic islets and the portal triad in the *gld.ApoE* liver, there was a VCAM1+ reticular network that enmeshed the lymphocytes. It is possible that PA activation relies on different progenitors depending on the species and organ site as suggested for fibrotic processes (214, 215). In any case, these data caution that extrapolation from the study of small to midsized perivascular events in the mouse to the parallel human settings may be anatomically constrained.

Using these various skin pathologies to define PA fibroblast transition states, we see progression from relatively minor change in SSc to the major inflammatory events in CSD and DLE. These PA events may lie on a continuum and in this sense parallel observations on peripheral interferon signatures in SSc and SLE (290). In the case of DLE, the perivascular infiltrates probably reside within the spectrum of tertiary structures. The transition from the T-cell dominant vascular lesions in CSD to the TLS-like infiltrates in DLE may reflect a larger ensemble event, perhaps depending upon the known inter-connections between HEV, FRC program status and dendritic/myeloid cells (291–294). There has been much discussion of the potential pathological relevance of TLS in human disease; nonetheless, it is likely that the poorly organized perivascular infiltrate is the more common event. If these local structures are critical to the generation or retention

of activated T or B cells as has been suggested, then the ability to erode these structures may be essential to breaking a cycle of chronic inflammatory disease. Conversely, their formation in tumors may be a crucial step to facilitate immunological responses. The description of the PA reticular elements provided here begin to lay the foundation to define the mechanisms for positioning and retention of both resident myeloid and lymphocytic cells in the resting state and effector cells in disease. Furthermore, it focuses attention on a relatively poorly explored anatomical compartment and potentially points towards an underappreciated role for VCAM1 in lymphocyte retention in extra-lymphoid locales.

CHAPTER FOUR: NERVE GROWTH FACTOR RECEPTOR EXPRESSION IDENTIFIES AN EXPANDED DERMAL PERIVASCULAR STROMAL CELL IN SYSTEMIC SCLEROSIS AND WOUND HEALING

Abstract

Vascular abnormalities, including Raynaud's phenomenon and digital ulcers, are considered early events in the pathogenesis of SSc. The PA compartment, including CD90+ fibroblasts, enlarges dramatically in SSc, yet the phenotype, activation status and driving events for this expansion remain poorly characterized. Expansion of PA fibroblasts may be due to activation of MSC, and NGFR is induced during proliferation and differentiation of both MSC and epithelial stem cells. Compared to healthy skin, NGFR-expressing PA fibroblasts were more frequent and expanded in the skin of both limited and diffuse SSc patients. NGFR+CD90+ and NGFR-CD90+ adventitial fibroblasts both contributed to the PA expansion in SSc. A further subset of NGFR+ cells also displayed CD34 and may be PA progenitor cells. Similar expansion of NGFR-expressing PA fibroblasts was detected in normal and pathologic scarring, as well as some dermal tumors. The expanded NGFR+ PA fibroblast population in SSc was absent in the equivalent compartment in the highly infiltrated discoid lupus lesions. These observations demonstrated that fibroblasts in the SSc PA compartment are not only expanded, but are phenotypically altered.

Introduction

Early studies consistently described alterations to the intima and adventitia of small arteries in SSc patients (79, 81, 82, 295), which culminated in LeRoy's 1975 proposal of the vascular hypothesis (296). Under this hypothesis adventitial thickening and myeloid infiltrates cause the loss of smaller vessels in the plexus, drive intimal pathology (296) and increase the risk of critical digital ischemia (23, 297). Although the vascular hypothesis was proposed over 40 years ago, most of the research on vasculopathy in SSc has focused on changes in the intima (endothelial/pericyte layer) and media (vascular smooth muscle layer) (298–300). In contrast to the intimal/medial regions, the PA compartment has received much less attention. Removal of the fibrotic adventitia around digital arteries in the early 1990's promoted the healing of ulcers and reduced pain (48, 49), further supporting the pathological role of the PA in SSc. Activation of PA fibroblastic cells is common to other diseases featuring vascular pathology including hypertension and cardiomyopathy (79, 250, 301–303). However, fibroblast expansion is the only PA change described in SSc (23).

PA fibroblasts, originally termed "veil cells" (not to be confused with "veiled cells", which was an early term describing DCs in afferent lymphatics), surround the *tunica media* of arterioles, post-capillary venules and larger blood vessels (71, 72, 304, 305). Myriad cell types are found in the adventitia, including nerves, macrophages, mast cells and MSC (213, 306, 307). As the outer-most vascular layer, the adventitia senses and responds to changes in both the vasculature

(inside-out signaling) and surrounding tissue (outside-in signaling) (303). In several diseases such as hypertension, atherosclerosis and transplant vasculopathy, PA fibroblasts initiate or perpetuate inflammation by recruiting and retaining leukocytes in the adventitia (308–310). Activation of PA fibroblasts and MSC may be early events after vascular injury that contribute to vascular occlusion through neointimal formation and medial hyperplasia (92, 311–314). Mounting evidence indicates that the perivascular space is home to at least one, and possibly several, types of mesenchymal progenitors or MSC (213, 315, 316); these MSC can differentiate into a variety of fibroblastic cells ranging from follicular dendritic cells (FDC) to vascular smooth muscle cells (VSMC) to adipocytes (177, 181, 317–320). Substantial work has shown that perivascular MSC make significant contributions to parenchymal fibrosis across organs (321, 322). Together, these features implicate the adventitia in both vascular and parenchymal remodeling during inflammation and fibrosis.

Several perivascular and non-perivascular mesenchymal cells express the p75 low-affinity nerve growth factor receptor/CD271/p75NTR (NGFR). PA and pericyte-like cells expressing NGFR have been noted in several human organs including the skin (323–327). MSC from many of these same organs express NGFR (190, 328). Pericyte expression of NGFR increases during ischemia in the eye and heart (329, 330). NGFR marks murine perivascular ADAM12+ MSC that are responsible for skin and heart fibrosis (331). NGFR-expressing PA fibroblasts also expand in several diseases, including rheumatoid arthritis, primary and

metastatic tumors in the bone marrow, muscular dystrophy and multiple sclerosis (325, 332–334). In a study of muscular dystrophy patients, perivascular fibrosis was the only pathological measure examined that correlated with disease severity (335, 336). Human and rodent hepatic stellate cells expressing NGFR localize to, and increase in, areas of fibrosis and regeneration (337–339). A marked increase in NGFR+ cells occurs in the skin of patients with desmoplastic melanoma and scars (327, 340). Despite these connections between perivascular fibroblastic cells, NGFR and extracellular matrix deposition no studies have linked these observations with cutaneous SSc.

Previously, we showed that CD90+CD34- PA fibroblasts expand in the skin of patients with SSc and DLE (154, 186). In DLE, the fibroblasts were clearly activated, indicated by expression of VCAM1, and appeared to support lymphocytic retention. Dense PA lymphocyte infiltrates are common in the skin of DLE patients (255, 341, 342). In SSc, we could not determine whether the PA fibroblasts were different or the normal cells simply occupied a larger area. This less differentiated state is consistent with sparse myeloid infiltrates in the PA of SSc skin (16). In this study, we sought to identify an alteration in PA fibroblasts that would distinguish the enlarged PA in SSc from those in healthy and DLE skin. Our hypothesis was that PA expansion in the absence of large infiltrates indicated a PA fibroblast activation state distinct from the VCAM1+ PA stroma we previously described. Here we describe an increase in frequency and area covered by NGFR-expressing PA fibroblastic cells in SSc, wound healing and fibromas.

Results

Rare Perivascular Cells Expressing NGFR in Healthy Human Skin are More Frequent and Cover Greater Area in SSc

Expression of NGFR in healthy human skin has been previously described in nerve bundles (both Schwann cells and neurons), eccrine gland epithelium, transit amplifying epithelial stem cell populations and around blood vessels (323, 324, 327, 343). Using immunohistochemistry, we confirmed the prior observations (Figure 12). Consistent with published data (323), we observed two patterns of perivascular NGFR expression in healthy human skin. Around larger vessels, cells expressing NGFR surrounded the vessel and were outside of the vascular media, indicating an adventitial localization (Fig. 12D). Capillary endothelial cells expressing CD31 were directly wrapped by NGFR-expressing cells consistent with pericytes (Fig. 12E). In these healthy skin samples, vascular units never had both pericyte- and adventitial-like NGFR+ layers. These patterns of perivascular NGFR expression were similar to our previously published CD90 staining (154, 186, 344), although perivascular NGFR was seen much less frequently than CD90 in healthy human skin.

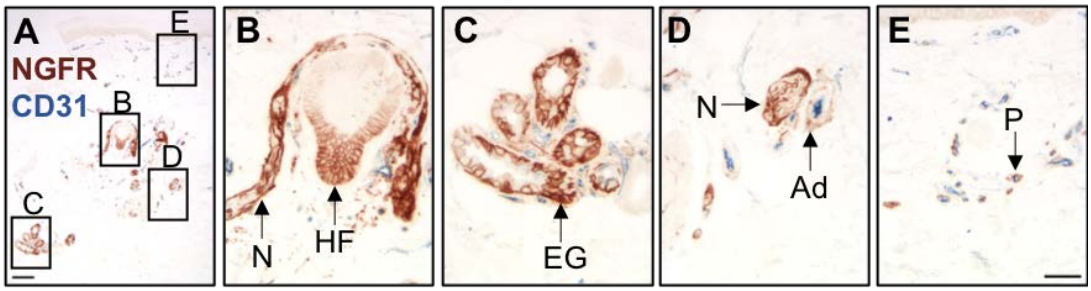

Figure 12. NGFR expression in healthy human skin.
(**A**) Immunohistochemical staining of a healthy human skin biopsy for NGFR (brown) and CD31 (blue) to define vasculature. Epidermis is at the top of the frame. Boxed and lettered areas correspond to higher magnification images shown in the following frames. (**B**) A higher magnification view of the boxed hair follicle (HF) and nerve (N). (**C**) Eccrine gland (EG) epithelium. (**D**) Rare NGFR+ perivascular adventitia (Ad) adjacent to a nerve (N). (**E**) The abluminal surface of a capillary (blue) wrapped by a pericyte (P) expressing NGFR. Scale bars are 150 μm (**A**) and 50 μm (**B**-**E**).

Previously we determined that CD90+ fibroblasts in the PA expand in the affected skin of SSc and DLE patients (154, 186). We hypothesized that this enlarged CD90+ population would also display NGFR in SSc and DLE. Immunohistochemistry demonstrated that the area per vascular unit covered by NGFR+ cells is larger in the skin of limited cutaneous SSc (lSSc, median 156 pixels, 95% CI 74-411, range 0-297994) and diffuse cutaneous SSc (dSSc, median 112 pixels, 95% CI 37-393, range 0-173462) than DLE (median 0 pixels, 95% CI 0-2, range 0-13675) and healthy (median 0 pixels, 95% CI 0-0 pixels, range 0-26936) patients as scored by two researchers (Fig. 13A-E). Although perivascular NGFR+ cells cover more area in the skin of patients from lSSc, dSSc and DLE, the median area covered by these cells was approximately two orders of magnitude larger in both SSc groups than in DLE patients (Fig.13E). Unlike CD90, perivascular NGFR expression was not observed in dermal fibroblasts in SSc and DLE patients (Fig. 13B-D)(154). The proportion of vessels surrounded by NGFR+ cells was also higher in both lSSc (median 33% of vessels, 95% CI 24-49%, range 24-54%) and dSSc (median 26% of vessels, 95% CI 16-36%, range 1-46%) compared to healthy (median 3% of vessels, 95% CI 1-6%, range 0-34%) and DLE (median 2% of vessels, 95% CI 0-4%, range 0-4%) skin (Fig. 13F). Although expansion of perivascular NGFR+ cells occurs in both SSc and DLE, the enlargement in SSc skin is dominant.

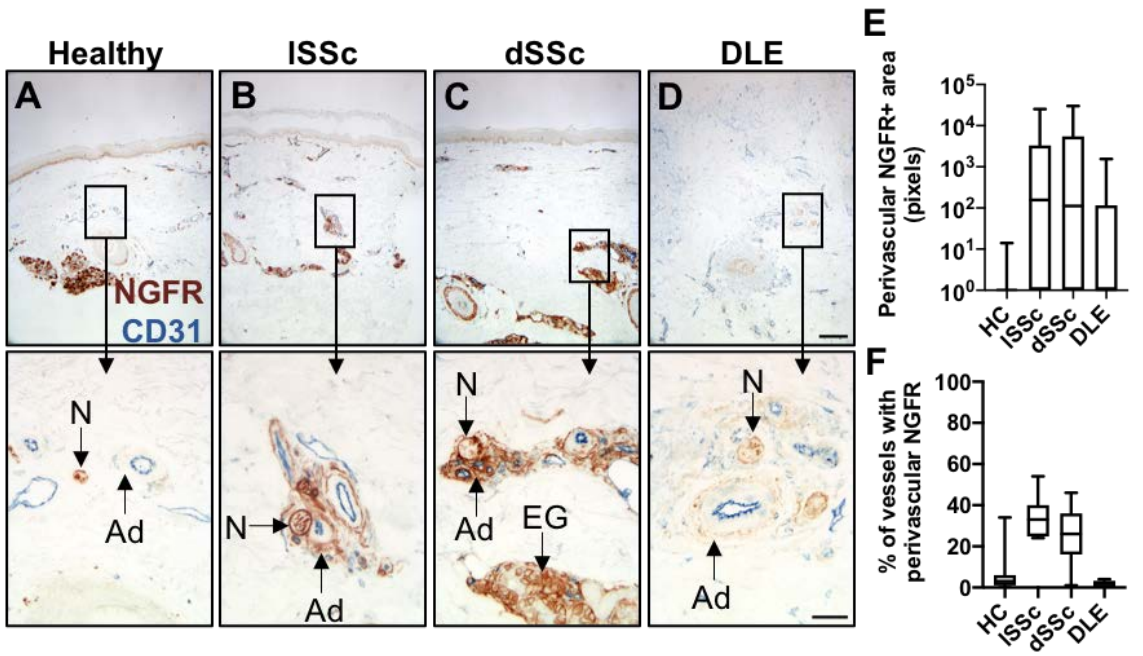

Figure 13. Perivascular cells expressing NGFR are more frequent and cover larger areas in the skin of SSc patients.
Immunohistochemical staining of human skin biopsies for NGFR (brown) and CD31 (blue) to define vasculature. Epidermis is at the top of the frame for all images. Boxed areas correspond to higher magnification images shown below. (**A**) Healthy skin, fibrotic forearm skin from an lSSc (**B**) and a dSSc (**C**) patient and a DLE (**D**) scalp lesion. In the bottom row, nerves (N), perivascular adventitia (Ad) and eccrine glands (EG) are indicated. (**E**) Morphometric analysis of the area of NGFR staining around vessels (excluding obvious nerves) in healthy skin (281 vascular units, 7 volunteers), skin from lSSc (235 vascular units, 5 patients) and dSSc patients (289 vascular units, 5 patients) and DLE skin lesions (285 vascular units, 5 patients). Area refers to the number of NGFR+ pixels per vascular unit. Thresholds for positive staining were set using internal nerve controls for each section. The median NGFR+ perivascular areas in lSSc and dSSc patients are larger than those for healthy and DLE patients (both $p<0.0001$). (**F**) Proportions of vessels with positive perivascular NGFR staining from 15 healthy, 10 lSSc, 15 dSSc and 6 DLE patients. Positivity was determined as in (**E**). Both lSSc and dSSc skin have higher proportions of NGFR+ vessels than healthy and DLE patients (HC vs lSSc, $p=0.0011$; HC vs dSSc, $p=0.0251$; DLE vs lSSc, $p=0.0008$; DLE vs dSSc, $p=0.011$). (**A-D**) Top scale bar is 200 μm, bottom scale bar is 50 μm. (**E**-**F**) Kruskal-Wallis followed by post-hoc pairwise Dunn's multiple comparison tests.

Human Dermal PA Cells Expressing NGFR are Mesenchymal

Several mesenchymal populations have been found in vascular units in human skin: pericytes, vascular smooth muscle cells, adventitial fibroblasts and CD34+ adventitial MSC (186, 345, 346). Around smaller vessels, such as arterioles and venules, it can be difficult to distinguish pericytes from adventitial cells (347). Cells expressing PDGFRβ, CD90 and NGFR around larger vessels lacked SMA and melanoma cell adhesion molecule (MCAM), and were outside of the vascular intima and media consistent with PA fibroblasts in healthy, SSc and DLE skin (Fig. 14A-E). Both NGFR+CD90+ and NGFR-CD90+ cells contributed to the PA expansion around dermal vessels in SSc (Fig. 14B). Nerve bundles abut the PA and individual axons terminate there (323, 324), so distinguishing between NGFR+ mesenchymal, neuronal and Schwann cells was critical. Schwann cells were clearly distinct from PA mesenchymal cells as they lacked PDGFRβ and CD90 (Fig. 14A-B). Peripheral nerves were distinguished from PA mesenchymal cells and Schwann cells by their expression of ubiquitin carboxyl-terminal esterase L1 (UCHL1/PGP9.5) and the absence of PDGFRβ (Fig. 14E, A). Some neurons expressed CD90 (Fig. 14B), but there was considerable heterogeneity. Together, these data support our hypothesis of expanded NGFR+ PA fibroblasts in SSc skin.

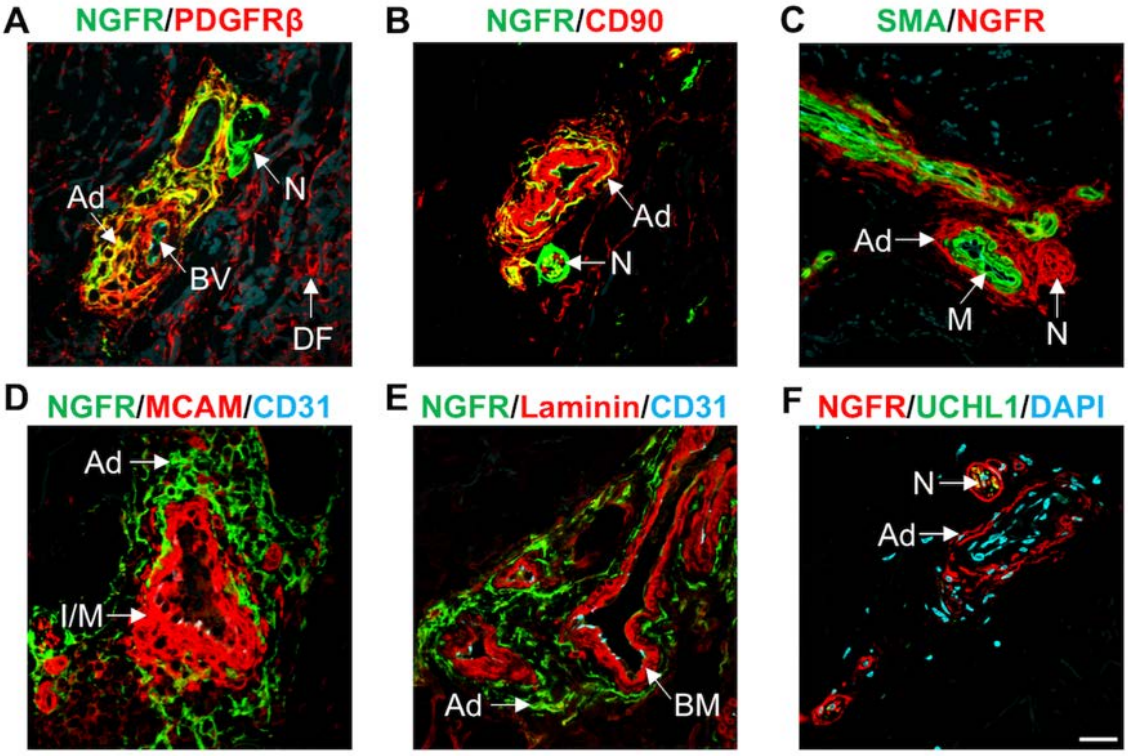

Figure 14. Perivascular adventitial NGFR+ cells are mesenchymal.
Representative images of immunofluorescent staining in skin biopsies from SSc patients. (**A**) NGFR (green) and mesenchymal marker PDGFRβ (red); (**B**) NGFR (green) and PA fibroblast marker CD90 (red); (**C**) NGFR (red) and SMA (green) to highlight the vascular media; (**D**) NGFR (green) along with intimal marker MCAM (red) and CD31 (cyan) to mark vasculature; (**E**) NGFR (green), basement membrane protein laminin (red) and CD31 (cyan); (**F**) NGFR (red), neuronal marker UCHL1 (green) and DAPI (cyan). Ad, adventitia; BV, blood vessel; N, nerve bundle; DF, dermal fibroblast; M, perivascular media; I/M, both intima and media; BM, basement membrane. All images captured with a 60x objective, scale bar is 25 μm.

Relationships Between NGFR+ PA Cells and Adventitial MSC

NGFR has been widely used to purify MSC from several human tissues including the skin (189, 190). CD34 marks a PA MSC population in several human organs, and similar cells have been observed in human skin (154, 162, 345). Thus, we asked whether PA cells expressing NGFR also expressed CD34. Overlap of CD34 and NGFR in the PA of larger vessels was not observed in healthy skin (4/4 biopsies, Fig. 15A), and CD34+ MSC were more common in the PA than cells expressing NGFR. Dermal fibroblasts also expressed CD34 in healthy skin, consistent with previous publications (154, 162, 348). In SSc (4/4 biopsies), rare co-localization of CD34 and NGFR could be seen on adventitial cells around larger vessels (Fig. 15A). However, it was more common to see outer CD34+ NGFR- and inner CD34- NGFR+ adventitial layers (Fig. 15A). Both CD34+ PA and NGFR+ dermal MSC expressed CD73 after isolation (190, 345), and this marker is part of the International Society for Cellular Therapy (ISCT) minimal criteria for defining MSC (349). However, isolation and culture change mesenchymal cell phenotypes, and direct demonstration of *in situ* co-localization of CD73 with CD34+ or NGFR+ cells is lacking. Neither pericyte-like nor PA cells expressed both CD73 and NGFR in healthy or SSc skin (Fig. 15B). Instead, adventitial CD73+ cells were consistently farther from the intima than PA cells expressing NGFR. Dermal fibroblasts in the skin of healthy patients also expressed CD73, which served as an internal positive control (Fig. 15B).

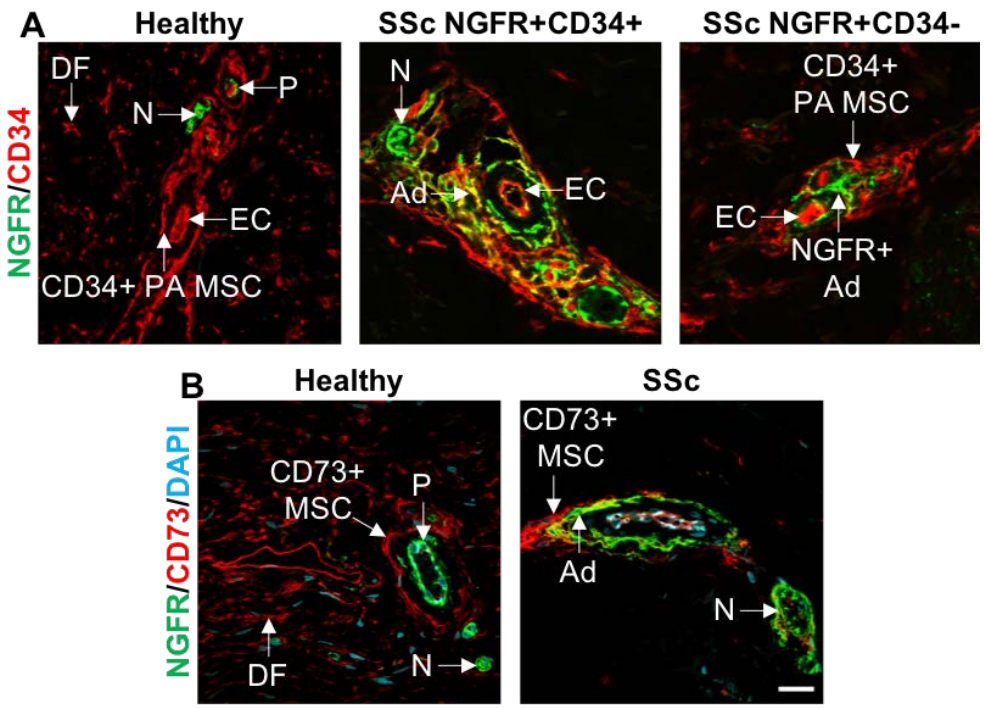

Figure 15. Relationship between NGFR+ PA cells and PA MSC.
Representative immunofluorescent images of healthy and SSc skin stained for NGFR and the MSC markers CD34 (**A**) and CD73 (**B**). (**A**) No PA cells expressing both NGFR and CD34 were observed in healthy skin (left). In fibrotic SSc skin, co-localization (yellow) of NGFR and CD34 was visible in the PA of <10% of vessels (middle). More than 90% of vessels in SSc skin had NGFR+ layers adjacent to CD34+ cells, but closer to the vessel lumen (right). (**B**) No co-localization of NGFR and CD73 was observed in healthy skin. In two fibrotic SSc biopsies PA NGFR+ layers were adjacent to CD73+ MSC layers, positioned closer to the intima. (**A-B**) All images were captured with a 60x objective and scale bars are 25 μm.

Perivascular NGFR-Expressing Cells are More Frequent and Occupy Larger Areas in Human Reparative and Pathologic Dermal Scarring than Healthy Skin

One hypothesis is that SSc represents a dysregulation of the normal tissue repair process. Human dermal scars display more frequent NGFR expression (327) and expansion of CD90+ PA fibroblasts (344) relative to healthy skin. However, it is unclear whether the expanded PA fibroblasts in human scars express NGFR. IHC demonstrated that NGFR+ perivascular populations covered more area per vessel in reparative (RS, 8/8), hypertrophic (HS, 8/8) and keloid (KS, 8/8) scars compared to healthy skin (Fig. 16A-F). Median area per vessel occupied by cells expressing NGFR in RS (2391 pixels, 95% CI 1283-4526, range 0-555713), HS (3204 pixels, 95% CI 2274-4427, range 0-744177) and KS (3130 pixels, 95% CI 3130-6179, range 0-953749) were larger than in healthy skin (0 pixels, 95% CI 0-1, range 0-13020) (Fig. 16E). In fact, the median perivascular area covered by NGFR-expressing cells in both reparative and pathologic scars was approximately an order of magnitude larger than in SSc patients (2391 pixels for RS, 3204 for HS and 3130 for KS versus 156 for lSSc and 112 for dSSc). Vascular units containing NGFR+ cells were also more common in RS (median 44% of vessels, 95% CI 29-60%, range 29-60%), HS (median 39% of vessels, 95% CI 34-63%, range 34-63%) and KS (median 39% of vessels, 95% CI 25-81%, range 25-81%) than healthy (median 9% of vessels, 95% CI 2-18%, range 2-18%) skin (Fig. 16F). These data are consistent with PA fibroblasts responding similarly in SSc and during normal and pathologic dermal wound repair.

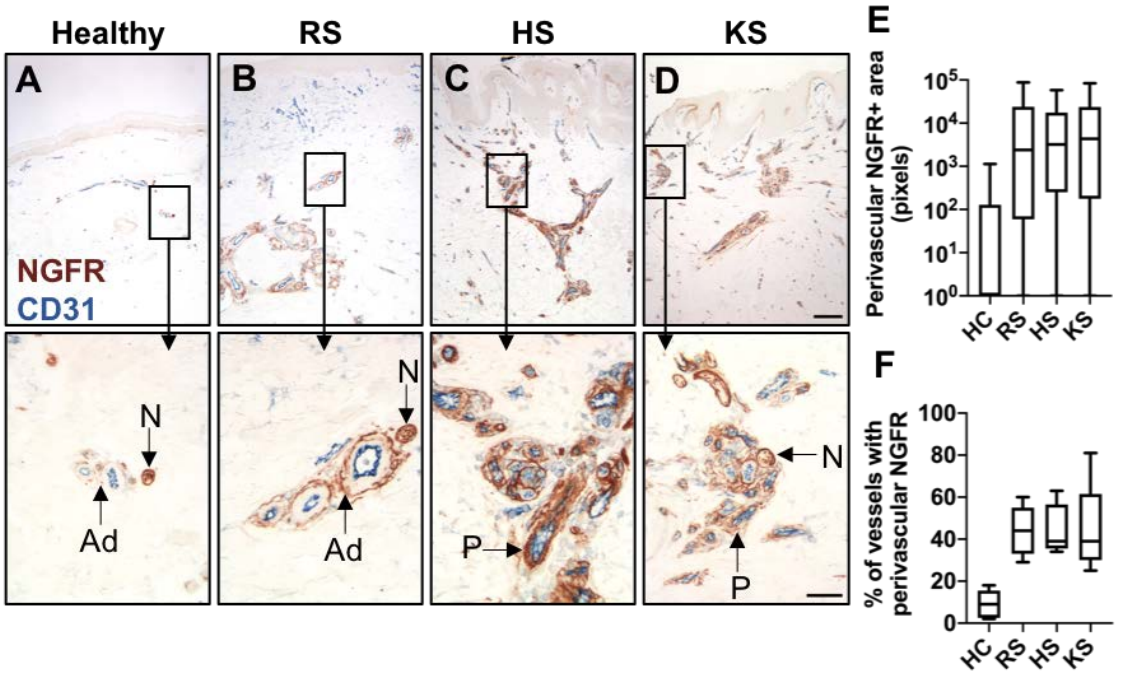

Figure 16. Expansion of perivascular cells expressing NGFR in reparative and pathologic scars.

Immunohistochemical staining of human skin biopsies for NGFR (brown) and CD31 (blue) to define vasculature. Epidermis is at the top of the frame for all images. Boxed areas correspond to higher magnification images shown below. (**A**) Healthy skin, a reparative scar (RS) (**B**), a hypertrophic scar (HS) (**C**) and a keloid scar (KS) (**D**). In the bottom row, nerves (N), perivascular adventitia (Ad) and pericytes (P) are indicated. (**E**) Morphometric analysis of the area of NGFR staining around vessels (excluding obvious nerves) in healthy skin (247 vascular units, 10 volunteers), RS (286 vascular units, 8 patients), HS (515 vascular units, 8 patients) and KS (495 vascular units, 8 patients). Area refers to the number of NGFR+ pixels per vascular unit. Thresholds for positive staining were set using internal nerve controls for each section. The median NGFR+ perivascular areas in RS, HS and KS were larger than those for healthy volunteers (all $p<0.0001$). (**F**) Proportions of vessels with positive perivascular NGFR staining from 5 healthy skin biopsies, 5 RS, 5 HS and 5 KS. Positivity was determined as in (**E**). RS, HS and KS all have higher proportions of NGFR+ vessels than healthy skin (HC vs RS, $p=0.0162$; HC vs HS, $p=0.0176$; HC vs KS, $p=0.0385$). (**E**-**F**) Kruskal-Wallis followed by post-hoc pairwise Dunn's multiple comparison tests. Top scale bar is 200 μm, bottom scale bar is 50 μm.

NGFR Expression in the Hypodermis During Early Wound Healing in Mice

Given the differences between murine and human skin (350), we next examined whether mice would recapitulate the expansion of perivascular NGFR+ populations observed in humans. Incisional wounds were made in the dorsal skin of female C57BL/6 mice (see methods) and allowed to heal for one, two or four days. No perivascular NGFR staining was observed in the healthy skin of unwounded mice (Fig. 17A-C). Keratinocytes expressed NGFR in the healthy skin of unwounded mice (Fig. 17A), but disappeared from the wound margins (Fig. 17B-E). Epithelial cells in hair follicles displayed heterogeneous NGFR expression at all time points in both healthy and wounded skin (Fig. 17B-D).

Perivascular NGFR expression was only detected four dpw, and was generally restricted to the hypodermal fat adjacent to the wound (Fig. 17B-E). In human scars and SSc skin, NGFR-expressing mesenchymal cells were not detected anywhere other than the perivascular space (Figs. 13 and 16). This was different in murine wounds where, at four dpw, NGFR-expressing fibroblastic cells were spread throughout the hypodermis (Fig. 17D-E). Images from serial sections stained with Masson’s trichrome are shown below each immunohistochemistry image to indicate the wound (Fig. 17F-J). NGFR expression by fibroblastic cells is not restricted to the PA during murine wound healing.

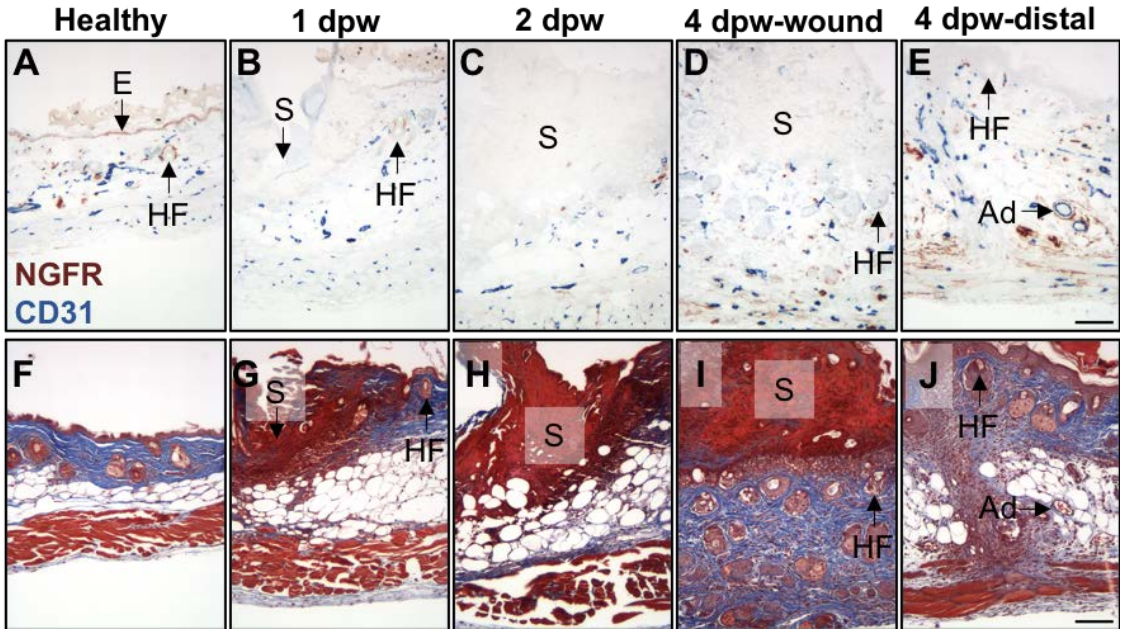

Figure 17. NGFR+ cells appear in the murine hypodermis 4 days post-incisional wound in skin adjacent to the wound.
Serial sections from healthy skin (**A**, **F**), and incisional wounds at 1 (**B**, **G**), 2 (**C**, **H**) and 4 (**D**, **I**) days-post wounding (dpw), as well as skin distal to the wound at 4 dpw (**E**, **J**) stained for NGFR (brown) and CD31 (blue) (**A**-**E**) or Masson's trichrome (blue, collagen; red, muscle and keratin; pink, fibrin; brown/black, nuclei) (**F**-**J**). Epidermis is at the top of the pictures. Images were representative of two C57BL/6 mice per group. E, epidermis; HF, hair follicle; S, scar; Ad, perivascular adventitia. Scale bars are 100 μm.

Perivascular NGFR Expression is Common in Four Types of Dermal Tumors

Fibromas and sarcomas represent other conditions where mesenchymal proliferation and extracellular matrix deposition occur, and vascular activation is common within and around tumors. Previous publications have shown that cutaneous neurofibromas frequently express NGFR (323, 351), and we observed diffuse NGFR staining in the dermis of all (2/2) cutaneous neurofibroma specimens studied (Fig. 18). Similarly, the dermatofibrosarcoma protuberans specimens (2/2) we examined had diffuse NGFR expression (Fig. 18). Because of the diffuse NGFR expression in neurofibromas and dermatofibrosarcoma protuberans it was difficult and beyond the scope of our current study to distinguish between perivascular and tumor-associated NGFR. Neither dermatofibromas (2/2) nor atypical fibroxanthomas (2/2) had wide-spread NGFR expression in the dermis; rather, both of these entities demonstrated perivascular NGFR expression similar to our observations in SSc and scars (Fig. 18). These data are consistent with the association of perivascular NGFR expression with dermal conditions marked by fibroproliferation and extracellular matrix deposition.

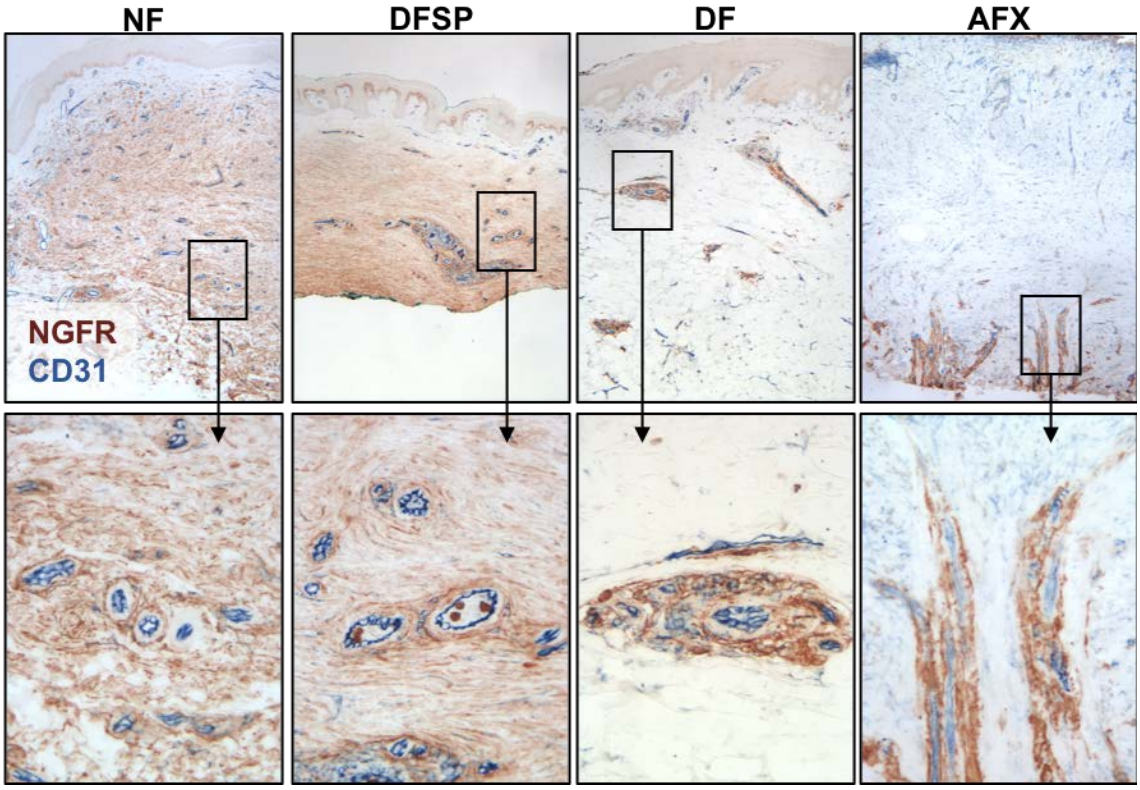

Figure 18. Patterns of NGFR expression in four dermal tumors.
Immunohistochemical staining of human skin biopsies for NGFR (brown) and CD31 (blue) to define vasculature. Epidermis is at the top of the frame for all images. Boxed areas correspond to higher magnification images shown below. NF, neurofibroma; DFSP, dermatofibrosarcoma protuberans; DF, dermatofibroma; AFX, atypical fibroxanthoma. Top scale bar is 200 μm, bottom scale bar is 50 μm.

Expanded PA Fibroblasts in SSc and DLE Distinguished by NGFR and VCAM1 Expression

Our previous work demonstrated that VCAM1-expressing PA fibroblasts are common in DLE skin lesions and rare in the skin of healthy and SSc patients (186). We hypothesized that expression of NGFR or VCAM1 is exclusive on PA cells in SSc and DLE. PA cells expressing both VCAM1 and NGFR were only seen around one vessel of over 80 examined in two SSc and two DLE biopsies. In DLE biopsy specimens (2/2), PA fibroblasts were VCAM1+NGFR-, while PA fibroblasts in SSc skin were VCAM1-NGFR+ (Fig. 19A). Plotting the perivascular areas of VCAM1 and NGFR expression demonstrated larger perivascular areas of NGFR+ than VCAM1+ in SSc and the converse in DLE (Fig. 19B-C). As previously reported (186), NGFR-VCAM1+ PA fibroblasts correlated with perivascular infiltration. Vessels surrounded by NGFR+VCAM1- PA fibroblasts lacked perivascular infiltrates (Fig. 19A). These data demonstrate nearly exclusive expression of NGFR or VCAM1 by PA fibroblasts in SSc or DLE, respectively, and suggest activation states associated with distinct vascular pathologies in these two diseases.

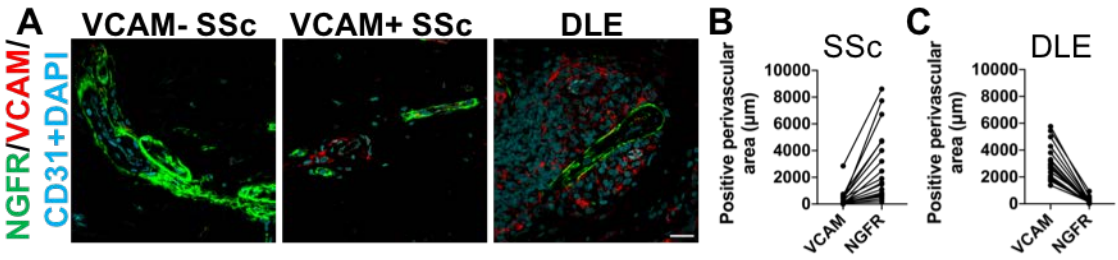

Figure 19. PA fibroblasts expressing NGFR in SSc and VCAM1 in DLE are in distinct states.

Immunofluorescent staining of SSc and DLE skin biopsies for NGFR (green), VCAM1 (red) and CD31 with DAPI (both cyan). (**A**) Representative images of the more common VCAM1-NGFR+ (left) and rarer VCAM1+NGFR- PA fibroblasts in SSc skin, along with a perivascular infiltrate from DLE skin showing VCAM1+NGFR- PA fibroblasts and an adjacent VCAM1-NGFR+ nerve bundle (right). (**B-C**) Measurements of the perivascular areas covered by NGFR+ and VCAM1+ cells in SSc (**B**) and DLE (**C**). Each pair of dots connected by a line represents one vascular unit (20 SSc and 18 DLE vessels from two biopsies of each disease). In SSc (**B**), the perivascular area covered by NGFR is greater than that covered by VCAM1. The opposite is true in DLE (**C**), where VCAM1 covers more perivascular area than NGFR. Wilcox matched-pairs signed rank test, $p<0.0001$ for **B** and **C**. (**A**) Scale bar is 25 μm.

Polar Solvents Induce NGFR, While the Combination of TNF and IFNγ Stimulates VCAM1 Expression by Cultured Primary Human Dermal Fibroblasts

The nearly exclusive expression of NGFR by PA fibroblasts in SSc and healing wounds, and VCAM1 by PA fibroblasts in DLE suggested that different stimuli induce the expression of these two proteins by fibroblasts. Stimuli capable of inducing NGFR expression by fibroblasts remain partially uncharacterized, but include nerve growth factor and TGFβ1 (352–354). Given the proximity of NGFR+ PA fibroblasts to perivascular MSC, we next tested the hypothesis that differentiation-inducing stimuli DMSO, DMF and RA (355, 356) would induce NGFR on primary cultured human dermal fibroblasts. Both DMSO and DMF stimulated NGFR expression (Fig. 20; 4% DMSO vs untreated, $p<0.0001$; 4% DMSO vs TNF+IFNγ, $p=0.0004$; 2% DMF vs untreated and 2% DMF vs TNF+IFNγ, $p<0.0001$). 1 μM RA, the concentration commonly used in leukemia cell differentiation *in vitro*, failed to alter NGFR levels (Fig. 20B; 1 μM RA vs untreated, $p>0.9999$; 4% DMSO vs 1μM RA, $p=0.0014$; 2% DMF vs 1 μM RA, $p<0.0001$).

Prior publications have demonstrated that the combination of TNFα and IFNγ induces VCAM1 on human dermal fibroblasts (357), which we reproduced (Fig. 20A, C; TNF+IFNγ vs untreated, $p<0.0001$). As we hypothesized, this combination of cytokines failed to induce NGFR on cultured fibroblasts (Fig. 20A-B; 4% DMSO vs untreated, $p=0.3567$; 2% DMF vs untreated, $p>0.9999$; TNF+IFNγ vs 4% DMSO, $p=0.0242$; TNF+IFNγ vs 2% DMF, $p=0.0022$). The different stimuli did not antagonize each other, however, suggesting that the NGFR+ and VCAM1+

states are different but not mutually exclusive (Fig. 20; for NGFR, 4% DMSO vs 4% DMSO+TNF+IFNγ, $p>0.9999$; for VCAM1, TNF+IFNγ vs 4% DMSO+TNF+IFNγ, $p>0.9999$).

In situ, dermal PA fibroblasts express CD90 while MSC are CD34+; either or both of these perivascular cells may contribute to the changes in NGFR expression seen in SSc (115–117, 186). Levels of CD90 were also measured to evaluate the relationship between CD90 and NGFR display on the surface of fibroblasts. Cultures of primary human dermal fibroblasts become uniformly CD90+ upon passaging *in vitro* (Fig. 20D-E) (117, 358, 359). Neither 4% DMSO ($p>0.9999$ versus untreated) nor 2% DMF ($p=1683$ versus untreated), the compounds that induced NGFR, reduced the high baseline expression of CD90 (Fig. 20D-E).

ICAM1 is another protein that is produced by fibroblasts in response to inflammatory stimuli and, in addition to VCAM1, marks differentiating FRC during embryonic development (176, 177, 360–363). The combination of TNF and IFNγ increased levels of ICAM1 on the surface of cultured fibroblasts ($p<0.0001$, Fig. 20D, F), as was previously described (357). Elevation of ICAM1 expression by TNF and IFNγ was not antagonized by the addition of either 4 ($p>0.9999$) or 2% DMSO ($p>0.9999$, Fig. 20F). Nor did 4% DMSO ($p=0.1930$) or 2% DMF ($p=0.5796$) increase ICAM1 expression by cultured fibroblasts (Fig. 20F). Together, these data support our assessment that NGFR and VCAM1 mark distinctly activated PA

fibroblasts in SSc and DLE while also indicating that these activation states may not be mutually exclusive.

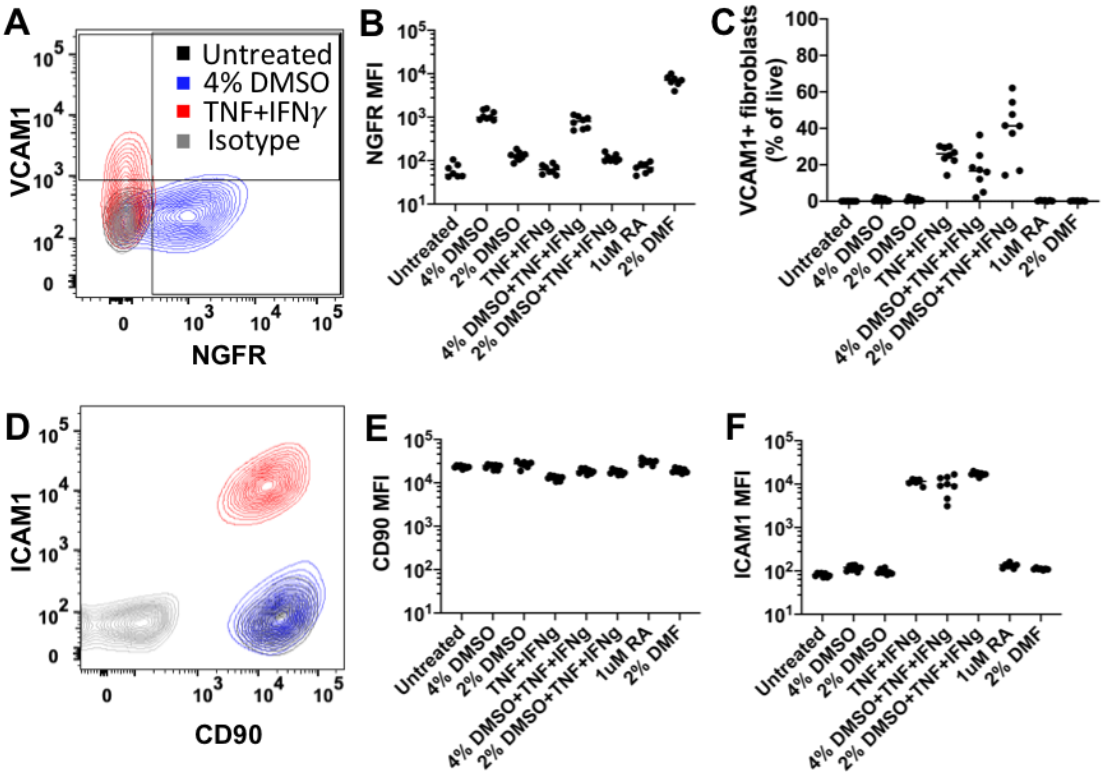

Figure 20. Polar solvents induce NGFR expression by primary human dermal fibroblasts, whereas the combination of TNF and IFNγ stimulates VCAM1 and ICAM1 production without altering CD90.

Primary human fibroblasts isolated from neonatal foreskin were treated with differentiation-inducing stimuli (dimethyl sulfoxide, dimethylformamide and retinoic acid) or a combination of TNF and IFNγ. (**A**) Representative contour plot of untreated fibroblasts (black) or fibroblasts treated with 4% DMSO (blue), TNF and IFNγ (red) or a mix of cells treated as above and stained with isotype control antibodies. Gates were set based on fluorescence-minus-one controls. (**B**) Median fluorescence intensity (MFI) of NGFR expression on primary human fibroblasts after three days of treatment with the stimuli listed on the X-axis. (**C**) The percent of primary human fibroblasts positive for VCAM1 as dictated by a fluorescence-minus-one control (see gates in (**A**)). (**D**) Contour plot of ICAM1 and CD90 expression in the same cells as in (**A**). (**E**) CD90 and (**F**) ICAM1 MFI. Data in (**A**, **D**) show population-level expression from one biological replicate in (**B**-**C, E**-**F**). (**B**-**C, E**-**F**) Each dot is a biological replicate, with data from three experiments amalgamated in these graphs.

Discussion

Augmenting our prior observations (154, 186), these data indicate that PA enlargement in SSc includes activation or differentiation marked by NGFR expression. Expanded, NGFR+ PA cells in SSc expressed the mesenchymal markers PDGFRβ and CD90, but lacked SMA and MCAM. Although neurons also display CD90, NGFR+ PA cells lacked the peripheral nerve marker UCHL1 (364). One interpretation of these data is that CD90+ PA fibroblasts turn on NGFR in SSc; this was demonstrated to be feasible *in vitro* as untreated primary human dermal fibroblasts express CD90, and DMSO and DMF induced NGFR without altering CD90 expression. However, without *in vivo* lineage tracing data we cannot formally exclude the possibility of phenotypic conversion by other perivascular residents such as Schwann cells or nerves. For decades it was assumed that activated fibroblasts drove PA enlargement in SSc skin (81, 82, 295, 296), but our study is the first to provide direct support for this hypothesis.

An alternative hypothesis is that NGFR expression is enhanced in proliferating or differentiating MSC. NGFR identifies MSC in several human settings (189–191). The presence of rare, perivascular NGFR+ cells in healthy skin, and the increased frequency and area covered by NGFR+ PA cells in SSc is consistent with a proliferating MSC (323, 326). Vascular units are a potential source of MSC (114, 216, 321), and PA MSC have been identified in both humans and mice by a variety of proteins including CD34 and CD73 (115, 117, 180). Our results suggest a potential PA MSC differentiation sequence in SSc based on

phenotype and relative location. CD34+CD73+NGFR- outer PA MSC-like cells may give rise to CD34+NGFR+ or NGFR+CD90+ transit amplifying MSC through asymmetric division (Fig. 21). These cells may then differentiate into NGFR-CD90+ PA fibroblasts (Fig. 21). This proposed progression is similar to other progenitor differentiation programs. Quiescent basal epithelial stem cells lack expression of NGFR, but turn it on while in the transit amplifying state. NGFR on transit amplifying cells inhibits differentiation in favor of proliferation, and it is lost during differentiation in the suprabasal transition (343, 365). Similar results have been observed for myoblasts, which express NGFR prior to differentiation and lose it upon joining a myotube (366–369), and MSC (370). The induction of NGFR on fibroblasts by differentiation-inducing polar compounds (355, 356, 371) is consistent with PA MSC activation. PA MSC receiving chronic repair signals or stuck in an intermediate differentiation state in SSc, could be an alternative explanation for the expanded NGFR+ PA population.

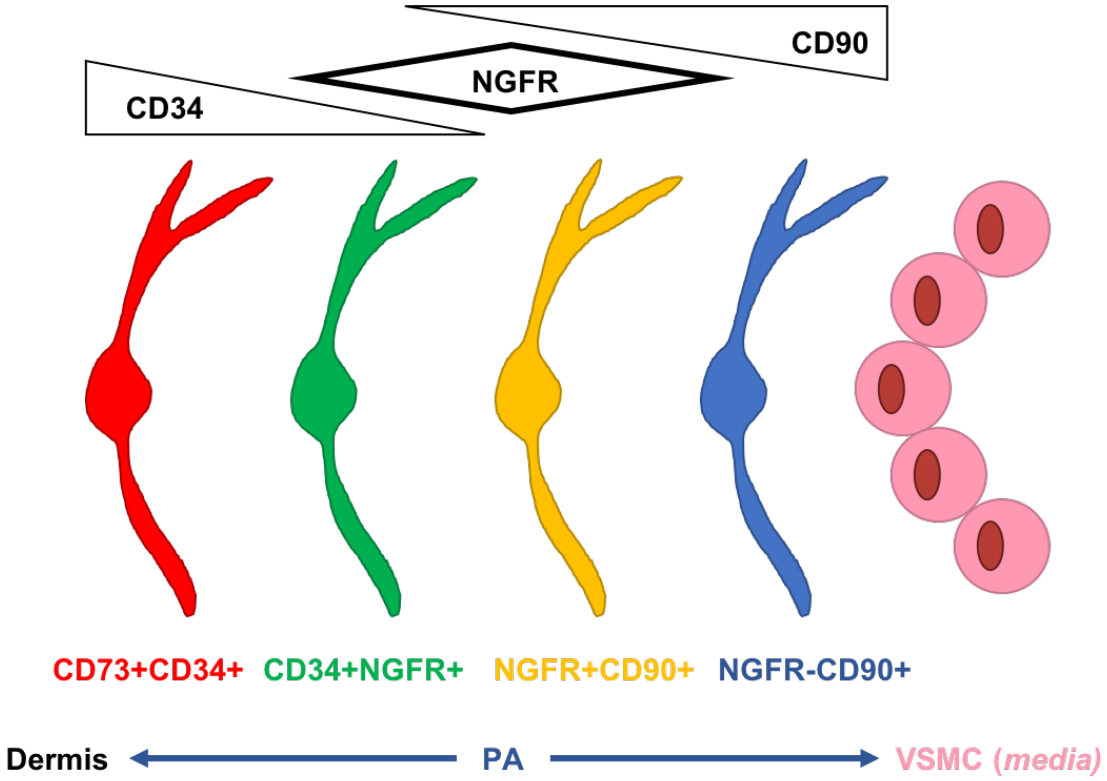

Figure 21. Model of PA mesenchymal cell phenotypes and layers observed in affected SSc skin.
The diagram shows an expanded view of part of the PA with the surrounding dermis (left) and the *tunica media* comprised of VSMC (right). Red cells at the outer rim of the PA represent the previously described CD73+CD34+ MSC. To the right are CD73-CD34+NGFR+ (green), CD34-NGFR+CD90+ (yellow) and NGFR-CD90+ (blue) PA mesenchymal cells. For clarity, the most commonly detected phenotypes are shown, but gradients in the expression of CD34, NGFR and CD90 were also observed as denoted by the triangles and diamond above the PA cells. The highest expression is indicated by the widest point of the shape.

Parallel growth of PA NGFR in reparative and pathologic scars, and in dermal fibromas, suggest that this vascular change is fundamental to settings of fibroblast proliferation and extracellular matrix deposition. This observation places SSc, scars and fibromas alongside multiple sclerosis, muscular dystrophy and arthritis (332, 334, 372). Proliferating, NGFR+ PA mesenchymal cells may be associated with “central vein sign” fibrosis in multiple sclerosis patients (372–374). NGFR-expressing cells in arthritic joints were specialized for attracting myeloid cells, and may be similar to the recently identified synovial perivascular CD90+ stromal cells ((123, 334), K. Slowikowski and K. Wei personal communications). If dermal NGFR+CD90+ PA fibroblasts resemble those in arthritis, they may attract the monocyte-rich perivascular infiltrates in SSc skin (16). Macrophage activation associates with endomysial fibrosis in human muscular dystrophy patients (375). In the murine *mdx* model of muscular dystrophy, infiltrating CCR2+ macrophages produce TGFβ and injured myofibers secrete PDGF-AA to induce perivascular fibroblast proliferation and fibrosis (39, 376). Serum CCL2 levels are increased in SSc patients, and fibroblasts are a substantial source (18, 377–379) suggesting a similar macrophage- and fibroblast-driven repair response may occur in the SSc PA.

Discrete expression of NGFR on expanded PA fibroblasts in SSc, and of VCAM1 in DLE is suggestive of cells with distinct functions. This interpretation is reinforced by the association of VCAM1+ PA fibroblasts with large perivascular lymphocyte infiltrates, and the scarcity of leukocytes in NGFR-expressing PA. We

previously proposed that PA fibroblasts in healthy, SSc, dermatitis and DLE skin existed on a continuum of activation or differentiation states (186). Our most recent data suggest that rather than existing on a continuum, the NGFR state in SSc may represent a differentiation pathway separate from that marked by VCAM1. The VCAM1+ state likely lies on the “inflammation recapitulates ontogeny” spectrum with mature TLS at the far end (141, 183, 380, 381). Placing the NGFR+ PA state into a similar differentiation scheme will require further study. Delineating the differences between these states will be aided by the growth of single-cell RNA sequencing data (145, 382–387), and our phenotypic definitions could serve as a touchstone for these analyses. Building on our previous study, these data demonstrate that human dermal PA fibroblasts can adopt separate activation states that correlate with discrete vascular alterations in SSc and DLE.

PA fibroblast-specific functions of NGFR await investigation. Other groups have, however, demonstrated roles for NGFR in dermal fibroblasts and other mesenchymal cells. Nerve growth factor (NGF), an NGFR ligand, is expressed in human scars and produced by cultured dermal fibroblasts. Fibroblasts express the high-affinity neurotrophic receptor tyrosine kinase 1 (NTRK1/TrkA), which responded to nerve growth factor (NGF) by inducing TGFβ secretion, migration and collagen gel contraction (352–354). Hepatic stellate cells make similar use of the neurotrophin system, where NGFR is important for myofibroblast activation, hepatocyte growth factor production and liver regeneration (388, 389). Whole-mouse NGFR knockout results in embryonically lethal vasculopathy and

neuropathy (390), but the critical NGFR-expressing vascular compartment and ligands await identification. Binding of pro-NGF to NGFR on pericytes in murine models of diabetic retinopathy and during recovery from myocardial infarction causes microvascular dysfunction and ischemia (329, 330, 391), while mature NGF has the opposite effect (392). NGFR is a promiscuous receptor with many potential signaling outcomes that are determined by the receptors with which it pairs and the ligands to which it binds (393). If NGFR expression by PA fibroblasts contributes to either vascular constriction or dermal fibrosis in SSc, parsing ways to manipulate this complex system may yield therapeutic benefits.

CHAPTER FIVE: CONCLUDING REMARKS

Summary of Results and Integration with the Literature

These studies demonstrated that dermal PA fibroblasts expanded in both DLE and SSc, and adopted distinct activation or differentiation states associated with discrete vascular alterations (Fig. 22). Expression of VCAM1 was most common in DLE and dermatitis, and correlated with dense perivascular T cell infiltrates. Thickening of the PA in the absence of large infiltrates was the norm in SSc, where fibroblasts expressed NGFR. In healthy human skin, PA fibroblasts were phenotypically distinct from dermal fibroblasts, suggesting cells specialized to perform separate tasks. Modifying fibroblasts by blocking activating signals or selectively depleting altered cells is being tested as a therapeutic avenue for both inflammatory and fibrotic diseases (8, 141, 143, 145, 148, 394), and these studies support the involvement of PA fibroblasts in SSc and DLE pathology.

Neither VCAM1+ PA fibroblasts nor large perivascular T cell cuffs were observed in skin lesions from MRL/lpr mice, which are considered a model for cutaneous lupus. In other murine models of inflammatory diseases, non-obese diabetic (NOD) and *gld.ApoE*, fibroblasts expressing VCAM1 enmeshed dense T cell infiltrates around large vessels in the pancreas and liver. PA fibroblasts expressing NGFR were observed around large vessels in the murine hypodermis during wound healing, but, consistent with a previous report (163), mesenchymal cells expressing NGFR extended through the skin unlike humans where it was restricted to vascular units. Collectively, these data demonstrate that PA fibroblast

activation is a common feature of human skin diseases, and suggest that the activation state may influence the observed vascular pathology.

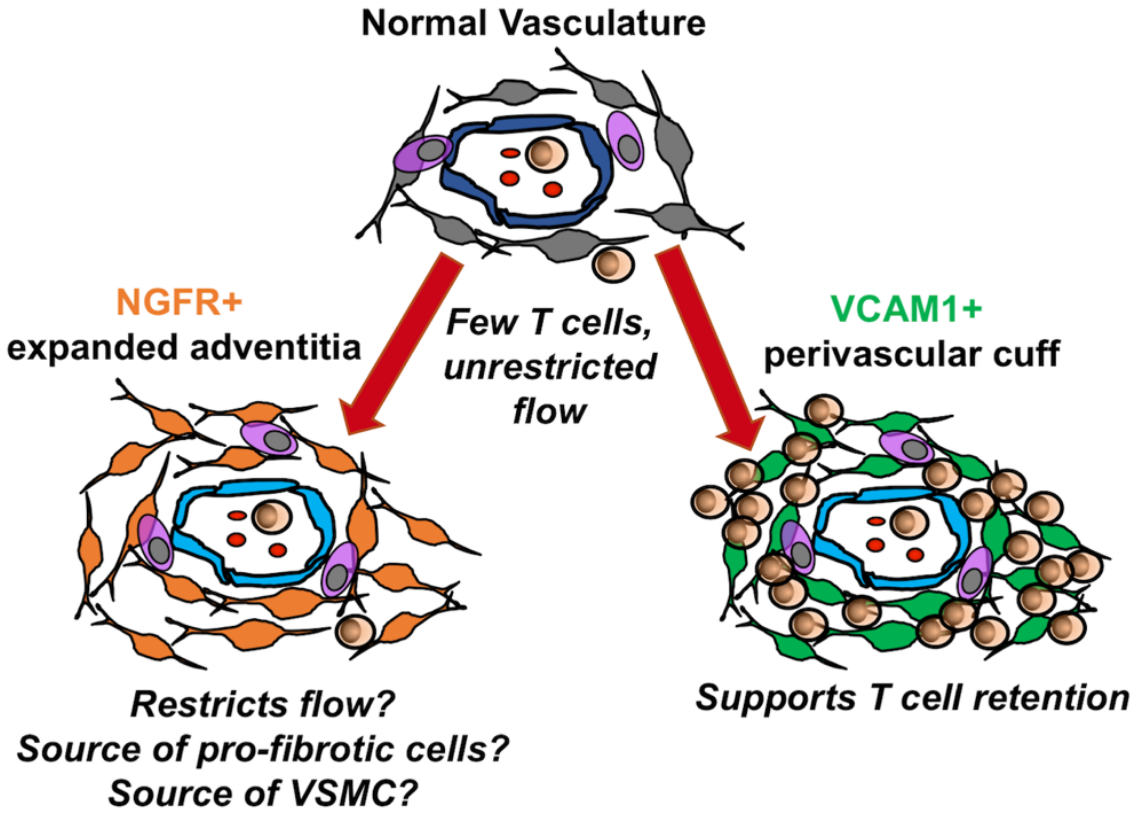

Figure 22. Proposed model of PA fibroblast activation states in DLE and SSc.

PA fibroblasts in healthy skin are CD90+VCAM1-NGFR- and form a thin layer—one to a few cells thick—within the outer layer of vascular units. In SSc, healing wounds and dermal fibromas, PA fibroblasts expand and express NGFR (left arrow). Although the PA grows in these settings, the activation of PA fibroblasts is not accompanied by dense lymphocyte infiltrates. The physiologically-relevant activating stimuli that trigger(s) NGFR expression is currently unknown, but the induction of NGFR in cultured fibroblasts by differentiation-inducing polar compounds suggests activation and elaboration of perivascular MSC. Contrast this with the PA fibroblast expansion and activation in DLE and dermatitis (right arrow). Conversion to a VCAM1+ state in these inflammatory diseases may promote the perivascular accumulation of dense T cell infiltrates. Initiating stimuli for this conversion have not been definitively proven, but *in vitro* stimuli that induce VCAM1 on primary human fibroblasts include combinations of TNF with IFNγ, IL-4 or IL-13.

Mesenchymal Cell Heterogeneity and PA Fibroblast Functions in Healthy Skin

These studies distinguish dermal PA fibroblasts from other fibroblast populations in the human skin. This distinction adds to the field of dermal fibroblast heterogeneity, which has existed for at least 40 years. Dermal fibroblast lines isolated from a single skin biopsy displayed variable rates of homeostatic and prostaglandin E_2-stimulated cell division, discrete rates and methods of metabolizing testosterone, as well as discrepancies between removal of the N-terminal propeptide that were stable across several passages *in vitro* (395–398). Contractile “myofibroblasts” that appeared during wound healing and disappeared from the mature scar were an early instance of a dermal fibroblast activation state (399, 400). Researchers also discovered two discrete populations around the hair follicles, dermal papilla and follicular sheath fibroblasts (401, 402). Recent findings further illuminated dermal fibroblast complexity by identifying temporal shifts in dermal fibroblast populations during development that contribute to neonatal regeneration as well as postnatal scarring and dermal fibrosis, but also indicate limitations in comparing murine and human dermal fibroblast subsets (40, 125–127, 129, 163, 403, 404). Despite the rich literature covering dermal fibroblast heterogeneity, PA fibroblasts in human skin have received little attention.

The evidence that PA fibroblasts in healthy human skin are phenotypically distinct from reticular dermal fibroblasts suggests that these populations may have unique functions. The functions of healthy dermal PA fibroblasts were not examined, but animal models provide suggestions. As members of the vascular

unit, PA fibroblasts participate in controlling vascular tone. Aortic adventitial fibroblasts express the angiotensin II receptor 1, and respond to angiotensin II by proliferating and producing the vasoconstrictor peptide endothelin 1 (86, 88). Endothelin 1 increases vascular smooth muscle cell contraction and nitric oxide release by endothelial cells with the net effect usually being vasoconstriction (405). Angiotensin II-driven endothelin 1 production by PA fibroblasts depends upon NADPH oxidase, which also produces reactive oxygen species that can counteract nitric oxide-mediated vasodilation (87, 89). Thus, PA fibroblasts in healthy human skin may be specialized to regulate vascular dilation and contraction.

Adventitial fibroblasts around hair follicles, sweat and sebaceous glands share the PA fibroblast CD90+CD34- phenotype (154, 186, 344) and play critical roles in regulating epithelial stem cells. During the earliest stages of hair follicle and sweat gland development, matrix metalloproteinases (MMP), such as MMP2, produced by adventitial fibroblasts appear to be important for degrading the basement membrane and forming tubes and shafts for the invading epithelial cells (406, 407). Subsequently, secretion of bone morphogenetic proteins (BMP) by mesenchymal cells promotes specification to sweat gland epithelium, while mesenchymal production of the BMP inhibitor, noggin, drives hair follicle epithelial fate (128, 140, 408, 409). After development, progressive signaling between mesenchymal and epithelial cells, including TGFβ and BMP, controls stem cell proliferation and differentiation, necessary for hair growth (160, 410). This fibroblast-epithelial guided growth and maintenance of adnexal structures may be

paralleled by fibroblast-endothelial cell crosstalk during angiogenesis. CD90-expressing fibroblasts in murine lymph nodes produce vascular endothelial growth factor to promote blood vessel growth during inflammation-stimulated enlargement (411). Control of vascular maintenance and growth, similar to that exerted on epithelial structures, may be another function of PA fibroblasts in healthy skin.

Another potential role for PA fibroblasts during homeostasis is the maintenance of a leukocyte survival niche. An elegant imaging study of human skin demonstrated that leukocytes are predominantly perivascular from 60 μm below the dermo-epidermal junction to the hypodermis (412). In healthy tissues, perivascular leukocytes include mast cells, macrophages, dendritic cells, type 2 innate lymphoid cells and T cells (412–418). Why these leukocytes accumulate around blood vessels in healthy skin is unclear, although CD90-expressing perivascular fibroblasts from multiple settings produce chemokines, such as CCL2 (95, 118, 279). Treg are critical for controlling inflammation and maintaining dermal homeostasis, and are found among perivascular T cells in healthy skin (419, 420). Fibroblasts within or isolated from healthy organs, including the skin, appear to support immunological homeostasis by promoting Treg survival and proliferation, and directly suppressing T cell activity in response to IFNγ (358, 415, 421, 422). Perhaps homeostatic PA fibroblasts contribute to the balance between immunosuppression and inflammation in the skin, similar to fibroblastic cells in Peyer's patches, epididymal visceral adipose tissue and the lungs (146, 151, 413, 421).

Fibroblasts in the healthy reticular dermis are predominantly CD34+CD90- but in SSc, healing wounds and pathologic scars many dermal fibroblasts express CD90 not CD34 (154, 162, 344, 348), thus resembling healthy PA fibroblasts. In SSc, the decrease in CD34 and increase in CD90 transcripts positively correlated with cutaneous sclerosis as measured by the MRSS (154). This CD34-to-CD90 transition occurred as early as 48 hours post-injury, followed by a time-dependent reversion to CD34 dominating the reticular dermis (344). Similarly, CD34 expression disappears from isolated mesenchymal cells within a few passages in culture (423, 424), although it is not clear whether this is due to outgrowth of a rare cell population or phenotypic conversion. Does this phenotypic convergence indicate that dermal fibroblasts in SSc and healing wounds adopt a functional program constitutively expressed by PA fibroblasts, or is CD90 a promiscuous marker of multiple mesenchymal states? Future studies, including comparative single-cell RNA-seq data, may help to unravel this.

Expansion and Activation of PA Fibroblasts in DLE and Dermatitis

These studies demonstrated that perivascular cuffs form in the adventitia of dermatitis and DLE skin lesions. The interpretation was put forth that activated, VCAM1+ PA fibroblasts drove this cuffing by producing a suite of molecules. Binding of α4β1 integrin-expressing innate lymphoid cells (ILCs) to VCAM1 on mesenchymal cells was necessary for developing the full complement and size of Peyer's patches (168). VCAM1 is also an early marker of differentiating lymph node fibroblasts, and is thought to retain organogenesis-driving ILC (176, 177,

425–427). Depleting inflamed fibroblasts using either fibroblast activation protein- or CCL19-diptheria toxin receptor mice decreased T and B cell accumulation in the salivary gland, lung and central nervous system (141, 150, 182). Activated FRC in lymph nodes draining an inflamed site are also critical for maintaining elevated T cell numbers (143). Yet, macrophages and dendritic cells were sufficient to form small, perivascular T cell clusters in a murine model of contact hypersensitivity (185). Thus, the question of whether activated, VCAM1-expressing PA fibroblasts are necessary for dense T cell accumulation remains open.

Data from these studies are consistent with the hypothesis that PA fibroblast activation precedes T cell accumulation. Although no causal data were presented, several published examples support this notion. Initiating events in lymph node and Peyer's patch organogenesis remain murky (428–430), but interactions between nerves, endothelial cells, mesenchymal cells and innate lymphoid cells (ILC) occur prior to the influx of lymphocytes (165, 176, 177, 360, 425, 426, 431–434). Fibroblast activation during inflammation in non-lymphoid tissues is also a multi-step dialogue between several cell types; however the initial priming can occur in the absence of lymphocytes, likely driven by a combination of ILC, myeloid cells, epithelial cells and fibroblasts (141, 381). Fibroblasts express pattern recognition receptors (435), which are important for the expansion of peritoneal fat-associated lymphoid clusters (146), indicating that at least partial inflammatory activation could be autocrine. T and B cells do play important roles in initiating the development of splenic white pulp (179), and the formation of lymphocyte

aggregates in the central nervous system (148), lungs (436, 437) and thyroid (438). Further work is necessary to determine whether PA fibroblast activation or T cell infiltration occurs first.

VCAM1 expression can signify one of several fibroblast programs ranging from attracting myeloid cells (118, 439, 440) and retaining T cells (186) to fully mature FRC (177, 360). This may represent a continuum of activation states. Attracting monocytes and macrophages by producing CCL2 is a common feature of activated perivascular fibroblasts (95, 118, 123, 279, 440–442). Once in the vascular unit, PA fibroblasts activate these myeloid cells by secreting IL-6 (118, 123, 440, 441, 443). This may parallel the initial perivascular macrophage activation described in murine contact hypersensitivity (185). Activated macrophages attract DCs and then T cells to blood vessels (185). During this step-wise dialogue with myeloid cells and lymphocytes, PA fibroblasts may mature along a similar path to that proposed for lymphoid organ fibroblasts (177, 428). The range of PA fibroblast activation states, from those specialized for macrophage accumulation to FRC and FDC in TLS, suggests that the VCAM1+ cells observed in dermatitis and DLE may lie on a continuum between these stages.

The general assumption is that leukocyte aggregates, such as those in DLE and dermatitis, promote tissue destruction in inflammatory diseases (109, 110). Inhibiting lymphotoxin-β receptor (LTβR) signaling in reactive lymph nodes halts immune responses by dampening activated fibroblasts (143). In the murine NOD model of type 1 diabetes, disruption of TLS by blocking LTβR signaling inhibits and

reverses disease, while overexpressing an LTβR ligand induces diabetes in the absence of pancreatic draining lymph nodes (444, 445).

In certain settings these structures may be protective. Mature TLS occur in the aortic adventitia near atherosclerotic plaques in both humans and mice (103–107, 112, 446), and, conversely, dissolving these TLS by blocking LTβR signaling worsens disease (104). However, the net effect of deactivating PA fibroblasts in atherosclerosis requires further clarification as there may be a time-dependent switch in whether TLS are protective or pathogenic (104, 107, 112). Perivascular cuffs, like those in DLE and dermatitis, may serve as efficient sites to activate Tregs, foster contact-mediated Treg suppression and generate new Tregs (104, 415) to control dermal inflammation (419, 420). FRC and fibroblasts stimulated with IFNγ can directly suppress T cell activity (358, 447, 448). While these mechanisms may initially constrain pathogenic lymphocytes, Treg and fibroblast suppression can fail turning the TLS into a site of local immune priming (440). If perivascular cuffs in DLE and dermatitis behave similarly, dissolving these structures in patients with overly flaring disease may halt or exacerbate local inflammatory destruction of the skin.

Targeting fibroblasts to treat inflammatory diseases and cancers is under investigation (449–451). However, fibroblast heterogeneity within an organ makes this difficult (123, 129, 145). Pharmacological deactivation or killing of only the pathogenic cells while sparing the beneficial ones requires precise knowledge. Similarly, time-dependent changes in fibroblast functions within lymphoid

aggregates pose the challenge of matching the treatment to the course of the disease (112). Boosting immunosuppressive and Treg augmenting fibroblast functions early in disease may control pathology, but if patients only present after local regulatory mechanisms have irreparably failed, deleting or reprogramming of the fibroblasts may be necessary (8, 452).

Expansion of NGFR+ PA Mesenchymal Cells in SSc, Wound Healing and Fibromas

Physicians and researchers have known for several decades that the perivascular adventitia expands in many SSc patients (81, 82, 295), but it is still unclear why. This gap in our knowledge contributes to the difficulty physicians face in treating SSc-associated vascular complications. Similar adventitial enlargements are implicated in several cardiovascular and fibrotic diseases (73, 216). In the 1990's, surgeons discovered that stripping the adventitia from arteries feeding the ulcerated fingers of SSc patients sped ulcer healing and decreased pain (48, 49). Evidence in Chapter Four demonstrated that expansion of specialized fibroblasts contributes to perivascular adventitial thickening in SSc. This is due, in part, to an amplification of perivascular NGFR-expressing mesenchymal cells. Similar elaborations of NGFR+ PA cells were observed in both reparative and pathologic human scars, as well as dermal fibromas. Collectively, these data suggest that perivascular NGFR expression correlates with fibroblast proliferation or ECM remodeling. A better understanding of adventitial thickening

and PA fibroblast activation may aid the treatment of digital ulcers and other symptoms in SSc patients.

The presence of scarce, NGFR+ PA mesenchymal cells in the skin of healthy patients suggested that these may be activated MSC repairing normal wear and tear. MSC have been described in every vascular layer (114, 115, 216, 321, 453, 454), although some of these populations are under debate (347, 455–457). NGFR is turned on by transit amplifying epithelial cells, myoblasts, dermal papilla fibroblasts and MSC. In all of these, NGFR expression appears to promote proliferation and prevent differentiation. Cells in the transit amplifying state are proliferating prior to their final differentiation (458). Once transit amplifying cells have proliferated to fully fill their niche, they differentiate and lose NGFR expression (343, 365, 366, 370, 459). Based on phenotype and location, expanded NGFR+ PA were proposed to be transit amplifying cells derived from CD34+CD73+ PA MSC (115, 116, 180). This notion fits with the expression of NGFR on transit amplifying cells mentioned above, and with the idea that normal repair signals are chronically active in SSc patients (460). Induction of NGFR on cultured dermal fibroblasts by differentiation-inducing polar compounds further supports this hypothesis. However, at least two alternative hypotheses need to be considered.

First, the expanded NGFR+ PA mesenchymal cells in SSc may signify an activation state of existing CD90+NGFR- PA fibroblasts. Fibroblastic cells are capable of proliferating *in vivo* and *in vitro*, indicating they can expand when

activated rather than requiring precursor proliferation (141, 411). Although fibroblasts are thought of as being more differentiated than MSC, the differentiation capabilities and relationships between these cells remain unclear. If NGFR represents a PA fibroblast activation state, rather than an MSC transit amplifying cell, it may be associated with vascular or dermal repair. NGFR expression by murine hepatic stellate cells (also mesenchymal) was necessary for myofibroblast differentiation, ECM deposition, hepatocyte proliferation and liver repair (388). Fibroblast activation and myofibroblast conversion are thought to be critical drivers of fibrosis in SSc. Murine models have implicated the vascular unit as a source of fibrosis-driving fibroblasts (114, 321). However, NGFR was restricted to dermal vascular units in the SSc biopsies used in this study, and was never observed on dermal SMA+ myofibroblasts. While NGFR may indicate a transient PA fibroblast activation state, the current data appear more consistent with NGFR marking an activated PA MSC in SSc.

Second, activated pericytes expressing NGFR may detach from endothelial cells, migrate into the adventitia and continue to expand there. Pericyte proliferation in SSc (461, 462) is consistent with their progenitor potential (453). This proliferation may be, in part, due to increased expression and signaling through PDGFRβ in pericytes in the skin of SSc patients (346, 463, 464). Especially around small vessels, where there is little, if any, media between the intima and adventitia, asymmetric division of pericytes would place one of the daughter cells in the PA. Expansion of ADAM12-expressing pericytes has also

been noted in SSc (465). In mice, rare ADAM12+ pericyte-like cells proliferated and migrated into the dermis where they deposited ECM. These ADAM12+ cells increased expression of NGFR during and after expansion (163), similar to our data from murine skin wounds. While pericyte activation and detachment may be responsible for the appearance of NGFR+ PA cells around small vessels, this seems less likely around larger arteries where movement through thick a thick media layer would be necessary to reach the adventitia. Additional experimentation will be necessary to discern if any of these three hypotheses is occurring in the skin of SSc patients.

How might PA fibroblast NGFR signaling influence SSc pathology? Ligand-independent NGFR signaling was necessary for the conversion of hepatic stellate cells into myofibroblasts in a murine model of liver injury. The authors formed this conclusion based on data using NGFR knockout fibroblasts transduced with either full-length NGFR or a construct expressing only the intracellular domain (388). However, this may not have been truly ligand independent as the NGFR intracellular domain potentiates Trk-induced Akt activity, and nerve growth factor signaling through TrkA and NGFR induces myofibroblast conversion in dermal fibroblasts (352, 354, 466). NGFR signaling can also be pro-apoptotic, which has an important role in controlling transit amplifying cell expansion (343). Pro-nerve growth factor binding to NGFR has similar apoptosis-inducing effects in pericytes in murine models of diabetic retinopathy, erectile dysfunction and myocardial infarction (392, 467–471). These examples highlight the complicated signaling

system in which NGFR participates. Understanding the effects of NGFR on PA fibroblasts in SSc and healing wounds will require a thorough analysis of the other neurotrophin receptors expressed by these cells, the neurotrophins secreted in the skin of these patients and the maturation status of these ligands.

The restriction of NGFR to the vascular unit in SSc and human scars contrasted with the diffuse distribution in murine scars (163) and some human fibromas (472–474). Perhaps NGFR+ fibromas have found a way to subvert pro-apoptotic NGFR signaling. Or, NGFR expression could indicate that these fibromas are trapped in a transit amplifying state, similar to the block in differentiation seen in acute promyelocytic leukemia (475, 476). Following this logic, the NGFR+ PA fibroblasts in SSc may be differentiating in response to damage signals, or these cells could be undergoing pro-NGF-mediated apoptosis. Determining why mesenchymal cells in some settings express NGFR throughout the dermis, and why mesenchymal NGFR is spatially limited in other settings may illuminate the pathogenesis of these diseases.

Limitations

There are ample data demonstrating that fibroblasts can create microenvironments supporting T cell accumulation in the literature (111, 139, 164, 166, 167, 477–479). The experiments provide evidence that VCAM1+ PA fibroblasts may retain T cells around blood vessels in DLE and dermatitis. Another study has indicated that macrophages and DCs can promote perivascular T cell accumulation (185). Both macrophages and DCs are found in the PA (73). These

studies do not exclude macrophages and DCs from being important drivers of perivascular T cell infiltration.

Expansion of NGFR-expressing PA fibroblasts was associated with conditions featuring fibroblast proliferation and ECM deposition. Yet, neither the function of NGFR on PA fibroblasts, nor the contributions of these cells to PA growth or remodeling were directly demonstrated. Published roles for NGFR on mesenchymal cells include blocking the differentiation of progenitor cells, promoting the myofibroblast conversion, supporting the HIF1α-driven hypoxia response and inducing apoptosis (343, 365, 366, 370, 388, 389, 459, 480). All of these are potentially relevant to SSc, wound healing and fibromas. Neurotrophin signaling is complex, and elucidating which of these functional outcomes is relevant to SSc PA thickening will require an additional study.

Conclusions are strengthened by obtaining concordant results through independent means. Confirming increased VCAM1 expression and T cell infiltration in DLE by both immunohistochemistry and whole-biopsy RNA microarrays is an example of this. Due to several restrictions, not all of the results from these studies were orthogonally confirmed. Using these same tools to validate the expanded NGFR+ PA fibroblast population in SSc was infeasible as many cells in the skin express this protein (326, 473). Such support will require isolating PA fibroblasts expressing NGFR for either bulk or single-cell RNA or protein analysis. Despite these limitations, these studies present a coherent introduction to the potential importance of PA fibroblasts in human skin diseases.

APPENDIX: COPYRIGHT PERMISSION

CHAPTERS TWO (METHODS) and *THREE (PERIVASCULAR ADVENTITIAL FIBROBLAST SPECIALIZATION ACCOMPANIES T CELL RETENTION IN THE INFLAMED HUMAN DERMIS)*

Data and portions of the text in these chapters were originally published as:

Barron, A. M. S., Mantero, J. C., Ho, J. D., Nazari, B., Horback, K. L., Bhawan, J., Lafyatis, R., Lam, C., and Browning, J. L. (2019) Perivascular Adventitial Fibroblast Specialization Accompanies T Cell Retention in the Inflamed Human Dermis. *Journal of immunology (Baltimore, Md.: 1950)*. **202**, 56–68.

Alexander Barron <amb253@bu.edu>

Barron Permission Request

Catherine Wattenberg <cwattenberg@aai.org> Wed, Aug 21, 2019 at 5:43 PM
To: "amb253@bu.edu" <amb253@bu.edu>

Dear Dr. Barron,

Permission is granted for the reuse of the material below in your PhD thesis.

Best wishes,

Catherine

Catherine Wattenberg
Director of Publications
The American Association of Immunologists, Inc.
1451 Rockville Pike, Suite 650
Rockville, MD 20852
Phone: 301-634-7835

www.aai.org

From: Web Email
Sent: Saturday, July 27, 2019 7:21 PM
To: Copyright Requests
Subject: Permission Request

Name	Alexander Barron
* Institution	Boston University School of Medicine
* Address	72 E. Concord St., Evans Bldg. 5th floor, rm 520
* City, State, and Postal Code	Boston, MA 02118
* Country	USA
* Phone	503-522-1417
Fax	

* E-mail	amb253@bu.edu
* Title of Article	Perivascular Adventitial Fibroblast Specialization Accompanies T Cell Retention in the Inflamed Human Dermis
* Volume Number	202
* Page Range	56-68
* Year	2019
DOI Number	10.4049/jimmunol.1801209
* Will figure be reproduced without changes from the original?	Yes
* Will figure be modified from the original?	No
* Figure or Table Number(s)	All
Other Reproduction (please describe)	I am requesting permission to reproduce the text and tables of this article with slight modifications (e.g. removing a few sentences and changing the font size and font of table text), and the figures without modification for my Ph.D. dissertation.
* Are you the author of the requested material?	Yes
* Is this for your Ph.D. thesis?	Yes
* Title of Publication (not article title)	To be determined. Working title is currently, "Perivascular Fibroblast Activation States in Human Skin Diseases".

* Publisher	Boston University
Date of Publication (optional)	To be determined. Likely sometime in Sept. 2019.
* Provide a brief explanation of how the material will be used	As noted above, I am requesting rights to reproduce the text, figures and tables from this article in my Ph.D. dissertation. The text will be modified by removing sentences containing "data not shown" references, and changing some of the figure numbers. Tables will be reproduced with changes to font size and typeface, but no alterations in the data. Figures will be reproduced without alteration. I will include text citing the original article in the Journal of Immunology, including a link to the article on the Journal of Immunology website. Also, if you supply an official document granting the requested permissions I will include it in an appendix to my dissertation. Many thanks.

BIBLIOGRAPHY

1. Lim, H. W., Collins, S. A. B., Resneck, J. S., Bolognia, J. L., Hodge, J. A., Rohrer, T. A., Van Beek, M. J., Margolis, D. J., Sober, A. J., Weinstock, M. A., Nerenz, D. R., Smith Begolka, W., and Moyano, J. V. (2017) The burden of skin disease in the United States. *Journal of the American Academy of Dermatology*. **76**, 958-972.e2

2. Tuckman, A. (2017) The Potential Psychological Impact of Skin Conditions. *Dermatology and Therapy*. **7**, 53–57

3. Durosaro, O., Davis, M. D. P., Reed, K. B., and Rohlinger, A. L. (2009) Incidence of cutaneous lupus erythematosus, 1965-2005: a population-based study. *Archives of Dermatology*. **145**, 249–53

4. Grönhagen, C. M., Fored, C. M., Granath, F., and Nyberg, F. (2011) Cutaneous lupus erythematosus and the association with systemic lupus erythematosus: a population-based cohort of 1088 patients in Sweden. *The British Journal of Dermatology*. **164**, 1335–41

5. Walling, H. W., and Sontheimer, R. D. (2009) Cutaneous Lupus Erythematosus. *American Journal of Clinical Dermatology*. **10**, 365–381

6. Knobler, R., Moinzadeh, P., Hunzelmann, N., Kreuter, A., Cozzio, A., Mouthon, L., Cutolo, M., Rongioletti, F., Denton, C. P., Rudnicka, L., Frasin, L. A., Smith, V., Gabrielli, A., Aberer, E., Bagot, M., Bali, G., Bouaziz, J., Braae Olesen, A., Foeldvari, I., Frances, C., Jalili, A., Just, U., Kähäri, V., Kárpáti, S., Kofoed, K., Krasowska, D., Olszewska, M., Orteu, C., Panelius, J., Parodi, A., Petit, A., Quaglino, P., Ranki, A., Sanchez Schmidt, J. M., Seneschal, J., Skrok, A., Sticherling, M., Sunderkötter, C., Taieb, A., Tanew, A., Wolf, P., Worm, M., Wutte, N. J., and Krieg, T. (2017) European Dermatology Forum S1-guideline on the diagnosis and treatment of sclerosing diseases of the skin, Part 1: localized scleroderma, systemic sclerosis and overlap syndromes. *Journal of the European Academy of Dermatology and Venereology : JEADV*. **31**, 1401–1424

7. Gordon, K. B., Blauvelt, A., Papp, K. A., Langley, R. G., Luger, T., Ohtsuki, M., Reich, K., Amato, D., Ball, S. G., Braun, D. K., Cameron, G. S., Erickson, J., Konrad, R. J., Muram, T. M., Nickoloff, B. J., Osuntokun, O. O., Secrest, R. J., Zhao, F., Mallbris, L., Leonardi, C. L., UNCOVER-1 Study Group, UNCOVER-2 Study Group, and UNCOVER-3 Study Group (2016) Phase 3 Trials of Ixekizumab in Moderate-to-Severe Plaque Psoriasis. *The New England Journal of Medicine*. **375**, 345–56

8. Dakin, S. G., Coles, M., Sherlock, J. P., Powrie, F., Carr, A. J., and

Buckley, C. D. (2018) Pathogenic stromal cells as therapeutic targets in joint inflammation. *Nature Reviews. Rheumatology*. **14**, 714–726

9. Schett, G., and Neurath, M. F. (2018) Resolution of chronic inflammatory disease: universal and tissue-specific concepts. *Nature Communications*. 10.1038/s41467-018-05800-6

10. Comen, E. A., Bowman, R. L., and Kleppe, M. (2018) Underlying Causes and Therapeutic Targeting of the Inflammatory Tumor Microenvironment. *Frontiers in Cell and Developmental Biology*. **6**, 1–24

11. Denton, C. P., and Khanna, D. (2017) Systemic sclerosis. *Lancet (London, England)*. **390**, 1685–1699

12. Obermoser, G., Sontheimer, R. D., and Zelger, B. (2010) Overview of common, rare and atypical manifestations of cutaneous lupus erythematosus and histopathological correlates. *Lupus*. **19**, 1050–70

13. Jabbari, A., Suárez-Fariñas, M., Fuentes-Duculan, J., Gonzalez, J., Cueto, I., Franks, A. G., and Krueger, J. G. (2014) Dominant Th1 and minimal Th17 skewing in discoid lupus revealed by transcriptomic comparison with psoriasis. *The Journal of Investigative Dermatology*. **134**, 87–95

14. Wenzel, J., Wörenkämper, E., Freutel, S., Henze, S., Haller, O., Bieber, T., and Tüting, T. (2005) Enhanced type I interferon signalling promotes Th1-biased inflammation in cutaneous lupus erythematosus. *The Journal of Pathology*. **205**, 435–42

15. Toro, J. R., Finlay, D., Dou, X., Zheng, S. C., LeBoit, P. E., and Connolly, M. K. (2000) Detection of type 1 cytokines in discoid lupus erythematosus. *Archives of Dermatology*. **136**, 1497–501

16. Kraling, B. M., Maul, G. G., and Jimenez, S. A. (1995) Mononuclear cellular infiltrates in clinically involved skin from patients with systemic sclerosis of recent onset predominantly consist of monocytes/macrophages. *Pathobiology*. **63**, 48–56

17. Prescott, R. J., Freemont, A. J., Jones, C. J. P., Hoyland, J., and Fielding, P. (1992) Sequential dermal microvascular and perivascular changes in the development of scleroderma. *The Journal of Pathology*. **166**, 255–63

18. Greenblatt, M. B., Sargent, J. L., Farina, G., Tsang, K., Lafyatis, R., Glimcher, L. H., Whitfield, M. L., and Aliprantis, A. O. (2012) Interspecies comparison of human and murine scleroderma reveals IL-13 and CCL2 as disease subset-specific targets. *American Journal of Pathology*. **180**,

1080–1094

19. Mollica Poeta, V., Massara, M., Capucetti, A., and Bonecchi, R. (2019) Chemokines and Chemokine Receptors: New Targets for Cancer Immunotherapy. *Frontiers in Immunology*. **10**, 379

20. Lim, S. Y., Yuzhalin, A. E., Gordon-Weeks, A. N., and Muschel, R. J. (2016) Targeting the CCL2-CCR2 signaling axis in cancer metastasis. *Oncotarget*. **7**, 28697–710

21. Haringman, J. J., Gerlag, D. M., Smeets, T. J. M., Baeten, D., van den Bosch, F., Bresnihan, B., Breedveld, F. C., Dinant, H. J., Legay, F., Gram, H., Loetscher, P., Schmouder, R., Woodworth, T., and Tak, P. P. (2006) A randomized controlled trial with an anti-CCL2 (anti-monocyte chemotactic protein 1) monoclonal antibody in patients with rheumatoid arthritis. *Arthritis and Rheumatism*. **54**, 2387–92

22. Lebre, M. C., Vergunst, C. E., Choi, I. Y. K., Aarrass, S., Oliveira, A. S. F., Wyant, T., Horuk, R., Reedquist, K. A., and Tak, P. P. (2011) Why CCR2 and CCR5 blockade failed and why CCR1 blockade might still be effective in the treatment of rheumatoid arthritis. *PLoS ONE*. **6**, e21772

23. Allanore, Y., Simms, R., Distler, O., Trojanowska, M., Pope, J., Denton, C. P., and Varga, J. (2015) Systemic sclerosis. *Nature Reviews. Disease Primers*. **1**, 15002

24. Barnes, J., and Mayes, M. D. (2012) Epidemiology of systemic sclerosis. *Current Opinion in Rheumatology*. **24**, 165–170

25. LeRoy, E. C., Black, C., Fleischmajer, R., Jablonska, S., Krieg, T., Medsger, T. A., Rowell, N., and Wollheim, F. (1988) Scleroderma (systemic sclerosis): classification, subsets and pathogenesis. *The Journal of Rheumatology*. **15**, 202–5

26. Chifflot, H., Fautrel, B., Sordet, C., Chatelus, E., and Sibilia, J. (2008) Incidence and prevalence of systemic sclerosis: a systematic literature review. *Seminars in Arthritis and Rheumatism*. **37**, 223–35

27. Katsumoto, T. R., Whitfield, M. L., and Connolly, M. K. (2011) The pathogenesis of systemic sclerosis. *Annual Review of Pathology*. **6**, 509–537

28. Mayes, M. D., Lacey, J. V, Beebe-Dimmer, J., Gillespie, B. W., Cooper, B., Laing, T. J., and Schottenfeld, D. (2003) Prevalence, incidence, survival, and disease characteristics of systemic sclerosis in a large US population.

Arthritis and Rheumatism. **48**, 2246–55

29. Martyanov, V., and Whitfield, M. L. (2016) Molecular stratification and precision medicine in systemic sclerosis from genomic and proteomic data. *Current Opinion in Rheumatology*. **28**, 83–8

30. Stifano, G., Sornasse, T., Rice, L. M., Na, L., Chen-Harris, H., Khanna, D., Jahreis, A., Zhang, Y., Siegel, J., and Lafyatis, R. (2018) Skin Gene Expression Is Prognostic for the Trajectory of Skin Disease in Patients With Diffuse Cutaneous Systemic Sclerosis. *Arthritis & Rheumatology (Hoboken, N.J.)*. **70**, 912–919

31. Campbell, P. M., and LeRoy, E. C. (1975) Pathogenesis of systemic sclerosis: a vascular hypothesis. *Seminars in Arthritis and Rheumatism*. **4**, 351–68

32. Furst, D. E., Clements, P. J., Steen, V. D., Medsger, T. A., Masi, A. T., D'Angelo, W. A., Lachenbruch, P. A., Grau, R. G., and Seibold, J. R. (1998) The modified Rodnan skin score is an accurate reflection of skin biopsy thickness in systemic sclerosis. *The Journal of Rheumatology*. **25**, 84–8

33. Freemont, A. J., Hoyland, J., Fielding, P., Hodson, N., and Jayson, M. I. (1992) Studies of the microvascular endothelium in uninvolved skin of patients with systemic sclerosis: direct evidence for a generalized microangiopathy. *The British Journal of Dermatology*. **126**, 561–8

34. Fleischmajer, R., Perlish, J. S., Shaw, K. V, and Pirozzi, D. J. (1976) Skin capillary changes in early systemic scleroderma. Electron microscopy and "in vitro" autoradiography with tritiated thymidine. *Archives of Dermatology*. **112**, 1553–7

35. Salojin, K. V., Le Tonquèze, M., Saraux, A., Nassonov, E. L., Dueymes, M., Piette, J. C., and Youinou, P. Y. (1997) Antiendothelial cell antibodies: useful markers of systemic sclerosis. *The American Journal of Medicine*. **102**, 178–85

36. Barbano, B., Marra, A. M., Quarta, S., Gigante, A., Barilaro, G., Gasperini, M. L., and Rosato, E. (2017) In systemic sclerosis skin perfusion of hands is reduced and may predict the occurrence of new digital ulcers. *Microvascular Research*. **110**, 1–4

37. Bourji, K., Meyer, A., Chatelus, E., Pincemail, J., Pigatto, E., Defraigne, J.-O., Singh, F., Charlier, C., Geny, B., Gottenberg, J.-E., Punzi, L., Cozzi, F., and Sibilia, J. (2015) High reactive oxygen species in fibrotic and

nonfibrotic skin of patients with diffuse cutaneous systemic sclerosis. *Free Radical Biology & Medicine*. **87**, 282–9

38. Marie, I., Gehanno, J.-F., Bubenheim, M., Duval-Modeste, A.-B., Joly, P., Dominique, S., Bravard, P., Noël, D., Cailleux, A.-F., Benichou, J., Levesque, H., and Goullé, J.-P. (2017) Systemic sclerosis and exposure to heavy metals: A case control study of 100 patients and 300 controls. *Autoimmunity Reviews*. **16**, 223–230

39. Lemos, D. R., Babaeijandaghi, F., Low, M., Chang, C.-K., Lee, S. T., Fiore, D., Zhang, R.-H., Natarajan, A., Nedospasov, S. A., and Rossi, F. M. V (2015) Nilotinib reduces muscle fibrosis in chronic muscle injury by promoting TNF-mediated apoptosis of fibro/adipogenic progenitors. *Nature Medicine*. **21**, 786–94

40. Shook, B. A., Wasko, R. R., Rivera-Gonzalez, G. C., Salazar-Gatzimas, E., López-Giráldez, F., Dash, B. C., Muñoz-Rojas, A. R., Aultman, K. D., Zwick, R. K., Lei, V., Arbiser, J. L., Miller-Jensen, K., Clark, D. A., Hsia, H. C., and Horsley, V. (2018) Myofibroblast proliferation and heterogeneity are supported by macrophages during skin repair. *Science*. 10.1126/science.aar2971

41. Mavalia, C., Scaletti, C., Romagnani, P., Carossino, A. M., Pignone, A., Emmi, L., Pupilli, C., Pizzolo, G., Maggi, E., and Romagnani, S. (1997) Type 2 helper T-cell predominance and high CD30 expression in systemic sclerosis. *The American Journal of Pathology*. **151**, 1751–8

42. Serpier, H., Gillery, P., Salmon-Ehr, V., Garnotel, R., Georges, N., Kalis, B., and Maquart, F. X. (1997) Antagonistic effects of interferon-gamma and interleukin-4 on fibroblast cultures. *The Journal of Investigative Dermatology*. **109**, 158–62

43. Riccieri, V., Rinaldi, T., Spadaro, A., Scrivo, R., Ceccarelli, F., Franco, M. Di, Taccari, E., and Valesini, G. (2003) Interleukin-13 in systemic sclerosis: relationship to nailfold capillaroscopy abnormalities. *Clinical Rheumatology*. **22**, 102–6

44. Jinnin, M., Ihn, H., Yamane, K., and Tamaki, K. (2004) Interleukin-13 stimulates the transcription of the human alpha2(I) collagen gene in human dermal fibroblasts. *The Journal of Biological Chemistry*. **279**, 41783–91

45. Pearson, D. R., Werth, V. P., and Pappas-Taffer, L. (2018) Systemic sclerosis: Current concepts of skin and systemic manifestations. *Clinics in Dermatology*. **36**, 459–474

46. Wigley, F. M., and Flavahan, N. A. (2016) Raynaud's Phenomenon. *The New England Journal of Medicine*. **375**, 556–65

47. Flatt, A. E. (1980) Digital artery sympathectomy. *The Journal of Hand Surgery*. **5**, 550–6

48. el-Gammal, T. A., and Blair, W. F. (1991) Digital periarterial sympathectomy for ischaemic digital pain and ulcers. *Journal of Hand Surgery (Edinburgh, Scotland)*. **16**, 382–5

49. O'Brien, B. M., Kumar, P. A., Mellow, C. G., and Oliver, T. V (1992) Radical microarteriolysis in the treatment of vasospastic disorders of the hand, especially scleroderma. *Journal of Hand Surgery (Edinburgh, Scotland)*. **17**, 447–52

50. Jarrett, P., Thornley, S., and Scragg, R. (2016) Ethnic differences in the epidemiology of cutaneous lupus erythematosus in New Zealand. *Lupus*. **25**, 1497–1502

51. Andersen, L. K., and Davis, M. D. P. (2016) Prevalence of Skin and Skin-Related Diseases in the Rochester Epidemiology Project and a Comparison with Other Published Prevalence Studies. *Dermatology (Basel, Switzerland)*. **232**, 344–52

52. Rothfield, N., Sontheimer, R. D., and Bernstein, M. (2006) Lupus erythematosus: systemic and cutaneous manifestations. *Clinics in Dermatology*. **24**, 348–362

53. Oh, E. H., Kim, E. J., Ro, Y. S., and Ko, J. Y. (2018) Ten-year retrospective clinicohistological study of cutaneous lupus erythematosus in Korea. *The Journal of Dermatology*. **45**, 436–443

54. McDaniel, B., and Tanner, L. S. (2019) Discoid Lupus Erythematosus. *StatPearls [Internet].* [online] https://www.ncbi.nlm.nih.gov/books/NBK493145/ (Accessed February 7, 2019)

55. Lehmann, P., Hölzle, E., Kind, P., Goerz, G., and Plewig, G. (1990) Experimental reproduction of skin lesions in lupus erythematosus by UVA and UVB radiation. *Journal of the American Academy of Dermatology*. **22**, 181–187

56. Järvinen, T. M., Hellquist, A., Koskenmies, S., Einarsdottir, E., Koskinen, L. L. E., Jeskanen, L., Berglind, L., Panelius, J., Hasan, T., Ranki, A., Kere, J., and Saarialho-Kere, U. (2010) Tyrosine kinase 2 and interferon

regulatory factor 5 polymorphisms are associated with discoid and subacute cutaneous lupus erythematosus. *Experimental Dermatology*. **19**, 123–131

57. Wenzel, J., Uerlich, M., Wörrenkämper, E., Freutel, S., Bieber, T., and Tüting, T. (2005) Scarring skin lesions of discoid lupus erythematosus are characterized by high numbers of skin-homing cytotoxic lymphocytes associated with strong expression of the type I interferon-induced protein MxA. *British Journal of Dermatology*. **153**, 1011–1015

58. Sarkar, M. K., Hile, G. A., Tsoi, L. C., Xing, X., Liu, J., Liang, Y., Berthier, C. C., Swindell, W. R., Patrick, M. T., Shao, S., Tsou, P.-S., Uppala, R., Beamer, M. A., Srivastava, A., Bielas, S. L., Harms, P. W., Getsios, S., Elder, J. T., Voorhees, J. J., Gudjonsson, J. E., and Kahlenberg, J. M. (2018) Photosensitivity and type I IFN responses in cutaneous lupus are driven by epidermal-derived interferon kappa. *Annals of the Rheumatic Diseases*. **77**, 1653–1664

59. Achtman, J. C., and Werth, V. P. (2015) Pathophysiology of cutaneous lupus erythematosus. *Arthritis Research & Therapy*. **17**, 182

60. Farkas, L., Beiske, K., Lund-Johansen, F., Brandtzaeg, P., and Jahnsen, F. L. (2001) Plasmacytoid dendritic cells (natural interferon- alpha/beta-producing cells) accumulate in cutaneous lupus erythematosus lesions. *The American Journal of Pathology*. **159**, 237–43

61. Jones, S. M., Mathew, C. M., Dixey, J., Lovell, C. R., and McHugh, N. J. (1996) VCAM-1 expression on endothelium in lesions from cutaneous lupus erythematosus is increased compared with systemic and localized scleroderma. *The British Journal of Dermatology*. **135**, 678–86

62. Alsaad, K. O., and Ghazarian, D. (2005) My approach to superficial inflammatory dermatoses. *Journal of Clinical Pathology*. **58**, 1233–41

63. Flier, J., Boorsma, D. M., van Beek, P. J., Nieboer, C., Stoof, T. J., Willemze, R., and Tensen, C. P. (2001) Differential expression of CXCR3 targeting chemokines CXCL10, CXCL9, and CXCL11 in different types of skin inflammation. *The Journal of Pathology*. **194**, 398–405

64. Wenzel, J., Henze, S., Wörenkämper, E., Basner-Tschakarjan, E., Sokolowska-Wojdylo, M., Steitz, J., Bieber, T., and Tüting, T. (2005) Role of the chemokine receptor CCR4 and its ligand thymus- and activation-regulated chemokine/CCL17 for lymphocyte recruitment in cutaneous lupus erythematosus. *Journal of Investigative Dermatology*. **124**, 1241–1248

65. Chen, K. L., Krain, R. L., and Werth, V. P. (2019) Advancing understanding, diagnosis, and therapies for cutaneous lupus erythematosus within the broader context of systemic lupus erythematosus. *F1000Research*. **8**, 332

66. Jessop, S., Whitelaw, D. A., Grainge, M. J., and Jayasekera, P. (2017) Drugs for discoid lupus erythematosus. *Cochrane Database of Systematic Reviews*. 10.1002/14651858.CD002954.pub3

67. Ruzicka, T., Sommerburg, C., Goerz, G., Kind, P., and Mensing, H. (1992) Treatment of cutaneous lupus erythematosus with acitretin and hydroxychloroquine. *The British Journal of Dermatology*. **127**, 513–8

68. Kabashima, K., Honda, T., Ginhoux, F., and Egawa, G. (2019) The immunological anatomy of the skin. *Nature Reviews. Immunology*. **19**, 19–30

69. Ho, A. W., and Kupper, T. S. (2019) T cells and the skin: from protective immunity to inflammatory skin disorders. *Nature Reviews. Immunology*. 10.1038/s41577-019-0162-3

70. Ho, K.-L. (1986) Ultrastructure of cerebellar capillary hemangioblastoma. *Acta Neuropathologica*. **70**, 117–126

71. Rhodin, J. A. (1967) The ultrastructure of mammalian arterioles and precapillary sphincters. *Journal of Ultrastructure Research*. **18**, 181–223

72. Rhodin, J. A. (1968) Ultrastructure of mammalian venous capillaries, venules, and small collecting veins. *Journal of Ultrastructure Research*. **25**, 452–500

73. Stenmark, K. R., Yeager, M. E., El Kasmi, K. C., Nozik-Grayck, E., Gerasimovskaya, E. V, Li, M., Riddle, S. R., and Frid, M. G. (2013) The adventitia: essential regulator of vascular wall structure and function. *Annual Review of Physiology*. **75**, 23–47

74. Sorrell, J. M., and Caplan, A. I. (2004) Fibroblast heterogeneity: more than skin deep. *Journal of Cell Science*. **117**, 667–75

75. McMahan, Z. H., and Wigley, F. M. Raynaud's phenomenon and digital ischemia: a practical approach to risk stratification, diagnosis and management. *International Journal of Clinical Rheumatology*. **5**, 355–370

76. Coelho Horimoto, A. M., de Souza, A. S., Rodrigues, S. H., and Kayser, C. (2019) Risk of digital ulcers occurrence in systemic sclerosis: A cross-

sectional study. *Advances in Rheumatology*. **59**, 1–7

77. Galluccio, F., and Matucci-Cerinic, M. (2011) Two faces of the same coin: Raynaud phenomenon and digital ulcers in systemic sclerosis. *Autoimmunity Reviews*. **10**, 241–3

78. Bruni, C., Frech, T., Manetti, M., Rossi, F. W., Furst, D. E., De Paulis, A., Rivellese, F., Guiducci, S., Matucci-Cerinic, M., and Bellando-Randone, S. (2018) Vascular Leaking, a Pivotal and Early Pathogenetic Event in Systemic Sclerosis: Should the Door Be Closed? *Frontiers in Immunology*. **9**, 2045

79. Rodnan, G. P., Myerowitz, R. L., and Justh, G. O. (1980) Morphologic changes in the digital arteries of patients with progressive systemic sclerosis (scleroderma) and Raynaud phenomenon. *Medicine*. **59**, 393–408

80. Matucci-Cerinic, M., Kahaleh, B., and Wigley, F. M. (2013) Review: evidence that systemic sclerosis is a vascular disease. *Arthritis and Rheumatism*. **65**, 1953–62

81. Matsui, S. (1924) Uber die Pathologie und pathogenese von Sklerodermia universalis. *Mitteilungen aus der Medizinischen Fakultät der Kaiserlichen Universität zu Tokyo*. **31**, 55–116

82. Lewis, T. (1938) The pathological changes in the arteries supplying the fingers in warm-handed people and in cases of so-called Raynaud's disease. *Clinical Science*. **3**, 287–319

83. Lewis, T. (1940) Notes on Scleroderma (Dermatomyositis). *British Journal of Dermatology*. **52**, 233–242

84. Qian, J., Tian, W., Jiang, X., Tamosiuniene, R., Sung, Y. K., Shuffle, E. M., Tu, A. B., Valenzuela, A., Jiang, S., Zamanian, R. T., Fiorentino, D. F., Voelkel, N. F., Peters-Golden, M., Stenmark, K. R., Chung, L., Rabinovitch, M., and Nicolls, M. R. (2015) Leukotriene B4 Activates Pulmonary Artery Adventitial Fibroblasts in Pulmonary Hypertension. *Hypertension (Dallas, Tex. : 1979)*. **66**, 1227–1239

85. Derrett-Smith, E. C., Dooley, A., Khan, K., Shi-wen, X., Abraham, D., and Denton, C. P. (2010) Systemic vasculopathy with altered vasoreactivity in a transgenic mouse model of scleroderma. *Arthritis Research & Therapy*. **12**, R69

86. An, S. J., Boyd, R., Wang, Y., Qiu, X., and Wang, H. D. (2006) Endothelin-

1 expression in vascular adventitial fibroblasts. *American Journal of Physiology. Heart and Circulatory Physiology*. **290**, H700-8

87. An, S. J., Boyd, R., Zhu, M., Chapman, A., Pimentel, D. R., and Wang, H. D. (2007) NADPH oxidase mediates angiotensin II-induced endothelin-1 expression in vascular adventitial fibroblasts. *Cardiovascular Research*. **75**, 702–9

88. An, S. J., Liu, P., Shao, T. M., Wang, Z. J., Lu, H. G., Jiao, Z., Li, X., and Fu, J. Q. (2015) Characterization and functions of vascular adventitial fibroblast subpopulations. *Cellular Physiology and Biochemistry : International Journal of Experimental Cellular Physiology, Biochemistry, and Pharmacology*. **35**, 1137–50

89. Wang, H. D., Pagano, P. J., Du, Y., Cayatte, A. J., Quinn, M. T., Brecher, P., and Cohen, R. A. (1998) Superoxide anion from the adventitia of the rat thoracic aorta inactivates nitric oxide. *Circulation Research*. **82**, 810–8

90. Vanhoutte, P. M., Shimokawa, H., Feletou, M., and Tang, E. H. C. (2017) Endothelial dysfunction and vascular disease - a 30th anniversary update. *Acta Physiologica (Oxford, England)*. **219**, 22–96

91. Meyrick, B., and Reid, L. (1979) Hypoxia and incorporation of 3H-thymidine by cells of the rat pulmonary arteries and alveolar wall. *The American Journal of Pathology*. **96**, 51–70

92. Scott, N. A., Cipolla, G. D., Ross, C. E., Dunn, B., Martin, F. H., Simonet, L., and Wilcox, J. N. (1996) Identification of a potential role for the adventitia in vascular lesion formation after balloon overstretch injury of porcine coronary arteries. *Circulation*. **93**, 2178–87

93. Sangiorgi, G., Taylor, A. J., Farb, A., Carter, A. J., Edwards, W. D., Holmes, D. R., Schwartz, R. S., and Virmani, R. (1999) Histopathology of postpercutaneous transluminal coronary angioplasty remodeling in human coronary arteries. *American Heart Journal*. **138**, 681–7

94. Sun, M., Ji, J., Guo, X., Liu, W., Wang, Y., Ma, S., Hu, W., Wang, J., and Jiang, F. (2016) Early adventitial activation characterized by NADPH oxidase expression and neovascularization in an aortic transplantation model. *Experimental and Molecular Pathology*. **100**, 67–73

95. Ji, J., Xu, F., Li, L., Chen, R., Wang, J., and Hu, W. (2010) Activation of adventitial fibroblasts in the early stage of the aortic transplant vasculopathy in rat. *Transplantation*. **89**, 945–53

96. Kuwabara, J. T., and Tallquist, M. D. (2017) Tracking Adventitial Fibroblast Contribution to Disease: A Review of Current Methods to Identify Resident Fibroblasts. *Arteriosclerosis, Thrombosis, and Vascular Biology*. 10.1161/ATVBAHA.117.308199

97. Kirabo, A., Fontana, V., de Faria, A. P. C., Loperena, R., Galindo, C. L., Wu, J., Bikineyeva, A. T., Dikalov, S., Xiao, L., Chen, W., Saleh, M. A., Trott, D. W., Itani, H. A., Vinh, A., Amarnath, V., Amarnath, K., Guzik, T. J., Bernstein, K. E., Shen, X. Z., Shyr, Y., Chen, S., Mernaugh, R. L., Laffer, C. L., Elijovich, F., Davies, S. S., Moreno, H., Madhur, M. S., Roberts, J., and Harrison, D. G. (2014) DC isoketal-modified proteins activate T cells and promote hypertension. *The Journal of Clinical Investigation*. **124**, 4642–56

98. Elman, S. A., Joyce, C., Nyberg, F., Furukawa, F., Goodfield, M., Hasegawa, M., Marinovic, B., Szepietowski, J. C., Dutz, J., Werth, V. P., and Merola, J. F. (2017) Development of classification criteria for discoid lupus erythematosus: Results of a Delphi exercise. *Journal of the American Academy of Dermatology*. **77**, 261–267

99. Nyberg, F., Hasan, T., Skoglund, C., and Stephansson, E. (1999) Early events in ultraviolet light-induced skin lesions in lupus erythematosus: expression patterns of adhesion molecules ICAM-1, VCAM-1 and E-selectin. *Acta Dermato-Venereologica*. **79**, 431–6

100. Lesiak, A., Narbutt, J., Kobos, J., Kordek, R., Sysa-Jedrzejowska, A., Norval, M., and Wozniacka, A. (2009) Systematic administration of chloroquine in discoid lupus erythematosus reduces skin lesions via inhibition of angiogenesis. *Clinical and Experimental Dermatology*. **34**, 570–5

101. Janeway, C. J., Travers, P., Walport, M., and Shlomchik, M. (2001) *Immunobiology: The Immune System in Health and Disease*, 5th Ed., Garland Science, New York, NY

102. Thorpe, R. B., Gray, A., Kumar, K. R., Susa, J. S., and Chong, B. F. (2014) Site-specific analysis of inflammatory markers in discoid lupus erythematosus skin. *The Scientific World Journal*. **2014**, 925805

103. Schwartz, C. J., and Mitchell, J. R. (1962) Cellular infiltration of the human arterial adventitia associated with atheromatous plaques. *Circulation*. **26**, 73–8

104. Hu, D., Mohanta, S. K., Yin, C., Peng, L., Ma, Z., Srikakulapu, P., Grassia, G., MacRitchie, N., Dever, G., Gordon, P., Burton, F. L., Ialenti, A., Sabir,

S. R., McInnes, I. B., Brewer, J. M., Garside, P., Weber, C., Lehmann, T., Teupser, D., Habenicht, L., Beer, M., Grabner, R., Maffia, P., Weih, F., and Habenicht, A. J. R. (2015) Artery Tertiary Lymphoid Organs Control Aorta Immunity and Protect against Atherosclerosis via Vascular Smooth Muscle Cell Lymphotoxin β Receptors. *Immunity*. **42**, 1100–15

105. Akhavanpoor, M., Gleissner, C. A., Akhavanpoor, H., Lasitschka, F., Doesch, A. O., Katus, H. A., and Erbel, C. (2018) Adventitial tertiary lymphoid organ classification in human atherosclerosis. *Cardiovascular Pathology : the Official Journal of the Society for Cardiovascular Pathology*. **32**, 8–14

106. Moos, M. P. W., John, N., Gräbner, R., Nossmann, S., Günther, B., Vollandt, R., Funk, C. D., Kaiser, B., and Habenicht, A. J. R. (2005) The lamina adventitia is the major site of immune cell accumulation in standard chow-fed apolipoprotein E-deficient mice. *Arteriosclerosis, Thrombosis, and Vascular Biology*. **25**, 2386–91

107. Gräbner, R., Lötzer, K., Döpping, S., Hildner, M., Radke, D., Beer, M., Spanbroek, R., Lippert, B., Reardon, C. a, Getz, G. S., Fu, Y.-X., Hehlgans, T., Mebius, R. E., van der Wall, M., Kruspe, D., Englert, C., Lovas, A., Hu, D., Randolph, G. J., Weih, F., and Habenicht, A. J. R. (2009) Lymphotoxin beta receptor signaling promotes tertiary lymphoid organogenesis in the aorta adventitia of aged ApoE-/- mice. *The Journal of Experimental Medicine*. **206**, 233–48

108. Link, A., Hardie, D. L., Favre, S., Britschgi, M. R., Adams, D. H., Sixt, M., Cyster, J. G., Buckley, C. D., and Luther, S. A. (2011) Association of T-zone reticular networks and conduits with ectopic lymphoid tissues in mice and humans. *The American Journal of Pathology*. **178**, 1662–75

109. Barone, F., Gardner, D. H., Nayar, S., Steinthal, N., Buckley, C. D., and Luther, S. A. (2016) Stromal Fibroblasts in Tertiary Lymphoid Structures: A Novel Target in Chronic Inflammation. *Frontiers in Immunology*. **7**, 477

110. Corsiero, E., Nerviani, A., Bombardieri, M., and Pitzalis, C. (2016) Ectopic Lymphoid Structures: Powerhouse of Autoimmunity. *Frontiers in Immunology*. **7**, 1–6

111. Malhotra, D., Fletcher, A. L., and Turley, S. J. (2013) Stromal and hematopoietic cells in secondary lymphoid organs: Partners in immunity. *Immunological Reviews*. **251**, 160–176

112. Yin, C., Mohanta, S. K., Srikakulapu, P., Weber, C., and Habenicht, A. J. R. (2016) Artery Tertiary Lymphoid Organs: Powerhouses of

Atherosclerosis Immunity. *Frontiers in Immunology*. **7**, 387

113. Majesky, M. W., Dong, X. R., Hoglund, V., Mahoney, W. M., and Daum, G. (2011) The adventitia: a dynamic interface containing resident progenitor cells. *Arteriosclerosis, Thrombosis, and Vascular Biology*. **31**, 1530–9

114. Di Carlo, S. E., and Peduto, L. (2018) The perivascular origin of pathological fibroblasts. *The Journal of Clinical Investigation*. **128**, 54–63

115. Corselli, M., Chen, C.-W., Sun, B., Yap, S., Rubin, J. P., and Péault, B. (2012) The tunica adventitia of human arteries and veins as a source of mesenchymal stem cells. *Stem Cells and Development*. **21**, 1299–308

116. Hoshino, A., Chiba, H., Nagai, K., Ishii, G., and Ochiai, A. (2008) Human vascular adventitial fibroblasts contain mesenchymal stem/progenitor cells. *Biochemical and Biophysical Research Communications*. **368**, 305–310

117. Feisst, V., Brooks, A. E. S., Chen, C.-J. J., and Dunbar, P. R. (2014) Characterization of mesenchymal progenitor cell populations directly derived from human dermis. *Stem Cells and Development*. **23**, 631–42

118. Li, M., Riddle, S. R., Frid, M. G., El Kasmi, K. C., McKinsey, T. a, Sokol, R. J., Strassheim, D., Meyrick, B., Yeager, M. E., Flockton, A. R., McKeon, B. A., Lemon, D. D., Horn, T. R., Anwar, A., Barajas, C., and Stenmark, K. R. (2011) Emergence of fibroblasts with a proinflammatory epigenetically altered phenotype in severe hypoxic pulmonary hypertension. *Journal of Immunology (Baltimore, Md. : 1950)*. **187**, 2711–22

119. Hay, E. D. (2005) The mesenchymal cell, its role in the embryo, and the remarkable signaling mechanisms that create it. *Developmental Dynamics : an Official Publication of the American Association of Anatomists*. **233**, 706–20

120. Marsh, E., Gonzalez, D. G., Lathrop, E. A., Boucher, J., and Greco, V. (2018) Positional Stability and Membrane Occupancy Define Skin Fibroblast Homeostasis In Vivo. *Cell*. **175**, 1620-1633.e13

121. Chang, H. Y., Chi, J.-T., Dudoit, S., Bondre, C., van de Rijn, M., Botstein, D., and Brown, P. O. (2002) Diversity, topographic differentiation, and positional memory in human fibroblasts. *Proceedings of the National Academy of Sciences of the United States of America*. **99**, 12877–82

122. Filer, A., Parsonage, G., Smith, E., Osborne, C., Thomas, A. M. C., Curnow, S. J., Rainger, G. E., Raza, K., Nash, G. B., Lord, J., Salmon, M., and Buckley, C. D. (2006) Differential survival of leukocyte subsets

mediated by synovial, bone marrow, and skin fibroblasts: Site-specific versus activation-dependent survival of T cells and neutrophils. *Arthritis and Rheumatism*. **54**, 2096–2108

123. Mizoguchi, F., Slowikowski, K., Wei, K., Marshall, J. L., Rao, D. A., Chang, S. K., Nguyen, H. N., Noss, E. H., Turner, J. D., Earp, B. E., Blazar, P. E., Wright, J., Simmons, B. P., Donlin, L. T., Kalliolias, G. D., Goodman, S. M., Bykerk, V. P., Ivashkiv, L. B., Lederer, J. A., Hacohen, N., Nigrovic, P. A., Filer, A., Buckley, C. D., Raychaudhuri, S., and Brenner, M. B. (2018) Functionally distinct disease-associated fibroblast subsets in rheumatoid arthritis. *Nature Communications*. **9**, 789

124. Croft, A. P., Naylor, A. J., Marshall, J. L., Hardie, D. L., Zimmermann, B., Turner, J., Desanti, G., Adams, H., Yemm, A. I., Müller-Ladner, U., Dayer, J. M., Neumann, E., Filer, A., and Buckley, C. D. (2016) Rheumatoid synovial fibroblasts differentiate into distinct subsets in the presence of cytokines and cartilage. *Arthritis Research and Therapy*. **18**, 1–11

125. Driskell, R. R., Lichtenberger, B. M., Hoste, E., Kretzschmar, K., Simons, B. D., Charalambous, M., Ferron, S. R., Herault, Y., Pavlovic, G., Ferguson-Smith, A. C., and Watt, F. M. (2013) Distinct fibroblast lineages determine dermal architecture in skin development and repair. *Nature*. **504**, 277–281

126. Philippeos, C., Telerman, S. B., Oulès, B., Pisco, A. O., Shaw, T. J., Elgueta, R., Lombardi, G., Driskell, R. R., Soldin, M., Lynch, M. D., and Watt, F. M. (2018) Spatial and Single-Cell Transcriptional Profiling Identifies Functionally Distinct Human Dermal Fibroblast Subpopulations. *The Journal of Investigative Dermatology*. **138**, 811–825

127. Tabib, T., Morse, C., Wang, T., Chen, W., and Lafyatis, R. (2018) SFRP2/DPP4 and FMO1/LSP1 Define Major Fibroblast Populations in Human Skin. *The Journal of Investigative Dermatology*. **138**, 802–810

128. Ma'ayan, A., Sennett, R., Roitershtein, N., Rendl, M., Rezza, A., Wang, Z., Heitman, N. J., Mok, K. W., Grisanti, L., Sicchio, C., and Clavel, C. (2015) An Integrated Transcriptome Atlas of Embryonic Hair Follicle Progenitors, Their Niche, and the Developing Skin. *Developmental Cell*. 10.1016/j.devcel.2015.06.023

129. Rinkevich, Y., Walmsley, G. G., Hu, M. S., Maan, Z. N., Newman, A. M., Drukker, M., Januszyk, M., Krampitz, G. W., Gurtner, G. C., Lorenz, H. P., Weissman, I. L., and Longaker, M. T. (2015) Skin fibrosis. Identification and isolation of a dermal lineage with intrinsic fibrogenic potential. *Science (New York, N.Y.)*. **348**, aaa2151

130. Rodda, L. B., Lu, E., Bennett, M. L., Sokol, C. L., Wang, X., Luther, S. A., Barres, B. A., Luster, A. D., Ye, C. J., and Cyster, J. G. (2018) Single-Cell RNA Sequencing of Lymph Node Stromal Cells Reveals Niche-Associated Heterogeneity. *Immunity*. **48**, 1014-1028.e6

131. Cremasco, V., Woodruff, M. C., Onder, L., Cupovic, J., Nieves-Bonilla, J. M., Schildberg, F. a, Chang, J., Cremasco, F., Harvey, C. J., Wucherpfennig, K., Ludewig, B., Carroll, M. C., and Turley, S. J. (2014) B cell homeostasis and follicle confines are governed by fibroblastic reticular cells. *Nature Immunology*. **15**, 1–11

132. Katakai, T., Hara, T., Sugai, M., Gonda, H., and Shimizu, A. (2004) Lymph node fibroblastic reticular cells construct the stromal reticulum via contact with lymphocytes. *The Journal of Experimental Medicine*. **200**, 783–795

133. Katakai, T., Suto, H., Sugai, M., Gonda, H., Togawa, A., Suematsu, S., Ebisuno, Y., Katagiri, K., Kinashi, T., and Shimizu, A. (2008) Organizer-like reticular stromal cell layer common to adult secondary lymphoid organs. *Journal of Immunology (Baltimore, Md. : 1950)*. **181**, 6189–200

134. Takeuchi, A., Ozawa, M., Kanda, Y., Kozai, M., Ohigashi, I., Kurosawa, Y., Rahman, M. A., Kawamura, T., Shichida, Y., Umemoto, E., Miyasaka, M., Ludewig, B., Takahama, Y., Nagasawa, T., and Katakai, T. (2018) A Distinct Subset of Fibroblastic Stromal Cells Constitutes the Cortex-Medulla Boundary Subcompartment of the Lymph Node. *Frontiers in Immunology*. **9**, 2196

135. Bogdanova, D., Takeuchi, A., Ozawa, M., Kanda, Y., Rahman, M. A., Ludewig, B., Kinashi, T., and Katakai, T. (2018) Essential Role of Canonical NF-κB Activity in the Development of Stromal Cell Subsets in Secondary Lymphoid Organs. *Journal of Immunology (Baltimore, Md. : 1950)*. **201**, 3580–3586

136. Jarjour, M., Jorquera, A., Mondor, I., Wienert, S., Narang, P., Coles, M. C., Klauschen, F., and Bajénoff, M. (2014) Fate mapping reveals origin and dynamics of lymph node follicular dendritic cells. *The Journal of Experimental Medicine*. **211**, 1109–22

137. Mionnet, C., Mondor, I., Jorquera, A., Loosveld, M., Maurizio, J., Arcangeli, M.-L., Ruddle, N. H., Nowak, J., Aurrand-Lions, M., Luche, H., and Bajénoff, M. (2013) Identification of a new stromal cell type involved in the regulation of inflamed B cell follicles. *PLoS Biology*. **11**, e1001672

138. Lu, T. T., and Browning, J. L. (2014) Role of the Lymphotoxin/LIGHT System in the Development and Maintenance of Reticular Networks and

Vasculature in Lymphoid Tissues. *Frontiers in Immunology*. **5**, 47

139. Malhotra, D., Fletcher, A. L., Astarita, J., Lukacs-Kornek, V., Tayalia, P., Gonzalez, S. F., Elpek, K. G., Chang, S. K., Knoblich, K., Hemler, M. E., Brenner, M. B., Carroll, M. C., Mooney, D. J., Turley, S. J., Zhou, Y., Shinton, S. a, Hardy, R. R., Bezman, N. a, Sun, J. C., Kim, C. C., Lanier, L. L., Miller, J., Brown, B., Merad, M., Fletcher, A. L., Elpek, K. G., Bellemare-Pelletier, A., Malhotra, D., Turley, S. J., Narayan, K., Sylvia, K., Kang, J., Gazit, R., Garrison, B., Rossi, D. J., Jojic, V., Koller, D., Jianu, R., Laidlaw, D., Costello, J., Collins, J., Cohen, N., Brennan, P., Brenner, M. B., Shay, T., Regev, A., Kim, F., Rao, T. N., Wagers, A., Gautier, E. L., Jakubzick, C., Randolph, G. J., Monach, P., Best, A. J., Knell, J., Goldrath, A., Heng, T., Kreslavsky, T., Painter, M., Mathis, D., and Benoist, C. (2012) Transcriptional profiling of stroma from inflamed and resting lymph nodes defines immunological hallmarks. *Nature Immunology*. **13**, 499–510

140. Lu, C. P., Polak, L., Keyes, B. E., and Fuchs, E. (2016) Spatiotemporal antagonism in mesenchymal-epithelial signaling in sweat versus hair fate decision. *Science (New York, N.Y.)*. 10.1126/science.aah6102

141. Nayar, S., Campos, J., Smith, C. G., Iannizzotto, V., Gardner, D. H., Mourcin, F., Roulois, D., Turner, J., Sylvestre, M., Asam, S., Glaysher, B., Bowman, S. J., Fearon, D. T., Filer, A., Tarte, K., Luther, S. A., Fisher, B. A., Buckley, C. D., Coles, M. C., and Barone, F. (2019) Immunofibroblasts are pivotal drivers of tertiary lymphoid structure formation and local pathology. *Proceedings of the National Academy of Sciences of the United States of America*. **116**, 13490–13497

142. Turley, S. J., Cremasco, V., and Astarita, J. L. (2015) Immunological hallmarks of stromal cells in the tumour microenvironment. *Nature Reviews. Immunology*. **15**, 669–82

143. Kumar, V., Dasoveanu, D. C. C., Chyou, S., Tzeng, T.-C., Rozo, C., Liang, Y., Stohl, W., Fu, Y.-X., Ruddle, N. H. H., and Lu, T. T. T. (2015) A dendritic-cell-stromal axis maintains immune responses in lymph nodes. *Immunity*. **42**, 719–30

144. Chang, S. K., Noss, E. H., Chen, M., Gu, Z., Townsend, K., Grenha, R., Leon, L., Lee, S. Y., Lee, D. M., and Brenner, M. B. (2011) Cadherin-11 regulates fibroblast inflammation. *Proceedings of the National Academy of Sciences of the United States of America*. **108**, 8402–7

145. Croft, A. P., Campos, J., Jansen, K., Turner, J. D., Marshall, J., Attar, M., Savary, L., Wehmeyer, C., Naylor, A. J., Kemble, S., Begum, J., Dürholz, K., Perlman, H., Barone, F., McGettrick, H. M., Fearon, D. T., Wei, K.,

Raychaudhuri, S., Korsunsky, I., Brenner, M. B., Coles, M., Sansom, S. N., Filer, A., and Buckley, C. D. (2019) Distinct fibroblast subsets drive inflammation and damage in arthritis. *Nature*. **570**, 246–251

146. Perez-Shibayama, C., Gil-Cruz, C., Cheng, H.-W., Onder, L., Printz, A., Mörbe, U., Novkovic, M., Li, C., Lopez-Macias, C., Buechler, M. B., Turley, S. J., Mack, M., Soneson, C., Robinson, M. D., Scandella, E., Gommerman, J., and Ludewig, B. (2018) Fibroblastic reticular cells initiate immune responses in visceral adipose tissues and secure peritoneal immunity. *Science Immunology*. **3**, eaar4539

147. Fasnacht, N., Huang, H.-Y., Koch, U., Favre, S., Auderset, F., Chai, Q., Onder, L., Kallert, S., Pinschewer, D. D., MacDonald, H. R., Tacchini-Cottier, F., Ludewig, B., Luther, S. A., and Radtke, F. (2014) Specific fibroblastic niches in secondary lymphoid organs orchestrate distinct Notch-regulated immune responses. *The Journal of Experimental Medicine*. **211**, 2265–2279

148. Pikor, N. B., Astarita, J. L., Summers-Deluca, L., Galicia, G., Qu, J., Ward, L. A., Armstrong, S., Dominguez, C. X., Malhotra, D., Heiden, B., Kay, R., Castanov, V., Touil, H., Boon, L., O'Connor, P., Bar-Or, A., Prat, A., Ramaglia, V., Ludwin, S., Turley, S. J., and Gommerman, J. L. (2015) Integration of Th17- and Lymphotoxin-Derived Signals Initiates Meningeal-Resident Stromal Cell Remodeling to Propagate Neuroinflammation. *Immunity*. **43**, 1160–73

149. Chung, J., Ebens, C. L., Perkey, E., Radojcic, V., Koch, U., Scarpellino, L., Tong, A., Allen, F., Wood, S., Feng, J., Friedman, A., Granadier, D., Tran, I. T., Chai, Q., Onder, L., Yan, M., Reddy, P., Blazar, B. R., Huang, A. Y., Brennan, T. V, Bishop, D. K., Ludewig, B., Siebel, C. W., Radtke, F., Luther, S. A., and Maillard, I. (2017) Fibroblastic niches prime T cell alloimmunity through Delta-like Notch ligands. *The Journal of Clinical Investigation*. **127**, 1574–1588

150. Cheng, H.-W., Onder, L., Cupovic, J., Boesch, M., Novkovic, M., Pikor, N., Tarantino, I., Rodriguez, R., Schneider, T., Jochum, W., Brutsche, M., and Ludewig, B. (2018) CCL19-producing fibroblastic stromal cells restrain lung carcinoma growth by promoting local antitumor T-cell responses. *The Journal of Allergy and Clinical Immunology*. 10.1016/j.jaci.2017.12.998

151. Gil-Cruz, C., Perez-Shibayama, C., Onder, L., Chai, Q., Cupovic, J., Cheng, H.-W., Novkovic, M., Lang, P. A., Geuking, M. B., McCoy, K. D., Abe, S., Cui, G., Ikuta, K., Scandella, E., and Ludewig, B. (2016) Fibroblastic reticular cells regulate intestinal inflammation via IL-15-mediated control of group 1 ILCs. *Nature Immunology*. **17**, 1388–1396

152. Trojanowska, M. (2010) Cellular and molecular aspects of vascular dysfunction in systemic sclerosis. *Nature Reviews. Rheumatology*. **6**, 453–60

153. Allanore, Y., Distler, O., Matucci-Cerinic, M., and Denton, C. P. (2018) Review: Defining a Unified Vascular Phenotype in Systemic Sclerosis. *Arthritis & Rheumatology (Hoboken, N.J.)*. **70**, 162–170

154. Nazari, B., Rice, L. M., Stifano, G., Barron, A. M. S., Wang, Y. M., Korndorf, T., Lee, J., Bhawan, J., Lafyatis, R., and Browning, J. L. (2016) Altered Dermal Fibroblasts in Systemic Sclerosis Display Podoplanin and CD90. *The American Journal of Pathology*. **186**, 2650–64

155. Hu, Y., Zhang, Z., Torsney, E., Afzal, A. R., Davison, F., Metzler, B., and Xu, Q. (2004) Abundant progenitor cells in the adventitia contribute to atherosclerosis of vein grafts in ApoE-deficient mice. *Journal of Clinical Investigation*. 10.1172/JCI19628

156. Sambasivan, R., Yao, R., Kissenpfennig, A., Van Wittenberghe, L., Paldi, A., Gayraud-Morel, B., Guenou, H., Malissen, B., Tajbakhsh, S., and Galy, A. (2011) Pax7-expressing satellite cells are indispensable for adult skeletal muscle regeneration. *Development (Cambridge, England)*. **138**, 3647–56

157. von Maltzahn, J., Jones, A. E., Parks, R. J., and Rudnicki, M. A. (2013) Pax7 is critical for the normal function of satellite cells in adult skeletal muscle. *Proceedings of the National Academy of Sciences of the United States of America*. **110**, 16474–9

158. Yin, H., Price, F., and Rudnicki, M. A. (2013) Satellite Cells and the Muscle Stem Cell Niche. *Physiological Reviews*. **93**, 23–67

159. Hsu, Y.-C., Li, L., and Fuchs, E. (2014) Transit-amplifying cells orchestrate stem cell activity and tissue regeneration. *Cell*. **157**, 935–49

160. Yang, H., Adam, R. C., Ge, Y., Hua, Z. L., and Fuchs, E. (2017) Epithelial-Mesenchymal Micro-niches Govern Stem Cell Lineage Choices. *Cell*. **169**, 483-496.e13

161. Díaz-Flores, L., Gutiérrez, R., García, M. P., Sáez, F. J., Díaz-Flores, L., Valladares, F., and Madrid, J. F. (2014) CD34+ stromal cells/fibroblasts/fibrocytes/telocytes as a tissue reserve and a principal source of mesenchymal cells. Location, morphology, function and role in pathology. *Histology and Histopathology*. **29**, 831–70

162. Manetti, M., Guiducci, S., Ruffo, M., Rosa, I., Faussone-Pellegrini, M. S., Matucci-Cerinic, M., and Ibba-Manneschi, L. (2013) Evidence for progressive reduction and loss of telocytes in the dermal cellular network of systemic sclerosis. *Journal of Cellular and Molecular Medicine*. **17**, 482–496

163. Dulauroy, S., Di Carlo, S. E., Langa, F., Eberl, G., and Peduto, L. (2012) Lineage tracing and genetic ablation of ADAM12(+) perivascular cells identify a major source of profibrotic cells during acute tissue injury. *Nature Medicine*. **18**, 1262–70

164. Luther, S. A., Tang, H. L., Hyman, P. L., Farr, A. G., and Cyster, J. G. (2000) Coexpression of the chemokines ELC and SLC by T zone stromal cells and deletion of the ELC gene in the plt/plt mouse. *Proceedings of the National Academy of Sciences of the United States of America*. **97**, 12694–9

165. Adachi, S., Yoshida, H., Kataoka, H., and Nishikawa, S. (1997) Three distinctive steps in Peyer's patch formation of murine embryo. *International Immunology*. **9**, 507–14

166. Bajénoff, M., Egen, J. G., Koo, L. Y., Laugier, J. P., Brau, F., Glaichenhaus, N., and Germain, R. N. (2006) Stromal cell networks regulate lymphocyte entry, migration, and territoriality in lymph nodes. *Immunity*. **25**, 989–1001

167. Link, A., Vogt, T. K., Favre, S., Britschgi, M. R., Acha-Orbea, H., Hinz, B., Cyster, J. G., and Luther, S. A. (2007) Fibroblastic reticular cells in lymph nodes regulate the homeostasis of naive T cells. *Nature Immunology*. **8**, 1255–65

168. Finke, D., Acha-Orbea, H., Mattis, A., Lipp, M., and Kraehenbuhl, J. (2002) CD4+CD3- cells induce Peyer's patch development: role of alpha4beta1 integrin activation by CXCR5. *Immunity*. **17**, 363–73

169. Schluns, K. S., Nowak, E. C., Cabrera-Hernandez, A., Puddington, L., Lefrançois, L., and Aguila, H. L. (2004) Distinct cell types control lymphoid subset development by means of IL-15 and IL-15 receptor alpha expression. *Proceedings of the National Academy of Sciences of the United States of America*. **101**, 5616–21

170. Onder, L., Narang, P., Scandella, E., Chai, Q., Iolyeva, M., Hoorweg, K., Halin, C., Richie, E., Kaye, P., Westermann, J., Cupedo, T., Coles, M., and Ludewig, B. (2012) IL-7-producing stromal cells are critical for lymph node remodeling. *Blood*. **120**, 4675–83

171. Rappl, G., Kapsokefalou, A., Heuser, C., Rössler, M., Ugurel, S., Tilgen, W., Reinhold, U., and Abken, H. (2001) Dermal fibroblasts sustain proliferation of activated T cells via membrane-bound interleukin-15 upon long-term stimulation with tumor necrosis factor-alpha. *The Journal of Investigative Dermatology*. **116**, 102–9

172. Ngo, V. N., Korner, H., Gunn, M. D., Schmidt, K. N., Riminton, D. S., Cooper, M. D., Browning, J. L., Sedgwick, J. D., and Cyster, J. G. (1999) Lymphotoxin alpha/beta and tumor necrosis factor are required for stromal cell expression of homing chemokines in B and T cell areas of the spleen. *The Journal of Experimental Medicine*. **189**, 403–12

173. Zhao, L., Chen, J., Liu, L., Gao, J., Guo, B., and Zhu, B. (2015) Essential role of TNF-alpha in development of spleen fibroblastic reticular cells. *Cellular Immunology*. **293**, 130–6

174. Saito, Y., Respatika, D., Komori, S., Washio, K., Nishimura, T., Kotani, T., Murata, Y., Okazawa, H., Ohnishi, H., Kaneko, Y., Yui, K., Yasutomo, K., Nishigori, C., Nojima, Y., and Matozaki, T. (2017) SIRPα + dendritic cells regulate homeostasis of fibroblastic reticular cells via TNF receptor ligands in the adult spleen . *Proceedings of the National Academy of Sciences*. **114**, E10151–E10160

175. Kuprash, D. V., Alimzhanov, M. B., Tumanov, A. V., Pfeffer, K., Nedospasov, S. A., and Anderson, A. O. (1999) TNF and lymphotoxin β cooperate in the maintenance of secondary lymphoid tissue microarchitecture but not in the development of lymph nodes. *Journal of Immunology*. **163**, 6575–6580

176. White, A., Carragher, D., Parnell, S., Msaki, A., Perkins, N., Lane, P., Jenkinson, E., Anderson, G., and Caamaño, J. H. (2007) Lymphotoxin a-dependent and -independent signals regulate stromal organizer cell homeostasis during lymph node organogenesis. *Blood*. **110**, 1950–9

177. Bénézech, C., White, A., Mader, E., Serre, K., Parnell, S., Pfeffer, K., Ware, C. F., Anderson, G., and Caamaño, J. H. (2010) Ontogeny of stromal organizer cells during lymph node development. *Journal of Immunology (Baltimore, Md. : 1950)*. **184**, 4521–30

178. Chai, Q., Onder, L., Scandella, E., Gil-Cruz, C., Perez-Shibayama, C., Cupovic, J., Danuser, R., Sparwasser, T., Luther, S., Thiel, V., Rülicke, T., Stein, J., Hehlgans, T., and Ludewig, B. (2013) Maturation of Lymph Node Fibroblastic Reticular Cells from Myofibroblastic Precursors Is Critical for Antiviral Immunity. *Immunity*. **38**, 1013–1024

179. Schaeuble, K., Britschgi, M. R., Scarpellino, L., Favre, S., Xu, Y., Koroleva, E., Lissandrin, T. K. A., Link, A., Matloubian, M., Ware, C. F., Nedospasov, S. A., Tumanov, A. V., Cyster, J. G., and Luther, S. A. (2017) Perivascular Fibroblasts of the Developing Spleen Act as LTα1β2-Dependent Precursors of Both T and B Zone Organizer Cells. *Cell Reports*. **21**, 2500–2514

180. Sitnik, K. M., Wendland, K., Weishaupt, H., Uronen-Hansson, H., White, A. J., Anderson, G., Kotarsky, K., and Agace, W. W. (2016) Context-Dependent Development of Lymphoid Stroma from Adult CD34(+) Adventitial Progenitors. *Cell Reports*. **14**, 2375–88

181. Krautler, N. J., Kana, V., Kranich, J., Tian, Y., Perera, D., Lemm, D., Schwarz, P., Armulik, A., Browning, J. L., Tallquist, M., Buch, T., Oliveira-Martins, J. B., Zhu, C., Hermann, M., Wagner, U., Brink, R., Heikenwalder, M., and Aguzzi, A. (2012) Follicular dendritic cells emerge from ubiquitous perivascular precursors. *Cell*. **150**, 194–206

182. Cupovic, J., Onder, L., Gil-Cruz, C., Weiler, E., Caviezel-Firner, S., Perez-Shibayama, C., Rülicke, T., Bechmann, I., and Ludewig, B. (2016) Central Nervous System Stromal Cells Control Local CD8(+) T Cell Responses during Virus-Induced Neuroinflammation. *Immunity*. **44**, 622–33

183. Kratz, A., Campos-Neto, A., Hanson, M. S., and Ruddle, N. H. (1996) Chronic inflammation caused by lymphotoxin is lymphoid neogenesis. *The Journal of Experimental Medicine*. **183**, 1461–72

184. Weninger, W., Carlsen, H. S., Goodarzi, M., Moazed, F., Crowley, M. a, Baekkevold, E. S., Cavanagh, L. L., and von Andrian, U. H. (2003) Naive T cell recruitment to nonlymphoid tissues: a role for endothelium-expressed CC chemokine ligand 21 in autoimmune disease and lymphoid neogenesis. *Journal of Immunology (Baltimore, Md. : 1950)*. **170**, 4638–4648

185. Natsuaki, Y., Egawa, G., Nakamizo, S., Ono, S., Hanakawa, S., Okada, T., Kusuba, N., Otsuka, A., Kitoh, A., Honda, T., Nakajima, S., Tsuchiya, S., Sugimoto, Y., Ishii, K. J., Tsutsui, H., Yagita, H., Iwakura, Y., Kubo, M., Ng, L. G., Hashimoto, T., Fuentes, J., Guttman-Yassky, E., Miyachi, Y., and Kabashima, K. (2014) Perivascular leukocyte clusters are essential for efficient activation of effector T cells in the skin. *Nature Immunology*. **15**, 1064–9

186. Barron, A. M. S., Mantero, J. C., Ho, J. D., Nazari, B., Horback, K. L., Bhawan, J., Lafyatis, R., Lam, C., and Browning, J. L. (2019) Perivascular Adventitial Fibroblast Specialization Accompanies T Cell Retention in the

Inflamed Human Dermis. *Journal of Immunology (Baltimore, Md. : 1950)*. **202**, 56–68

187. Baekkevold, E. S., Yamanaka, T., Palframan, R. T., Carlsen, H. S., Reinholt, F. P., von Andrian, U. H., Brandtzaeg, P., and Haraldsen, G. (2001) The CCR7 ligand elc (CCL19) is transcytosed in high endothelial venules and mediates T cell recruitment. *The Journal of Experimental Medicine*. **193**, 1105–1112

188. Luther, S. A., Bidgol, A., Hargreaves, D. C., Schmidt, A., Xu, Y., Paniyadi, J., Matloubian, M., and Cyster, J. G. (2002) Differing activities of homeostatic chemokines CCL19, CCL21, and CXCL12 in lymphocyte and dendritic cell recruitment and lymphoid neogenesis. *Journal of Immunology (Baltimore, Md. : 1950)*. **169**, 424–33

189. Álvarez-Viejo, M., Menéndez-Menéndez, Y., and Otero-Hernández, J. (2015) CD271 as a marker to identify mesenchymal stem cells from diverse sources before culture. *World Journal of Stem Cells*. **7**, 470–6

190. Vaculik, C., Schuster, C., Bauer, W., Iram, N., Pfisterer, K., Kramer, G., Reinisch, A., Strunk, D., and Elbe-Bürger, A. (2012) Human dermis harbors distinct mesenchymal stromal cell subsets. *The Journal of Investigative Dermatology*. **132**, 563–74

191. Kumar, A., D'Souza, S. S., Moskvin, O. V., Toh, H., Wang, B., Zhang, J., Swanson, S., Guo, L.-W., Thomson, J. A., and Slukvin, I. I. (2017) Specification and Diversification of Pericytes and Smooth Muscle Cells from Mesenchymoangioblasts. *Cell Reports*. **19**, 1902–1916

192. Ansell, D. M., Campbell, L., Thomason, H. A., Brass, A., and Hardman, M. J. A statistical analysis of murine incisional and excisional acute wound models. *Wound Repair and Regeneration : Official Publication of the Wound Healing Society and the European Tissue Repair Society*. **22**, 281–7

193. Aprahamian, T., Rifkin, I., Bonegio, R., Hugel, B., Freyssinet, J.-M., Sato, K., Castellot, J. J., and Walsh, K. (2004) Impaired Clearance of Apoptotic Cells Promotes Synergy between Atherogenesis and Autoimmune Disease. *The Journal of Experimental Medicine*. **199**, 1121–1131

194. Schindelin, J., Arganda-Carreras, I., Frise, E., Kaynig, V., Longair, M., Pietzsch, T., Preibisch, S., Rueden, C., Saalfeld, S., Schmid, B., Tinevez, J.-Y., White, D. J., Hartenstein, V., Eliceiri, K., Tomancak, P., and Cardona, A. (2012) Fiji: an open-source platform for biological-image analysis. *Nature Methods*. **9**, 676–82

195. Rueden, C. T., Schindelin, J., Hiner, M. C., DeZonia, B. E., Walter, A. E., Arena, E. T., and Eliceiri, K. W. (2017) ImageJ2: ImageJ for the next generation of scientific image data. *BMC Bioinformatics*. **18**, 529

196. Ruifrok, A. C., and Johnston, D. A. (2001) Quantification of histochemical staining by color deconvolution. *Analytical and Quantitative Cytology and Histology*. **23**, 291–9

197. Rice, L. M., Padilla, C. M., McLaughlin, S. R., Mathes, A., Ziemek, J., Goummih, S., Nakerakanti, S., York, M., Farina, G., Whitfield, M. L., Spiera, R. F., Christmann, R. B., Gordon, J. K., Weinberg, J., Simms, R. W., and Lafyatis, R. (2015) Fresolimumab treatment decreases biomarkers and improves clinical symptoms in systemic sclerosis patients. *The Journal of Clinical Investigation*. **125**, 2795–807

198. Rice, L. M., Ziemek, J., Stratton, E. A., McLaughlin, S. R., Padilla, C. M., Mathes, A. L., Christmann, R. B., Stifano, G., Browning, J. L., Whitfield, M. L., Spiera, R. F., Gordon, J. K., Simms, R. W., Zhang, Y., and Lafyatis, R. (2015) A Longitudinal Biomarker for the Extent of Skin Disease in Patients With Diffuse Cutaneous Systemic Sclerosis. *Arthritis & Rheumatology*. **67**, 3004–3015

199. Jabbari, A., Suárez-Fariñas, M., Fuentes-Duculan, J., Gonzalez, J., Cueto, I., Franks, A. G., and Krueger, J. G. (2014) Dominant Th1 and minimal Th17 skewing in discoid lupus revealed by transcriptomic comparison with psoriasis. *The Journal of Investigative Dermatology*. **134**, 87–95

200. Suárez-Fariñas, M., Tintle, S. J., Shemer, A., Chiricozzi, A., Nograles, K., Cardinale, I., Duan, S., Bowcock, A. M., Krueger, J. G., and Guttman-Yassky, E. (2011) Nonlesional atopic dermatitis skin is characterized by broad terminal differentiation defects and variable immune abnormalities. *Journal of Allergy and Clinical Immunology*. **127**, 954-964.e4

201. Lafyatis, R., Mantero, J. C., Gordon, J., Kishore, N., Carns, M., Dittrich, H., Spiera, R., Simms, R. W., and Varga, J. (2017) Inhibition of β-Catenin Signaling in the Skin Rescues Cutaneous Adipogenesis in Systemic Sclerosis: A Randomized, Double-Blind, Placebo-Controlled Trial of C-82. *Journal of Investigative Dermatology*. **137**, 2473–2483

202. Johnson, W. E., Li, C., and Rabinovic, A. (2007) Adjusting batch effects in microarray expression data using empirical Bayes methods. *Biostatistics (Oxford, England)*. **8**, 118–27

203. Newman, A. M., Liu, C. L., Green, M. R., Gentles, A. J., Feng, W., Xu, Y., Hoang, C. D., Diehn, M., and Alizadeh, A. A. (2015) Robust enumeration of

cell subsets from tissue expression profiles. *Nature Methods*. **12**, 453–457

204. Farina, G. A., York, M. R., Di Marzio, M., Collins, C. A., Meller, S., Homey, B., Rifkin, I. R., Marshak-Rothstein, A., Radstake, T. R. D. J., and Lafyatis, R. (2010) Poly(I:C) Drives Type I IFN- and TGFβ-Mediated Inflammation and Dermal Fibrosis Simulating Altered Gene Expression in Systemic Sclerosis. *Journal of Investigative Dermatology*. **130**, 2583–2593

205. Joshi, R. (2013) Interface dermatitis. *Indian Journal of Dermatology, Venereology and Leprology*. **79**, 349–59

206. Tanaka, R., Iwasaki, Y., and Koprowski, H. (1975) Ultrastructural studies of perivascular cuffing cells in multiple sclerosis brain. *The American Journal of Pathology*. **81**, 467–78

207. Pitzalis, C., Jones, G. W., Bombardieri, M., and Jones, S. A. (2014) Ectopic lymphoid-like structures in infection, cancer and autoimmunity. *Nature Reviews. Immunology*. **14**, 447–62

208. Ley, K., Laudanna, C., Cybulsky, M. I., and Nourshargh, S. (2007) Getting to the site of inflammation: the leukocyte adhesion cascade updated. *Nature Reviews. Immunology*. **7**, 678–89

209. Ruddle, N. H. (2016) High Endothelial Venules and Lymphatic Vessels in Tertiary Lymphoid Organs: Characteristics, Functions, and Regulation. *Frontiers in Immunology*. **7**, 491

210. Barone, F., Gardner, D. H., Nayar, S., Steinthal, N., Buckley, C. D., and Luther, S. A. (2016) Stromal Fibroblasts in Tertiary Lymphoid Structures: A Novel Target in Chronic Inflammation. *Frontiers in Immunology*. **7**, 477

211. Cuzner, M. L., Hayes, G. M., Newcombe, J., and Woodroofe, M. N. (1988) The nature of inflammatory components during demyelination in multiple sclerosis. *Journal of Neuroimmunology*. **20**, 203–9

212. Stenmark, K. R., Yeager, M. E., El Kasmi, K. C., Nozik-Grayck, E., Gerasimovskaya, E. V, Li, M., Riddle, S. R., and Frid, M. G. (2013) The Adventitia: Essential Regulator of Vascular Wall Structure and Function. *Annual Review of Physiology*. **75**, 23–47

213. Wörsdörfer, P., Mekala, S. R., Bauer, J., Edenhofer, F., Kuerten, S., and Ergün, S. (2017) The vascular adventitia: An endogenous, omnipresent source of stem cells in the body. *Pharmacology & Therapeutics*. **171**, 13–29

214. Lemos, D. R., and Duffield, J. S. (2018) Tissue-resident mesenchymal stromal cells: Implications for tissue-specific antifibrotic therapies. *Science Translational Medicine*. 10.1126/scitranslmed.aan5174

215. Di Carlo, S. E., and Peduto, L. (2018) The perivascular origin of pathological fibroblasts. *Journal of Clinical Investigation*. **128**, 54–63

216. Majesky, M. W. (2015) Adventitia and perivascular cells. *Arteriosclerosis, Thrombosis, and Vascular Biology*. **35**, e31-5

217. Yin, C., Mohanta, S. K., Srikakulapu, P., Weber, C., and Habenicht, A. J. R. (2016) Artery Tertiary Lymphoid Organs: Powerhouses of Atherosclerosis Immunity. *Frontiers in Immunology*. **7**, 387

218. Burke, D. L., Frid, M. G., Kunrath, C. L., Karoor, V., Anwar, A., Wagner, B. D., Strassheim, D., and Stenmark, K. R. (2009) Sustained hypoxia promotes the development of a pulmonary artery-specific chronic inflammatory microenvironment. *American Journal of Physiology-Lung Cellular and Molecular Physiology*. **297**, L238–L250

219. Li, M., Riddle, S. R., Frid, M. G., El Kasmi, K. C., McKinsey, T. a, Sokol, R. J., Strassheim, D., Meyrick, B., Yeager, M. E., Flockton, A. R., McKeon, B. A., Lemon, D. D., Horn, T. R., Anwar, A., Barajas, C., and Stenmark, K. R. (2011) Emergence of Fibroblasts with a Proinflammatory Epigenetically Altered Phenotype in Severe Hypoxic Pulmonary Hypertension. *The Journal of Immunology*. **187**, 2711–2722

220. Schlesinger, M., and Bendas, G. (2015) Vascular cell adhesion molecule-1 (VCAM-1)--an increasing insight into its role in tumorigenicity and metastasis. *International Journal of Cancer*. **136**, 2504–14

221. Lobb, R. R., and Hemler, M. E. (1994) The pathophysiologic role of alpha 4 integrins in vivo. *Journal of Clinical Investigation*. **94**, 1722–1728

222. Taooka, Y., Chen, J., Yednock, T., and Sheppard, D. (1999) The integrin alpha9beta1 mediates adhesion to activated endothelial cells and transendothelial neutrophil migration through interaction with vascular cell adhesion molecule-1. *The Journal of Cell Biology*. **145**, 413–20

223. Bevilacqua, M. P. (1993) Endothelial-leukocyte adhesion molecules. *Annual Review of Immunology*. **11**, 767–804

224. Rabquer, B. J., Hou, Y., Del Galdo, F., Kenneth Haines, G., Gerber, M. L., Jimenez, S. A., Seibold, J. R., and Koch, A. E. (2009) The proadhesive phenotype of systemic sclerosis skin promotes myeloid cell adhesion via

ICAM-1 and VCAM-1. *Rheumatology (Oxford, England)*. **48**, 734–40

225. Gao, J. X., and Issekutz, A. C. (1996) Expression of VCAM-1 and VLA-4 dependent T-lymphocyte adhesion to dermal fibroblasts stimulated with proinflammatory cytokines. *Immunology*. **89**, 375–383

226. Dakin, S. G., Buckley, C. D., Al-Mossawi, M. H., Hedley, R., Martinez, F. O., Wheway, K., Watkins, B., and Carr, A. J. (2017) Persistent stromal fibroblast activation is present in chronic tendinopathy. *Arthritis Research & Therapy*. **19**, 16

227. Morales-Ducret, J., Wayner, E., Elices, M. J., Alvaro-Gracia, J. M., Zvaifler, N. J., and Firestein, G. S. (1992) Alpha 4/beta 1 integrin (VLA-4) ligands in arthritis. Vascular cell adhesion molecule-1 expression in synovium and on fibroblast-like synoviocytes. *Journal of Immunology (Baltimore, Md. : 1950)*. **149**, 1424–31

228. Maggi, L., Margheri, F., Luciani, C., Capone, M., Rossi, M. C., Chillà, A., Santarlasci, V., Mazzoni, A., Cimaz, R., Liotta, F., Maggi, E., Cosmi, L., Del Rosso, M., and Annunziato, F. (2016) Th1-Induced CD106 Expression Mediates Leukocytes Adhesion on Synovial Fibroblasts from Juvenile Idiopathic Arthritis Patients. *PLoS ONE*. **11**, e0154422

229. Li, H., Cybulsky, M. I., Gimbrone, M. A., and Libby, P. (1993) Inducible expression of vascular cell adhesion molecule-1 by vascular smooth muscle cells in vitro and within rabbit atheroma. *The American Journal of Pathology*. **143**, 1551–9

230. Alpers, C. E., Hudkins, K. L., Davis, C. L., Marsh, C. L., Riches, W., McCarty, J. M., Benjamin, C. D., Carlos, T. M., Harlan, J. M., and Lobb, R. (1993) Expression of vascular cell adhesion molecule-1 in kidney allograft rejection. *Kidney International*. **44**, 805–16

231. Verbeek, M. M., Westphal, J. R., Ruiter, D. J., and de Waal, R. M. (1995) T lymphocyte adhesion to human brain pericytes is mediated via very late antigen-4/vascular cell adhesion molecule-1 interactions. *Journal of Immunology (Baltimore, Md. : 1950)*. **154**, 5876–84

232. Rosenman, S. J., Shrikant, P., Dubb, L., Benveniste, E. N., and Ransohoff, R. M. (1995) Cytokine-induced expression of vascular cell adhesion molecule-1 (VCAM-1) by astrocytes and astrocytoma cell lines. *Journal of Immunology (Baltimore, Md. : 1950)*. **154**, 1888–99

233. Salomon, D. R., Crisa, L., Mojcik, C. F., Ishii, J. K., Klier, G., and Shevach, E. M. (1997) Vascular cell adhesion molecule-1 is expressed by cortical

thymic epithelial cells and mediates thymocyte adhesion. Implications for the function of alpha4beta1 (VLA4) integrin in T-cell development. *Blood*. **89**, 2461–71

234. Dal Canton, A. (1995) Adhesion molecules in renal disease. *Kidney International*. **48**, 1687–96

235. Wilkinson, L. S., Edwards, J. C., Poston, R. N., and Haskard, D. O. (1993) Expression of vascular cell adhesion molecule-1 in normal and inflamed synovium. *Laboratory Investigation; a Journal of Technical Methods and Pathology*. **68**, 82–8

236. Fujii, M., Tanaka, H., Nakamura, A., Suzuki, C., Harada, Y., Takamatsu, T., and Hamaoka, K. (2016) Histopathological Characteristics of Post-inflamed Coronary Arteries in Kawasaki Disease-like Vasculitis of Rabbits. *Acta Histochemica et Cytochemica*. **49**, 29–36

237. Libby, P., and Li, H. (1993) Vascular cell adhesion molecule-1 and smooth muscle cell activation during atherogenesis. *Journal of Clinical Investigation*. **92**, 538–539

238. Link, A., Vogt, T. K., Favre, S., Britschgi, M. R., Acha-Orbea, H., Hinz, B., Cyster, J. G., and Luther, S. A. (2007) Fibroblastic reticular cells in lymph nodes regulate the homeostasis of naive T cells. *Nature Immunology*. **8**, 1255–65

239. Huang, M. J., Osborn, L., Svahn, J., Schiffer, S. B., Eliseo, L., Zhou, L. J., Rhynhart, K., Benjamin, C. D., and Freedman, A. S. (1995) Expression of vascular cell adhesion molecule-1 by follicular dendritic cells. *Leukemia & Lymphoma*. **18**, 259–64

240. Myers, R. C., King, R. G., Carter, R. H., and Justement, L. B. (2013) Lymphotoxin α1β2 expression on B cells is required for follicular dendritic cell activation during the germinal center response. *European Journal of Immunology*. **43**, 348–59

241. Malhotra, D., Fletcher, A. L., Astarita, J., Lukacs-Kornek, V., Tayalia, P., Gonzalez, S. F., Elpek, K. G., Chang, S. K., Knoblich, K., Hemler, M. E., Brenner, M. B., Carroll, M. C., Mooney, D. J., Turley, S. J., Zhou, Y., Shinton, S. a, Hardy, R. R., Bezman, N. a, Sun, J. C., Kim, C. C., Lanier, L. L., Miller, J., Brown, B., Merad, M., Fletcher, A. L., Elpek, K. G., Bellemare-Pelletier, A., Malhotra, D., Turley, S. J., Narayan, K., Sylvia, K., Kang, J., Gazit, R., Garrison, B., Rossi, D. J., Jojic, V., Koller, D., Jianu, R., Laidlaw, D., Costello, J., Collins, J., Cohen, N., Brennan, P., Brenner, M. B., Shay, T., Regev, A., Kim, F., Rao, T. N., Wagers, A., Gautier, E. L., Jakubzick,

C., Randolph, G. J., Monach, P., Best, A. J., Knell, J., Goldrath, A., Heng, T., Kreslavsky, T., Painter, M., Mathis, D., and Benoist, C. (2012) Transcriptional profiling of stroma from inflamed and resting lymph nodes defines immunological hallmarks. *Nature Immunology*. **13**, 499–510

242. Link, A., Hardie, D. L., Favre, S., Britschgi, M. R., Adams, D. H., Sixt, M., Cyster, J. G., Buckley, C. D., and Luther, S. A. (2011) Association of T-Zone Reticular Networks and Conduits with Ectopic Lymphoid Tissues in Mice and Humans. *The American Journal of Pathology*. **178**, 1662–1675

243. Marinkovic, T. (2006) Interaction of mature CD3+CD4+ T cells with dendritic cells triggers the development of tertiary lymphoid structures in the thyroid. *Journal of Clinical Investigation*. **116**, 2622–2632

244. Finke, D., Acha-Orbea, H., Mattis, A., Lipp, M., and Kraehenbuhl, J. P. (2002) CD4+CD3- cells induce Peyer's patch development: role of a4β1 integrin activation by CXCR5. *Immunity*. **17**, 363–373

245. Lo, C. G., Lu, T. T., and Cyster, J. G. (2003) Integrin-dependence of lymphocyte entry into the splenic white pulp. *The Journal of Experimental Medicine*. **197**, 353–61

246. Lu, T. T., and Cyster, J. G. (2002) Integrin-mediated long-term B cell retention in the splenic marginal zone. *Science (New York, N.Y.)*. **297**, 409–12

247. Enzler, T., Bonizzi, G., Silverman, G. J., Otero, D. C., Widhopf, G. F., Anzelon-Mills, A., Rickert, R. C., and Karin, M. (2006) Alternative and classical NF-kappa B signaling retain autoreactive B cells in the splenic marginal zone and result in lupus-like disease. *Immunity*. **25**, 403–415

248. DiLillo, D. J., Hamaguchi, Y., Ueda, Y., Yang, K., Uchida, J., Haas, K. M., Kelsoe, G., and Tedder, T. F. (2008) Maintenance of long-lived plasma cells and serological memory despite mature and memory B cell depletion during CD20 immunotherapy in mice. *Journal of Immunology (Baltimore, Md. : 1950)*. **180**, 361–71

249. Teixidó, J., Hemler, M. E., Greenberger, J. S., and Anklesaria, P. (1992) Role of beta 1 and beta 2 integrins in the adhesion of human CD34hi stem cells to bone marrow stroma. *The Journal of Clinical Investigation*. **90**, 358–67

250. Nevers, T., Salvador, A. M., Velazquez, F., Ngwenyama, N., Carrillo-Salinas, F. J., Aronovitz, M., Blanton, R. M., and Alcaide, P. (2017) Th1 effector T cells selectively orchestrate cardiac fibrosis in nonischemic heart

failure. *The Journal of Experimental Medicine*. **214**, 3311–3329

251. Koch, A. E., Kronfeld-Harrington, L. B., Szekanecz, Z., Cho, M. M., Haines, G. K., Harlow, L. A., Strieter, R. M., Kunkel, S. L., Massa, M. C., Barr, W. G., and et al. (1993) In situ expression of cytokines and cellular adhesion molecules in the skin of patients with systemic sclerosis. Their role in early and late disease. *Pathobiology*. **61**, 239–246

252. Jones, S. M., Mathew, C. M., Dixey, J., Lovell, C. R., and McHugh, N. J. (1996) VCAM-1 expression on endothelium in lesions from cutaneous lupus erythematosus is increased compared with systemic and localized scleroderma. *The British Journal of Dermatology*. **135**, 678–86

253. Kuhn, A., Sonntag, M., Lehmann, P., Megahed, M., Vestweber, D., and Ruzicka, T. (2002) Characterization of the inflammatory infiltrate and expression of endothelial cell adhesion molecules in lupus erythematosus tumidus. *Archives of Dermatological Research*. **294**, 6–13

254. Wang, X.-N., McGovern, N., Gunawan, M., Richardson, C., Windebank, M., Siah, T.-W., Lim, H.-Y., Fink, K., Yao Li, J. L., Ng, L. G., Ginhoux, F., Angeli, V., Collin, M., and Haniffa, M. (2014) A three-dimensional atlas of human dermal leukocytes, lymphatics, and blood vessels. *The Journal of Investigative Dermatology*. **134**, 965–974

255. Obermoser, G., Sontheimer, R., and Zelger, B. (2010) Overview of common, rare and atypical manifestations of cutaneous lupus erythematosus and histopathological correlates. *Lupus*. **19**, 1050–1070

256. Thorpe, R. B., Gray, A., Kumar, K. R., Susa, J. S., and Chong, B. F. (2014) Site-specific analysis of inflammatory markers in discoid lupus erythematosus skin. *The Scientific World Journal*. **2014**, 925805

257. Leung, D. Y., Bhan, A. K., Schneeberger, E. E., and Geha, R. S. (1983) Characterization of the mononuclear cell infiltrate in atopic dermatitis using monoclonal antibodies. *The Journal of Allergy and Clinical Immunology*. **71**, 47–56

258. Ho, J. D., Chung, H. J., MS Barron, A., Ho, D. A., Sahni, D., Browning, J. L., and Bhawan, J. (2019) Extensive CD34-to-CD90 Fibroblast Transition Defines Regions of Cutaneous Reparative, Hypertrophic, and Keloidal Scarring. *The American Journal of Dermatopathology*. **41**, 16–28

259. Corselli, M., Chen, C.-W., Sun, B., Yap, S., Rubin, J. P., and Péault, B. (2012) The tunica adventitia of human arteries and veins as a source of mesenchymal stem cells. *Stem Cells and Development*. **21**, 1299–308

260. Tigges, U., Komatsu, M., and Stallcup, W. B. (2013) Adventitial Pericyte Progenitor/Mesenchymal Stem Cells Participate in the Restenotic Response to Arterial Injury. *Journal of Vascular Research*. **50**, 134–144

261. Armulik, A., Genové, G., and Betsholtz, C. (2011) Pericytes: Developmental, Physiological, and Pathological Perspectives, Problems, and Promises. *Developmental Cell*. **21**, 193–215

262. Rappl, G., Kapsokefalou, A., Heuser, C., Rössler, M., Ugurel, S., Tilgen, W., Reinhold, U., and Abken, H. (2001) Dermal fibroblasts sustain proliferation of activated T cells via membrane-bound interleukin-15 upon long-term stimulation with tumor necrosis factor-alpha. *The Journal of Investigative Dermatology*. **116**, 102–9

263. Marsee, D. K., Pinkus, G. S., and Hornick, J. L. (2009) Podoplanin (D2-40) is a highly effective marker of follicular dendritic cells. *Applied Immunohistochemistry & Molecular Morphology : AIMM*. **17**, 102–7

264. Rodda, L. B., Lu, E., Bennett, M. L., Sokol, C. L., Wang, X., Luther, S. A., Barres, B. A., Luster, A. D., Ye, C. J., and Cyster, J. G. (2018) Single-Cell RNA Sequencing of Lymph Node Stromal Cells Reveals Niche-Associated Heterogeneity. *Immunity*. **48**, 1014-1028.e6

265. Mizoguchi, F., Slowikowski, K., Wei, K., Marshall, J. L., Rao, D. A., Chang, S. K., Nguyen, H. N., Noss, E. H., Turner, J. D., Earp, B. E., Blazar, P. E., Wright, J., Simmons, B. P., Donlin, L. T., Kalliolias, G. D., Goodman, S. M., Bykerk, V. P., Ivashkiv, L. B., Lederer, J. A., Hacohen, N., Nigrovic, P. A., Filer, A., Buckley, C. D., Raychaudhuri, S., and Brenner, M. B. (2018) Functionally distinct disease-associated fibroblast subsets in rheumatoid arthritis. *Nature Communications*. **9**, 789

266. Philippeos, C., Telerman, S. B., Oulès, B., Pisco, A. O., Shaw, T. J., Elgueta, R., Lombardi, G., Driskell, R. R., Soldin, M., Lynch, M. D., and Watt, F. M. (2018) Spatial and Single-Cell Transcriptional Profiling Identifies Functionally Distinct Human Dermal Fibroblast Subpopulations. *Journal of Investigative Dermatology*. **138**, 811–825

267. Hayakawa, M., Kobayashi, M., and Hoshino, T. (1990) Microfibrils: a constitutive component of reticular fibers in the mouse lymph node. *Cell and Tissue Research*. **262**, 199–201

268. Miyata, K., and Takaya, K. (1981) Elastic fibers associated with collagenous fibrils surrounded by reticular cells in lymph nodes of the rat as revealed by electron microscopy after orcein staining. *Cell and Tissue Research*. **220**, 445–8

269. Steiniger, B. S., Wilhelmi, V., Seiler, A., Lampp, K., and Stachniss, V. (2014) Heterogeneity of stromal cells in the human splenic white pulp. Fibroblastic reticulum cells, follicular dendritic cells and a third superficial stromal cell type. *Immunology*. **143**, 462–77

270. Stenmark, K. R., Meyrick, B., Galie, N., Mooi, W. J., and McMurtry, I. F. (2009) Animal models of pulmonary arterial hypertension: the hope for etiological discovery and pharmacological cure. *American Journal of Physiology-Lung Cellular and Molecular Physiology*. **297**, L1013–L1032

271. Benahmed, F., Chyou, S., Dasoveanu, D., Chen, J., Kumar, V., Iwakura, Y., and Lu, T. T. (2014) Multiple CD11c+ cells collaboratively express IL-1β to modulate stromal vascular endothelial growth factor and lymph node vascular-stromal growth. *Journal of Immunology (Baltimore, Md. : 1950)*. **192**, 4153–63

272. Ekwall, A.-K. H., Eisler, T., Anderberg, C., Jin, C., Karlsson, N., Brisslert, M., and Bokarewa, M. I. (2011) The tumour-associated glycoprotein podoplanin is expressed in fibroblast-like synoviocytes of the hyperplastic synovial lining layer in rheumatoid arthritis. *Arthritis Research & Therapy*. **13**, R40

273. Gil-Cruz, C., Perez-Shibayama, C., Onder, L., Chai, Q., Cupovic, J., Cheng, H.-W., Novkovic, M., Lang, P. A., Geuking, M. B., McCoy, K. D., Abe, S., Cui, G., Ikuta, K., Scandella, E., and Ludewig, B. (2016) Fibroblastic reticular cells regulate intestinal inflammation via IL-15-mediated control of group 1 ILCs. *Nature Immunology*. **17**, 1388–1396

274. Cui, G., Hara, T., Simmons, S., Wagatsuma, K., Abe, A., Miyachi, H., Kitano, S., Ishii, M., Tani-ichi, S., and Ikuta, K. (2014) Characterization of the IL-15 niche in primary and secondary lymphoid organs in vivo. *Proceedings of the National Academy of Sciences of the United States of America*. **111**, 1915–20

275. Schluns, K. S., Klonowski, K. D., and Lefrançois, L. (2004) Transregulation of memory CD8 T-cell proliferation by IL-15Ralpha+ bone marrow-derived cells. *Blood*. **103**, 988–94

276. Chen, L., Lin, S., Amin, S., Overbergh, L., Maggiolino, G., and Chan, L. S. VCAM-1 blockade delays disease onset, reduces disease severity and inflammatory cells in an atopic dermatitis model. *Immunology and Cell Biology*. **88**, 334–42

277. Cybulsky, M. I., Iiyama, K., Li, H., Zhu, S., Chen, M., Iiyama, M., Davis, V., Gutierrez-Ramos, J.-C., Connelly, P. W., and Milstone, D. S. (2001) A

major role for VCAM-1, but not ICAM-1, in early atherosclerosis. *Journal of Clinical Investigation*. **107**, 1255–1262

278. Matucci-Cerinic, M., Manetti, M., Bruni, C., Chora, I., Bellando-Randone, S., Lepri, G., De Paulis, A., and Guiducci, S. (2017) The “myth” of loss of angiogenesis in systemic sclerosis: a pivotal early pathogenetic process or just a late unavoidable event? *Arthritis Research & Therapy*. **19**, 162

279. Samaniego, R., Estecha, A., Relloso, M., Longo, N., Escat, J. L., Longo-Imedio, I., Avilés, J. a, del Pozo, M. Á., Puig-Kröger, A., and Sánchez-Mateos, P. (2013) Mesenchymal Contribution to Recruitment, Infiltration, and Positioning of Leukocytes in Human Melanoma Tissues. *Journal of Investigative Dermatology*. **133**, 2255–2264

280. Karnoub, A. E., Dash, A. B., Vo, A. P., Sullivan, A., Brooks, M. W., Bell, G. W., Richardson, A. L., Polyak, K., Tubo, R., and Weinberg, R. A. (2007) Mesenchymal stem cells within tumour stroma promote breast cancer metastasis. *Nature*. **449**, 557–63

281. Pestell, T. G., Jiao, X., Kumar, M., Peck, A. R., Prisco, M., Deng, S., Li, Z., Ertel, A., Casimiro, M. C., Ju, X., Di Rocco, A., Di Sante, G., Katiyar, S., Shupp, A., Lisanti, M. P., Jain, P., Wu, K., Rui, H., Hooper, D. C., Yu, Z., Goldman, A. R., Speicher, D. W., Laury-Kleintop, L., and Pestell, R. G. (2017) Stromal cyclin D1 promotes heterotypic immune signaling and breast cancer growth. *Oncotarget*. **8**, 81754–81775

282. Takahashi, H., Sakakura, K., Kawabata-Iwakawa, R., Rokudai, S., Toyoda, M., Nishiyama, M., and Chikamatsu, K. (2015) Immunosuppressive activity of cancer-associated fibroblasts in head and neck squamous cell carcinoma. *Cancer Immunology, Immunotherapy : CII*. **64**, 1407–17

283. Nakagawa, H., Liyanarachchi, S., Davuluri, R. V., Auer, H., Martin, E. W., de la Chapelle, A., and Frankel, W. L. (2004) Role of cancer-associated stromal fibroblasts in metastatic colon cancer to the liver and their expression profiles. *Oncogene*. **23**, 7366–77

284. Tirosh, I., Izar, B., Prakadan, S. M., Wadsworth, M. H., Treacy, D., Trombetta, J. J., Rotem, A., Rodman, C., Lian, C., Murphy, G., Fallahi-Sichani, M., Dutton-Regester, K., Lin, J., Cohen, O., Shah, P., Lu, D., Genshaft, A. S., Hughes, T. K., Ziegler, C. G. K., Kazer, S. W., Gaillard, A., Kolb, K. E., Villani, A.-C., Johannessen, C. M., Andreev, A. Y., Van Allen, E. M., Bertagnolli, M., Sorger, P. K., Sullivan, R. J., Flaherty, K. T., Frederick, D. T., Jané-Valbuena, J., Yoon, C. H., Rozenblatt-Rosen, O., Shalek, A. K., Regev, A., and Garraway, L. A. (2016) Dissecting the multicellular ecosystem of metastatic melanoma by single-cell RNA-seq.

Science (New York, N.Y.). **352**, 189–96

285. Bénézech, C., Mader, E., Desanti, G., Khan, M., Nakamura, K., White, A., Ware, C. F., Anderson, G., and Caamaño, J. H. (2012) Lymphotoxin-β receptor signaling through NF-κB2-RelB pathway reprograms adipocyte precursors as lymph node stromal cells. *Immunity*. **37**, 721–34

286. Sitnik, K. M., Wendland, K., Weishaupt, H., Uronen-Hansson, H., White, A. J., Anderson, G., Kotarsky, K., and Agace, W. W. (2016) Context-Dependent Development of Lymphoid Stroma from Adult CD34(+) Adventitial Progenitors. *Cell Reports*. **14**, 2375–88

287. Nishikawa, S., Nishikawa, S., Honda, K., Hashi, H., and Yoshida, H. (1998) Peyer's patch organogenesis as a programmed inflammation: a hypothetical model. *Cytokine & Growth Factor Reviews*. **9**, 213–20

288. Peduto, L., Dulauroy, S., Lochner, M., Späth, G. F., Morales, M. A., Cumano, A., and Eberl, G. (2009) Inflammation recapitulates the ontogeny of lymphoid stromal cells. *Journal of Immunology (Baltimore, Md. : 1950)*. **182**, 5789–99

289. Katakai, T., Hara, T., Sugai, M., Gonda, H., and Shimizu, A. (2004) Lymph Node Fibroblastic Reticular Cells Construct the Stromal Reticulum via Contact with Lymphocytes. *The Journal of Experimental Medicine*. **200**, 783–795

290. Assassi, S., Mayes, M. D., Arnett, F. C., Gourh, P., Agarwal, S. K., McNearney, T. A., Chaussabel, D., Oommen, N., Fischbach, M., Shah, K. R., Charles, J., Pascual, V., Reveille, J. D., and Tan, F. K. (2010) Systemic sclerosis and lupus: Points in an interferon-mediated continuum. *Arthritis & Rheumatism*. **62**, 589–598

291. Chyou, S., Ekland, E. H., Carpenter, A. C., Tzeng, T.-C. J., Tian, S., Michaud, M., Madri, J. A., and Lu, T. T. (2008) Fibroblast-type reticular stromal cells regulate the lymph node vasculature. *Journal of Immunology (Baltimore, Md. : 1950)*. **181**, 3887–96

292. Moussion, C., and Girard, J. P. (2011) Dendritic cells control lymphocyte entry to lymph nodes through high endothelial venules. *Nature*. **479**, 542–546

293. Kumar, V., Dasoveanu, D. C., Chyou, S., Tzeng, T.-C., Rozo, C., Liang, Y., Stohl, W., Fu, Y.-X., Ruddle, N. H., and Lu, T. T. (2015) A dendritic-cell-stromal axis maintains immune responses in lymph nodes. *Immunity*. **42**, 719–30

294. Saito, Y., Respatika, D., Komori, S., Washio, K., Nishimura, T., Kotani, T., Murata, Y., Okazawa, H., Ohnishi, H., Kaneko, Y., Yui, K., Yasutomo, K., Nishigori, C., Nojima, Y., and Matozaki, T. (2017) SIRPα+ dendritic cells regulate homeostasis of fibroblastic reticular cells via TNF receptor ligands in the adult spleen. *Proceedings of the National Academy of Sciences of the United States of America*. **114**, E10151–E10160

295. Lewis, T. (1940) Notes on Scleroderma (Dermatomyositis). *British Journal of Dermatology*. **52**, 233–242

296. Campbell, P. M., and LeRoy, E. C. (1975) Pathogenesis of systemic sclerosis: A vascular hypothesis. *Seminars in Arthritis and Rheumatism*. **4**, 351–368

297. Wigley, F. M., and Flavahan, N. A. (2016) Raynaud's Phenomenon. *New England Journal of Medicine*. **375**, 556–565

298. Allanore, Y., Distler, O., Matucci-Cerinic, M., and Denton, C. P. (2018) Review: Defining a Unified Vascular Phenotype in Systemic Sclerosis. *Arthritis & Rheumatology*. **70**, 162–170

299. Flavahan, N. A. (2015) A vascular mechanistic approach to understanding Raynaud phenomenon. *Nature Reviews. Rheumatology*. **11**, 146–58

300. Trojanowska, M. (2010) Cellular and molecular aspects of vascular dysfunction in systemic sclerosis. *Nature Reviews. Rheumatology*. **6**, 453–460

301. Manetti, M., Guiducci, S., Ibba-Manneschi, L., and Matucci-Cerinic, M. (2010) Mechanisms in the loss of capillaries in systemic sclerosis: angiogenesis versus vasculogenesis. *Journal of Cellular and Molecular Medicine*. **14**, 1241–1254

302. Stenmark, K. R., Meyrick, B., Galie, N., Mooi, W. J., and McMurtry, I. F. (2009) Animal models of pulmonary arterial hypertension: the hope for etiological discovery and pharmacological cure. *American Journal of Physiology-Lung Cellular and Molecular Physiology*. **297**, L1013–L1032

303. Majesky, M. W. (2015) Adventitia and Perivascular Cells. *Arteriosclerosis, Thrombosis, and Vascular Biology*. **35**, e31-5

304. Kelly, R. H., Balfour, B. M., Armstrong, J. A., and Griffith, S. (1978) Functional anatomy of lymph nodes. II. Peripheral lymph-borne mononuclear cells. *The Anatomical Record*. **190**, 5–21

305. Knight, S. C., Balfour, B. M., O'Brien, J., Buttifant, L., Sumerska, T., and Clarke, J. (1982) Role of veiled cells in lymphocyte activation. *European Journal of Immunology*. **12**, 1057–1060

306. Stenmark, K. R., Yeager, M. E., El Kasmi, K. C., Nozik-Grayck, E., Gerasimovskaya, E. V, Li, M., Riddle, S. R., and Frid, M. G. (2013) The Adventitia: Essential Regulator of Vascular Wall Structure and Function. *Annual Review of Physiology*. **75**, 23–47

307. Gu, W., Ni, Z., Tan, Y.-Q., Deng, J., Zhang, S.-J., Lv, Z.-C., Wang, X.-J., Chen, T., Zhang, Z., Hu, Y., Jing, Z.-C., and Xu, Q. (2019) Adventitial Cell Atlas of wt (Wild Type) and ApoE (Apolipoprotein E)-Deficient Mice Defined by Single-Cell RNA Sequencing. *Arteriosclerosis, Thrombosis, and Vascular Biology*. **39**, 1055–1071

308. Wang, J., Wang, Y., Wang, J., Guo, X., Chan, E. C., and Jiang, F. (2018) Adventitial Activation in the Pathogenesis of Injury-Induced Arterial Remodeling. *The American Journal of Pathology*. **188**, 838–845

309. Meijles, D. N., and Pagano, P. J. (2016) Nox and Inflammation in the Vascular Adventitia. *Hypertension*. **67**, 14–19

310. Yin, C., Mohanta, S. K., Srikakulapu, P., Weber, C., and Habenicht, A. J. R. (2016) Artery Tertiary Lymphoid Organs: Powerhouses of Atherosclerosis Immunity. *Frontiers in Immunology*. **7**, 387

311. Dutzmann, J., Koch, A., Weisheit, S., Sonnenschein, K., Korte, L., Haertlé, M., Thum, T., Bauersachs, J., Sedding, D. G., and Daniel, J.-M. (2017) Sonic hedgehog-dependent activation of adventitial fibroblasts promotes neointima formation. *Cardiovascular Research*. **113**, 1653–1663

312. Chen, Y., Wong, M. M., Campagnolo, P., Simpson, R., Winkler, B., Margariti, A., Hu, Y., and Xu, Q. (2013) Adventitial Stem Cells in Vein Grafts Display Multilineage Potential That Contributes to Neointimal Formation. *Arteriosclerosis, Thrombosis, and Vascular Biology*. **33**, 1844–1851

313. Hu, Y., Zhang, Z., Torsney, E., Afzal, A. R., Davison, F., Metzler, B., and Xu, Q. (2004) Abundant progenitor cells in the adventitia contribute to atherosclerosis of vein grafts in ApoE-deficient mice. *Journal of Clinical Investigation*. **113**, 1258–1265

314. Passman, J. N., Dong, X. R., Wu, S.-P., Maguire, C. T., Hogan, K. A., Bautch, V. L., and Majesky, M. W. (2008) A sonic hedgehog signaling domain in the arterial adventitia supports resident Sca1+ smooth muscle

progenitor cells. *Proceedings of the National Academy of Sciences of the United States of America*. **105**, 9349–54

315. Zhang, L., Issa Bhaloo, S., Chen, T., Zhou, B., and Xu, Q. (2018) Role of Resident Stem Cells in Vessel Formation and Arteriosclerosis. *Circulation Research*. **122**, 1608–1624

316. Psaltis, P. J., and Simari, R. D. (2015) Vascular Wall Progenitor Cells in Health and Disease. *Circulation Research*. **116**, 1392–1412

317. Hepler, C., Shan, B., Zhang, Q., Henry, G. H., Shao, M., Vishvanath, L., Ghaben, A. L., Mobley, A. B., Strand, D., Hon, G. C., and Gupta, R. K. (2018) Identification of functionally distinct fibro-inflammatory and adipogenic stromal subpopulations in visceral adipose tissue of adult mice. *eLife*. **7**, 1–36

318. Kramann, R., Goettsch, C., Wongboonsin, J., Iwata, H., Schneider, R. K., Kuppe, C., Kaesler, N., Chang-Panesso, M., Machado, F. G., Gratwohl, S., Madhurima, K., Hutcheson, J. D., Jain, S., Aikawa, E., and Humphreys, B. D. (2016) Adventitial MSC-like Cells Are Progenitors of Vascular Smooth Muscle Cells and Drive Vascular Calcification in Chronic Kidney Disease. *Cell Stem Cell*. **19**, 628–642

319. Sitnik, K. M., Wendland, K., Weishaupt, H., Uronen-Hansson, H., White, A. J., Anderson, G., Kotarsky, K., and Agace, W. W. (2016) Context-Dependent Development of Lymphoid Stroma from Adult CD34+ Adventitial Progenitors. *Cell Reports*. **14**, 2375–2388

320. Schaeuble, K., Britschgi, M. R., Scarpellino, L., Favre, S., Xu, Y., Koroleva, E., Lissandrin, T. K. A., Link, A., Matloubian, M., Ware, C. F., Nedospasov, S. A., Tumanov, A. V., Cyster, J. G., and Luther, S. A. (2017) Perivascular Fibroblasts of the Developing Spleen Act as LTα1β2-Dependent Precursors of Both T and B Zone Organizer Cells. *Cell Reports*. **21**, 2500–2514

321. Lemos, D. R., and Duffield, J. S. (2018) Tissue-resident mesenchymal stromal cells: Implications for tissue-specific antifibrotic therapies. *Science Translational Medicine*. 10.1126/scitranslmed.aan5174

322. Di Carlo, S. E., and Peduto, L. (2018) The perivascular origin of pathological fibroblasts. *Journal of Clinical Investigation*. **128**, 54–63

323. Perosio, P. M., and Brooks, J. J. (1988) Expression of nerve growth factor receptor in paraffin-embedded soft tissue tumors. *The American Journal of Pathology*. **132**, 152–60

324. Fantini, F., and Johansson, O. (1992) Expression of growth-associated protein 43 and nerve growth factor receptor in human skin: a comparative immunohistochemical investigation. *The Journal of Investigative Dermatology*. **99**, 734–42

325. Cattoretti, G., Schiró, R., Orazi, A., Soligo, D., and Colombo, M. P. (1993) Bone marrow stroma in humans: anti-nerve growth factor receptor antibodies selectively stain reticular cells in vivo and in vitro. *Blood*. **81**, 1726–38

326. Thompson, S. J., Schatteman, G. C., Gown, A. M., and Bothwell, M. (1989) A Monoclonal Antibody Against Nerve Growth Factor Receptor: Immunohistochemical Analysis of Normal and Neoplastic Human Tissue. *American Journal of Clinical Pathology*. **92**, 415–423

327. Otaibi, S., Jukic, D. M., Drogowski, L., Bhawan, J., and Radfar, A. (2011) NGFR (p75) Expression in Cutaneous Scars; Further Evidence for a Potential Pitfall in Evaluation of Reexcision Scars of Cutaneous Neoplasms, in Particular Desmoplastic Melanoma. *The American Journal of Dermatopathology*. **33**, 65–71

328. Lv, F.-J., Tuan, R. S., Cheung, K. M. C., and Leung, V. Y. L. (2014) Concise review: the surface markers and identity of human mesenchymal stem cells. *Stem Cells (Dayton, Ohio)*. **32**, 1408–19

329. Siao, C.-J., Lorentz, C. U., Kermani, P., Marinic, T., Carter, J., McGrath, K., Padow, V. a., Mark, W., Falcone, D. J., Cohen-Gould, L., Parrish, D. C., Habecker, B. A., Nykjaer, A., Ellenson, L. H., Tessarollo, L., and Hempstead, B. L. (2012) ProNGF, a cytokine induced after myocardial infarction in humans, targets pericytes to promote microvascular damage and activation. *The Journal of Experimental Medicine*. **209**, 2291–2305

330. Elshaer, S. L., and El-Remessy, A. B. (2017) Implication of the neurotrophin receptor p75 NTR in vascular diseases: beyond the eye. *Expert Review of Ophthalmology*. **12**, 149–158

331. Dulauroy, S., Di Carlo, S. E., Langa, F., Eberl, G., and Peduto, L. (2012) Lineage tracing and genetic ablation of ADAM12+ perivascular cells identify a major source of profibrotic cells during acute tissue injury. *Nature Medicine*. **18**, 1262–1270

332. Zhao, J., Yoshioka, K., Miike, T., Kageshita, T., and Arao, T. (1991) Nerve growth factor receptor immunoreactivity on the tunica adventitia of intramuscular blood vessels in childhood muscular dystrophies. *Neuromuscular Disorders : NMD*. **1**, 135–41

333. Iacobaeus, E., Sugars, R. V., Törnqvist Andrén, A., Alm, J. J., Qian, H., Frantzen, J., Newcombe, J., Alkass, K., Druid, H., Bottai, M., Röyttä, M., and Le Blanc, K. (2017) Dynamic Changes in Brain Mesenchymal Perivascular Cells Associate with Multiple Sclerosis Disease Duration, Active Inflammation, and Demyelination. *Stem Cells Translational Medicine*. **6**, 1840–1851

334. Del Rey, M. J., Faré, R., Usategui, A., Cañete, J. D., Bravo, B., Galindo, M., Criado, G., and Pablos, J. L. (2016) CD271+ stromal cells expand in arthritic synovium and exhibit a proinflammatory phenotype. *Arthritis Research & Therapy*. **18**, 66

335. Desguerre, I., Mayer, M., Leturcq, F., Barbet, J.-P., Gherardi, R. K., and Christov, C. (2009) Endomysial Fibrosis in Duchenne Muscular Dystrophy: A Marker of Poor Outcome Associated With Macrophage Alternative Activation. *Journal of Neuropathology & Experimental Neurology*. **68**, 762–773

336. Klingler, W., Jurkat-Rott, K., Lehmann-Horn, F., and Schleip, R. (2012) The role of fibrosis in Duchenne muscular dystrophy. *Acta Myologica : Myopathies and Cardiomyopathies : Official Journal of the Mediterranean Society of Myology*. **31**, 184–95

337. Trim, N., Morgan, S., Evans, M., Issa, R., Fine, D., Afford, S., Wilkins, B., and Iredale, J. (2000) Hepatic Stellate Cells Express the Low Affinity Nerve Growth Factor Receptor p75 and Undergo Apoptosis in Response to Nerve Growth Factor Stimulation. *The American Journal of Pathology*. **156**, 1235–1243

338. Asai, K., Tamakawa, S., Yamamoto, M., Yoshie, M., Tokusashi, Y., Yaginuma, Y., Kasai, S., and Ogawa, K. (2006) Activated hepatic stellate cells overexpress p75NTR after partial hepatectomy and undergo apoptosis on nerve growth factor stimulation. *Liver International*. **26**, 595–603

339. Amoras, E. da S. G., Gomes, S. T. M., Freitas, F. B., Santana, B. B., Ishak, G., de Araújo, M. T. F., Demachki, S., da Silva Conde, S. R. S., de Oliveira Guimarães Ishak, M., Ishak, R., and Vallinoto, A. C. R. (2015) NGF and P75NTR Gene Expression Is Associated with the Hepatic Fibrosis Stage Due to Viral and Non-Viral Causes. *PLoS ONE*. **10**, e0121754

340. Kanik, A. B., Yaar, M., and Bhawan, J. (1996) p75 nerve growth factor receptor staining helps identify desmoplastic and neurotropic melanoma. *Journal of Cutaneous Pathology*. **23**, 205–210

341. Thorpe, R. B., Gray, A., Kumar, K. R., Susa, J. S., and Chong, B. F. (2014) Site-Specific Analysis of Inflammatory Markers in Discoid Lupus Erythematosus Skin. *The Scientific World Journal*. **2014**, 1–12

342. Alsaad, K. O. (2005) My approach to superficial inflammatory dermatoses. *Journal of Clinical Pathology*. **58**, 1233–1241

343. Truzzi, F., Marconi, A., Atzei, P., Panza, M. C., Lotti, R., Dallaglio, K., Tiberio, R., Palazzo, E., Vaschieri, C., and Pincelli, C. (2011) p75 neurotrophin receptor mediates apoptosis in transit-amplifying cells and its overexpression restores cell death in psoriatic keratinocytes. *Cell Death & Differentiation*. **18**, 948–958

344. Ho, J. D., Chung, H. J., Ms Barron, A., Ho, D. A., Sahni, D., Browning, J. L., and Bhawan, J. (2019) Extensive CD34-to-CD90 Fibroblast Transition Defines Regions of Cutaneous Reparative, Hypertrophic, and Keloidal Scarring. *The American Journal of Dermatopathology*. **41**, 16–28

345. Corselli, M., Chen, C.-W., Sun, B., Yap, S., Rubin, J. P., and Péault, B. (2012) The Tunica Adventitia of Human Arteries and Veins As a Source of Mesenchymal Stem Cells. *Stem Cells and Development*. **21**, 1299–1308

346. Rajkumar, V. S., Sundberg, C., Abraham, D. J., Rubin, K., and Black, C. M. (1999) Activation of microvascular pericytes in autoimmune Raynaud's phenomenon and systemic sclerosis. *Arthritis & Rheumatism*. **42**, 930–941

347. Guimarães-Camboa, N., and Evans, S. M. (2017) Are Perivascular Adipocyte Progenitors Mural Cells or Adventitial Fibroblasts? *Cell Stem Cell*. **20**, 587–589

348. Aiba, S., Tabata, N., Ohtani, H., and Tagami, H. (1994) CD34+ spindle-shaped cells selectively disappear from the skin lesion of scleroderma. *Archives of Dermatology*. **130**, 593–7

349. Dominici, M., Le Blanc, K., Mueller, I., Slaper-Cortenbach, I., Marini, F., Krause, D., Deans, R., Keating, A., Prockop, D., and Horwitz, E. (2006) Minimal criteria for defining multipotent mesenchymal stromal cells. The International Society for Cellular Therapy position statement. *Cytotherapy*. **8**, 315–7

350. Zomer, H. D., and Trentin, A. G. (2018) Skin wound healing in humans and mice: Challenges in translational research. *Journal of Dermatological Science*. **90**, 3–12

351. Hoshi, N., Hiraki, H., Yamaki, T., Natsume, T., Watanabe, K., and Suzuki,

T. (1994) Frequent expression of 75 kDa nerve growth factor receptor and phosphotyrosine in human peripheral nerve tumours: an immunohistochemical study on paraffin-embedded tissues. *Virchows Archiv : an International Journal of Pathology*. **424**, 563–8

352. Palazzo, E., Marconi, A., Truzzi, F., Dallaglio, K., Petrachi, T., Humbert, P., Schnebert, S., Perrier, E., Dumas, M., and Pincelli, C. (2012) Role of neurotrophins on dermal fibroblast survival and differentiation. *Journal of Cellular Physiology*. **227**, 1017–1025

353. Micera, A., Puxeddu, I., Lambiase, A., Antonelli, A., Bonini, S., Bonini, S., Aloe, L., Pe'er, J., and Levi-Schaffer, F. (2005) The pro-fibrogenic effect of nerve growth factor on conjunctival fibroblasts is mediated by transforming growth factor-beta. *Clinical and experimental allergy : journal of the British Society for Allergy and Clinical Immunology*. **35**, 650–6

354. Micera, A., Vigneti, E., Pickholtz, D., Reich, R., Pappo, O., Bonini, S., Maquart, F. X., Aloe, L., and Levi-Schaffer, F. (2001) Nerve growth factor displays stimulatory effects on human skin and lung fibroblasts, demonstrating a direct role for this factor in tissue repair. *Proceedings of the National Academy of Sciences of the United States of America*. **98**, 6162–7

355. Friend, C., Scher, W., Holland, J. G., and Sato, T. (1971) Hemoglobin synthesis in murine virus-induced leukemic cells in vitro: stimulation of erythroid differentiation by dimethyl sulfoxide. *Proceedings of the National Academy of Sciences of the United States of America*. **68**, 378–82

356. Tanaka, M., Levy, J., Terada, M., Breslow, R., Rifkind, R. A., and Marks, P. A. (1975) Induction of erythroid differentiation in murine virus infected eythroleukemia cells by highly polar compounds. *Proceedings of the National Academy of Sciences*. **72**, 1003–1006

357. Gao, J. X., and Issekutz, A. C. (1996) Expression of VCAM-1 and VLA-4 dependent T-lymphocyte adhesion to dermal fibroblasts stimulated with proinflammatory cytokines. *Immunology*. **89**, 375–83

358. Haniffa, M. a, Wang, X., Holtick, U., Rae, M., Isaacs, J. D., Dickinson, A. M., Hilkens, C. M. U., and Collin, M. P. (2007) Adult human fibroblasts are potent immunoregulatory cells and functionally equivalent to mesenchymal stem cells. *Journal of Immunology (Baltimore, Md. : 1950)*. **179**, 1595–604

359. Vaculik, C., Schuster, C., Bauer, W., Iram, N., Pfisterer, K., Kramer, G., Reinisch, A., Strunk, D., and Elbe-Bürger, A. (2012) Human dermis harbors distinct mesenchymal stromal cell subsets. *Journal of Investigative*

Dermatology. 10.1038/jid.2011.355

360. Honda, K., Nakano, H., Yoshida, H., Nishikawa, S., Rennert, P., Ikuta, K., Tamechika, M., Yamaguchi, K., Fukumoto, T., Chiba, T., and Nishikawa, S.-I. (2001) Molecular Basis for Hematopoietic/Mesenchymal Interaction during Initiation of Peyer's Patch Organogenesis. *The Journal of Experimental Medicine*. **193**, 621–630

361. Saalbach, A., Klein, C., Sleeman, J., Sack, U., Kauer, F., Gebhardt, C., Averbeck, M., Anderegg, U., and Simon, J. C. (2007) Dermal fibroblasts induce maturation of dendritic cells. *Journal of Immunology (Baltimore, Md. : 1950)*. **178**, 4966–74

362. Blasi, A., Martino, C., Balducci, L., Saldarelli, M., Soleti, A., Navone, S. E., Canzi, L., Cristini, S., Invernici, G., Parati, E. a, and Alessandri, G. (2011) Dermal fibroblasts display similar phenotypic and differentiation capacity to fat-derived mesenchymal stem cells, but differ in anti-inflammatory and angiogenic potential. *Vascular Cell*. **3**, 5

363. Yellin, M. J., Winikoff, S., Fortune, S. M., Baum, D., Crow, M. K., Lederman, S., and Chess, L. (1995) Ligation of CD40 on fibroblasts induces CD54 (ICAM-1) and CD106 (VCAM-1) up-regulation and IL-6 production and proliferation. *Journal of Leukocyte Biology*. **58**, 209–16

364. Thompson, R. J., Doran, J. F., Jackson, P., Dhillon, A. P., and Rode, J. (1983) PGP 9.5—a new marker for vertebrate neurons and neuroendocrine cells. *Brain Research*. **278**, 224–228

365. Truzzi, F., Saltari, A., Palazzo, E., Lotti, R., Petrachi, T., Dallaglio, K., Gemelli, C., Grisendi, G., Dominici, M., Pincelli, C., and Marconi, A. (2015) CD271 Mediates Stem Cells to Early Progeny Transition in Human Epidermis. *Journal of Investigative Dermatology*. **135**, 786–795

366. Seidl, K., Erck, C., and Buchberger, A. (1998) Evidence for the participation of nerve growth factor and its low-affinity receptor (p75NTR) in the regulation of the myogenic program. *Journal of Cellular Physiology*. **176**, 10–21

367. Colombo, E., Romaggi, S., Medico, E., Menon, R., Mora, M., Falcone, C., Lochmüller, H., Confalonieri, P., Mantegazza, R., Morandi, L., and Farina, C. (2011) Human neurotrophin receptor p75NTR defines differentiation-oriented skeletal muscle precursor cells: Implications for muscle regeneration. *Journal of Neuropathology and Experimental Neurology*. **70**, 133–142

368. Deponti, D., Buono, R., Catanzaro, G., De Palma, C., Longhi, R., Meneveri, R., Bresolin, N., Bassi, M. T., Cossu, G., Clementi, E., and Brunelli, S. (2009) The Low-Affinity Receptor for Neurotrophins p75 NTR Plays a Key Role for Satellite Cell Function in Muscle Repair Acting via RhoA. *Molecular Biology of the Cell*. **20**, 3620–3627

369. Hicks, M. R., Hiserodt, J., Paras, K., Fujiwara, W., Eskin, A., Jan, M., Xi, H., Young, C. S., Evseenko, D., Nelson, S. F., Spencer, M. J., Handel, B. Van, and Pyle, A. D. (2018) ERBB3 and NGFR mark a distinct skeletal muscle progenitor cell in human development and hPSCs. *Nature Cell Biology*. **20**, 46–57

370. Mikami, Y., Ishii, Y., Watanabe, N., Shirakawa, T., Suzuki, S., Irie, S., Isokawa, K., and Honda, M. J. (2011) CD271/p75 NTR Inhibits the Differentiation of Mesenchymal Stem Cells into Osteogenic, Adipogenic, Chondrogenic, and Myogenic Lineages. *Stem Cells and Development*. **20**, 901–913

371. Li, J., Narayanan, C., Bian, J., Sambo, D., Brickler, T., Zhang, W., and Chetty, S. (2018) A transient DMSO treatment increases the differentiation potential of human pluripotent stem cells through the Rb family. *PLoS ONE*. **13**, 1–16

372. Iacobaeus, E., Sugars, R. V., Törnqvist Andrén, A., Alm, J. J., Qian, H., Frantzen, J., Newcombe, J., Alkass, K., Druid, H., Bottai, M., Röyttä, M., and Le Blanc, K. (2017) Dynamic Changes in Brain Mesenchymal Perivascular Cells Associate with Multiple Sclerosis Disease Duration, Active Inflammation, and Demyelination. *Stem Cells Translational Medicine*. **6**, 1840–1851

373. Absinta, M., Nair, G., Monaco, M. C. G., Maric, D., Lee, N. J., Ha, S.-K., Luciano, N. J., Sati, P., Jacobson, S., and Reich, D. S. (2019) The “central vein sign” in inflammatory demyelination: The role of fibrillar collagen type I. *Annals of Neurology*. **85**, 934–942

374. Mohan, H., Krumbholz, M., Sharma, R., Eisele, S., Junker, A., Sixt, M., Newcombe, J., Wekerle, H., Hohlfeld, R., Lassmann, H., and Meinl, E. (2010) Extracellular Matrix in Multiple Sclerosis Lesions: Fibrillar Collagens, Biglycan and Decorin are Upregulated and Associated with Infiltrating Immune Cells. *Brain Pathology*. **20**, no-no

375. Desguerre, I., Mayer, M., Leturcq, F., Barbet, J.-P., Gherardi, R. K., and Christov, C. (2009) Endomysial fibrosis in Duchenne muscular dystrophy: a marker of poor outcome associated with macrophage alternative activation. *Journal of neuropathology and experimental neurology*. **68**, 762–73

376. Ieronimakis, N., Hays, A., Prasad, A., Janebodin, K., Duffield, J. S., and Reyes, M. (2016) PDGFRα signalling promotes fibrogenic responses in collagen-producing cells in Duchenne muscular dystrophy. *The Journal of Pathology*. **240**, 410–424

377. Carulli, M. T., Ong, V. H., Ponticos, M., Shiwen, X., Abraham, D. J., Black, C. M., and Denton, C. P. (2005) Chemokine receptor CCR2 expression by systemic sclerosis fibroblasts: Evidence for autocrine regulation of myofibroblast differentiation. *Arthritis & Rheumatism*. **52**, 3772–3782

378. Carulli, M. T., Handler, C., Coghlan, J. G., Black, C. M., and Denton, C. P. (2008) Can CCL2 serum levels be used in risk stratification or to monitor treatment response in systemic sclerosis? *Annals of the Rheumatic Diseases*. **67**, 105–109

379. Bandinelli, F., Del Rosso, A., Gabrielli, A., Giacomelli, R., Bartoli, F., Guiducci, S., and Matucci-Cerinic, M. (2012) CCL2, CCL3 and CCL5 chemokines in systemic sclerosis: The correlation with SSc clinical features and the effect of prostaglandin E1 treatment. *Clinical and Experimental Rheumatology*. **30**, 1–6

380. Nishikawa, S.-I., Nishikawa, S., Honda, K., Hashi, H., and Yoshida, H. (1998) Peyers Patch Organogenesis as a Programmed Inflammation: a Hypothetical Model. *Cytokine & Growth Factor Reviews*. **9**, 213–220

381. Peduto, L., Dulauroy, S., Lochner, M., Späth, G. F., Morales, M. a, Cumano, A., and Eberl, G. (2009) Inflammation recapitulates the ontogeny of lymphoid stromal cells. *Journal of Immunology (Baltimore, Md. : 1950)*. **182**, 5789–5799

382. Tabib, T., Morse, C., Wang, T., Chen, W., and Lafyatis, R. (2018) SFRP2/DPP4 and FMO1/LSP1 Define Major Fibroblast Populations in Human Skin. *Journal of Investigative Dermatology*. **138**, 802–810

383. Philippeos, C., Telerman, S. B., Oulès, B., Pisco, A. O., Shaw, T. J., Elgueta, R., Lombardi, G., Driskell, R. R., Soldin, M., Lynch, M. D., and Watt, F. M. (2018) Spatial and Single-Cell Transcriptional Profiling Identifies Functionally Distinct Human Dermal Fibroblast Subpopulations. *Journal of Investigative Dermatology*. **138**, 811–825

384. Apostolidis, S. A., Stifano, G., Tabib, T., Rice, L. M., Morse, C. M., Kahaleh, B., and Lafyatis, R. (2018) Single Cell RNA Sequencing Identifies HSPG2 and APLNR as Markers of Endothelial Cell Injury in Systemic Sclerosis Skin. *Frontiers in Immunology*. **9**, 2191

385. Mizoguchi, F., Slowikowski, K., Wei, K., Marshall, J. L., Rao, D. A., Chang, S. K., Nguyen, H. N., Noss, E. H., Turner, J. D., Earp, B. E., Blazar, P. E., Wright, J., Simmons, B. P., Donlin, L. T., Kalliolias, G. D., Goodman, S. M., Bykerk, V. P., Ivashkiv, L. B., Lederer, J. A., Hacohen, N., Nigrovic, P. A., Filer, A., Buckley, C. D., Raychaudhuri, S., and Brenner, M. B. (2018) Functionally distinct disease-associated fibroblast subsets in rheumatoid arthritis. *Nature Communications*. **9**, 789

386. Stephenson, W., Donlin, L. T., Butler, A., Rozo, C., Bracken, B., Rashidfarrokhi, A., Goodman, S. M., Ivashkiv, L. B., Bykerk, V. P., Orange, D. E., Darnell, R. B., Swerdlow, H. P., and Satija, R. (2018) Single-cell RNA-seq of rheumatoid arthritis synovial tissue using low-cost microfluidic instrumentation. *Nature Communications*. **9**, 791

387. Nayar, S., Campos, J., Smith, C. G., Iannizzotto, V., Gardner, D. H., Mourcin, F., Roulois, D., Turner, J., Sylvestre, M., Asam, S., Glaysher, B., Bowman, S. J., Fearon, D. T., Filer, A., Tarte, K., Luther, S. A., Fisher, B. A., Buckley, C. D., Coles, M. C., and Barone, F. (2019) Immunofibroblasts are pivotal drivers of tertiary lymphoid structure formation and local pathology. *Proceedings of the National Academy of Sciences of the United States of America*. **116**, 13490–13497

388. Passino, M. A., Adams, R. A., Sikorski, S. L., and Akassoglou, K. (2007) Regulation of hepatic stellate cell differentiation by the neurotrophin receptor p75NTR. *Science (New York, N.Y.)*. **315**, 1853–6

389. Trim, N., Morgan, S., Evans, M., Issa, R., Fine, D., Afford, S., Wilkins, B., and Iredale, J. (2000) Hepatic Stellate Cells Express the Low Affinity Nerve Growth Factor Receptor p75 and Undergo Apoptosis in Response to Nerve Growth Factor Stimulation. *The American Journal of Pathology*. **156**, 1235–1243

390. von Schack, D., Casademunt, E., Schweigreiter, R., Meyer, M., Bibel, M., and Dechant, G. (2001) Complete ablation of the neurotrophin receptor p75NTR causes defects both in the nervous and the vascular system. *Nature Neuroscience*. **4**, 977–978

391. Barcelona, P. F., Sitaras, N., Galan, A., Esquiva, G., Jmaeff, S., Jian, Y., Sarunic, M. V., Cuenca, N., Sapieha, P., and Saragovi, H. U. (2016) p75 NTR and Its Ligand ProNGF Activate Paracrine Mechanisms Etiological to the Vascular, Inflammatory, and Neurodegenerative Pathologies of Diabetic Retinopathy. *The Journal of Neuroscience*. **36**, 8826–8841

392. Hammes, H. P., Federoff, H. J., and Brownlee, M. (1995) Nerve growth factor prevents both neuroretinal programmed cell death and capillary

pathology in experimental diabetes. *Molecular Medicine (Cambridge, Mass.)*. **1**, 527–34

393. Pramanik, S., Sulistio, Y. A., and Heese, K. (2017) Neurotrophin Signaling and Stem Cells—Implications for Neurodegenerative Diseases and Stem Cell Therapy. *Molecular Neurobiology*. **54**, 7401–7459

394. Lagares, D., Santos, A., Grasberger, P. E., Liu, F., Probst, C. K., Rahimi, R. A., Sakai, N., Kuehl, T., Ryan, J., Bhola, P., Montero, J., Kapoor, M., Baron, M., Varelas, X., Tschumperlin, D. J., Letai, A., and Tager, A. M. (2017) Targeted apoptosis of myofibroblasts with the BH3 mimetic ABT-263 reverses established fibrosis. *Science Translational Medicine*. **9**, eaal3765

395. Kaufman, M., Pinsky, L., Straisfeld, C., Shanfield, B., and Zilahi, B. (1975) Qualitative differences in testosterone metabolism as an indication of cellular heterogeneity in fibroblast monolayers derived from human preputial skin. *Experimental Cell Research*. **96**, 31–36

396. Tajima, S., and Pinnell, S. R. (1981) Collagen Synthesis by Human Skin Fibroblasts in Culture: Studies of Fibroblasts Explanted from Papillary and Reticular Dermis. *Journal of Investigative Dermatology*. **77**, 410–412

397. Ko, S. D., Page, R. C., and Narayanan, A. S. (1977) Fibroblast heterogeneity and prostaglandin regulation of subpopulations. *Proceedings of the National Academy of Sciences*. **74**, 3429–3432

398. Harper, R. A., and Grove, G. (1979) Human skin fibroblasts derived from papillary and reticular dermis: differences in growth potential in vitro. *Science (New York, N.Y.)*. **204**, 526–7

399. Skalli, O., Schürch, W., Seemayer, T., Lagacé, R., Montandon, D., Pittet, B., and Gabbiani, G. (1989) Myofibroblasts from diverse pathologic settings are heterogeneous in their content of actin isoforms and intermediate filament proteins. *Laboratory Investigation; a Journal of Technical Methods and Pathology*. **60**, 275–85

400. Schmitt-Gräff, A., Desmoulière, A., and Gabbiani, G. (1994) Heterogeneity of myofibroblast phenotypic features: an example of fibroblastic cell plasticity. *Virchows Archiv : an International Journal of Pathology*. **425**, 3–24

401. Grisanti, L., Clavel, C., Cai, X., Rezza, A., Tsai, S.-Y., Sennett, R., Mumau, M., Cai, C.-L., and Rendl, M. (2013) Tbx18 Targets Dermal Condensates for Labeling, Isolation, and Gene Ablation during Embryonic Hair Follicle

Formation. *Journal of Investigative Dermatology*. **133**, 344–353

402. Rahmani, W., Abbasi, S., Hagner, A., Raharjo, E., Kumar, R., Hotta, A., Magness, S., Metzger, D., and Biernaskie, J. (2014) Hair Follicle Dermal Stem Cells Regenerate the Dermal Sheath, Repopulate the Dermal Papilla, and Modulate Hair Type. *Developmental Cell*. **31**, 543–558

403. Jiang, D., Correa-Gallegos, D., Christ, S., Stefanska, A., Liu, J., Ramesh, P., Rajendran, V., De Santis, M. M., Wagner, D. E., and Rinkevich, Y. (2018) Two succeeding fibroblastic lineages drive dermal development and the transition from regeneration to scarring. *Nature Cell Biology*. **20**, 422–431

404. Guerrero-Juarez, C. F., Dedhia, P. H., Jin, S., Ruiz-Vega, R., Ma, D., Liu, Y., Yamaga, K., Shestova, O., Gay, D. L., Yang, Z., Kessenbrock, K., Nie, Q., Pear, W. S., Cotsarelis, G., and Plikus, M. V. (2019) Single-cell analysis reveals fibroblast heterogeneity and myeloid-derived adipocyte progenitors in murine skin wounds. *Nature Communications*. **10**, 1–17

405. Böhm, F., and Pernow, J. (2007) The importance of endothelin-1 for vascular dysfunction in cardiovascular disease. *Cardiovascular Research*. **76**, 8–18

406. Karelina, T. V., Bannikov, G. A., and Eisen, A. Z. (2000) Basement Membrane Zone Remodeling During Appendageal Development in Human Fetal Skin. The Absence of Type VII Collagen is Associated with Gelatinase-A (MMP2) Activity. *Journal of Investigative Dermatology*. **114**, 371–375

407. Sharov, A. A., Schroeder, M., Sharova, T. Y., Mardaryev, A. N., Peters, E. M. J., Tobin, D. J., and Botchkarev, V. A. (2011) Matrix Metalloproteinase-9 Is Involved in the Regulation of Hair Canal Formation. *Journal of Investigative Dermatology*. **131**, 257–260

408. Botchkarev, V. A., Botchkareva, N. V., Roth, W., Nakamura, M., Chen, L.-H., Herzog, W., Lindner, G., McMahon, J. A., Peters, C., Lauster, R., McMahon, A. P., and Paus, R. (1999) Noggin is a mesenchymally derived stimulator of hair-follicle induction. *Nature Cell Biology*. **1**, 158–164

409. Tsai, S.-Y., Sennett, R., Rezza, A., Clavel, C., Grisanti, L., Zemla, R., Najam, S., and Rendl, M. (2014) Wnt/β-catenin signaling in dermal condensates is required for hair follicle formation. *Developmental Biology*. **385**, 179–188

410. Oshimori, N., and Fuchs, E. (2012) Paracrine TGF-β Signaling

Counterbalances BMP-Mediated Repression in Hair Follicle Stem Cell Activation. *Cell Stem Cell*. **10**, 63–75

411. Benahmed, F., Chyou, S., Dasoveanu, D., Chen, J., Kumar, V., Iwakura, Y., and Lu, T. T. (2014) Multiple CD11c+ cells collaboratively express IL-1β to modulate stromal vascular endothelial growth factor and lymph node vascular-stromal growth. *Journal of Immunology (Baltimore, Md. : 1950)*. **192**, 4153–63

412. Wang, X.-N., McGovern, N., Gunawan, M., Richardson, C., Windebank, M., Siah, T.-W., Lim, H.-Y., Fink, K., Yao Li, J. L., Ng, L. G., Ginhoux, F., Angeli, V., Collin, M., and Haniffa, M. (2014) A Three-Dimensional Atlas of Human Dermal Leukocytes, Lymphatics, and Blood Vessels. *Journal of Investigative Dermatology*. **134**, 965–974

413. Dahlgren, M. W., Jones, S. W., Cautivo, K. M., Dubinin, A., Ortiz-Carpena, J. F., Farhat, S., Yu, K. S., Lee, K., Wang, C., Molofsky, A. V, Tward, A. D., Krummel, M. F., Peng, T., and Molofsky, A. B. (2019) Adventitial Stromal Cells Define Group 2 Innate Lymphoid Cell Tissue Niches. *Immunity*. **50**, 707-722.e6

414. Sontheimer, R. D., Matsubara, T., and Seelig, L. L. (1989) A Macrophage Phenotype for a Constitutive, Class II Antigen-Expressing, Human Dermal Perivascular Dendritic Cell. *Journal of Investigative Dermatology*. **93**, 154–159

415. Clark, R. A., and Kupper, T. S. (2007) IL-15 and dermal fibroblasts induce proliferation of natural regulatory T cells isolated from human skin. *Blood*. **109**, 194–202

416. Clark, R. a, Chong, B., Mirchandani, N., Brinster, N. K., Yamanaka, K.-I., Dowgiert, R. K., and Kupper, T. S. (2006) The vast majority of CLA+ T cells are resident in normal skin. *Journal of Immunology (Baltimore, Md. : 1950)*. **176**, 4431–9

417. Janssens, A. S. (2005) Mast cell distribution in normal adult skin. *Journal of Clinical Pathology*. **58**, 285–289

418. Cheng, L. E., Hartmann, K., Roers, A., Krummel, M. F., and Locksley, R. M. (2013) Perivascular Mast Cells Dynamically Probe Cutaneous Blood Vessels to Capture Immunoglobulin E. *Immunity*. **38**, 166–175

419. Dudda, J. C., Perdue, N., Bachtanian, E., and Campbell, D. J. (2008) Foxp3 + regulatory T cells maintain immune homeostasis in the skin. *The Journal of Experimental Medicine*. **205**, 1559–1565

420. Sather, B. D., Treuting, P., Perdue, N., Miazgowicz, M., Fontenot, J. D., Rudensky, A. Y., and Campbell, D. J. (2007) Altering the distribution of Foxp3 + regulatory T cells results in tissue-specific inflammatory disease. *The Journal of Experimental Medicine*. **204**, 1335–1347

421. Spallanzani, R. G., Zemmour, D., Xiao, T., Jayewickreme, T., Li, C., Bryce, P. J., Benoist, C., and Mathis, D. (2019) Distinct immunocyte-promoting and adipocyte-generating stromal components coordinate adipose tissue immune and metabolic tenors. *Science Immunology*. **4**, eaaw3658

422. Vasanthakumar, A., Moro, K., Xin, A., Liao, Y., Gloury, R., Kawamoto, S., Fagarasan, S., Mielke, L. A., Afshar-Sterle, S., Masters, S. L., Nakae, S., Saito, H., Wentworth, J. M., Li, P., Liao, W., Leonard, W. J., Smyth, G. K., Shi, W., Nutt, S. L., Koyasu, S., and Kallies, A. (2015) The transcriptional regulators IRF4, BATF and IL-33 orchestrate development and maintenance of adipose tissue–resident regulatory T cells. *Nature Immunology*. **16**, 276–285

423. Braun, J., Kurtz, A., Barutcu, N., Bodo, J., Thiel, A., and Dong, J. (2013) Concerted Regulation of CD34 and CD105 Accompanies Mesenchymal Stromal Cell Derivation from Human Adventitial Stromal Cell. *Stem Cells and Development*. **22**, 815–827

424. Walmsley, G. G., Rinkevich, Y., Hu, M. S., Montoro, D. T., Lo, D. D., McArdle, A., Maan, Z. N., Morrison, S. D., Duscher, D., Whittam, A. J., Wong, V. W., Weissman, I. L., Gurtner, G. C., and Longaker, M. T. (2015) Live Fibroblast Harvest Reveals Surface Marker Shift In Vitro. *Tissue Engineering Part C: Methods*. **21**, 314–321

425. Onder, L., Mörbe, U., Pikor, N., Novkovic, M., Cheng, H.-W., Hehlgans, T., Pfeffer, K., Becher, B., Waisman, A., Rülicke, T., Gommerman, J., Mueller, C. G., Sawa, S., Scandella, E., and Ludewig, B. (2017) Lymphatic Endothelial Cells Control Initiation of Lymph Node Organogenesis. *Immunity*. **47**, 80-92.e4

426. van de Pavert, S. a, Olivier, B. J., Goverse, G., Vondenhoff, M. F., Greuter, M., Beke, P., Kusser, K., Höpken, U. E., Lipp, M., Niederreither, K., Blomhoff, R., Sitnik, K., Agace, W. W., Randall, T. D., de Jonge, W. J., and Mebius, R. E. (2009) Chemokine CXCL13 is essential for lymph node initiation and is induced by retinoic acid and neuronal stimulation. *Nature Immunology*. **10**, 1193–1199

427. Cupedo, T., Jansen, W., Kraal, G., and Mebius, R. E. (2004) Induction of Secondary and Tertiary Lymphoid Structures in the Skin. *Immunity*. **21**, 655–667

428. Onder, L., and Ludewig, B. (2018) A Fresh View on Lymph Node Organogenesis. *Trends in Immunology*. **39**, 775–787

429. Koning, J. J., and Mebius, R. E. (2018) Complexity of Lymphoid Tissue Organizers: A Response to Onder and Ludewig. *Trends in Immunology*. **39**, 951–952

430. Onder, L., and Ludewig, B. (2018) Redefining the Nature of Lymphoid Tissue Organizer Cells: Response to 'Complexity of Lymphoid Tissue Organizers' by Koning and Mebius. *Trends in Immunology*. **39**, 952–953

431. Adachi, S., Yoshida, H., Honda, K., Maki, K., Saijo, K., Ikuta, K., Saito, T., and Nishikawa, S. I. (1998) Essential role of IL-7 receptor alpha in the formation of Peyer's patch anlage. *International Immunology*. **10**, 1–6

432. Onder, L., Danuser, R., Scandella, E., Firner, S., Chai, Q., Hehlgans, T., Stein, J. V, and Ludewig, B. (2013) Endothelial cell–specific lymphotoxin-β receptor signaling is critical for lymph node and high endothelial venule formation. *The Journal of Experimental Medicine*. **210**, 465–473

433. Veiga-Fernandes, H., Coles, M. C., Foster, K. E., Patel, A., Williams, A., Natarajan, D., Barlow, A., Pachnis, V., and Kioussis, D. (2007) Tyrosine kinase receptor RET is a key regulator of Peyer's Patch organogenesis. *Nature*. **446**, 547–551

434. Patel, A., Harker, N., Moreira-Santos, L., Ferreira, M., Alden, K., Timmis, J., Foster, K., Garefalaki, A., Pachnis, P., Andrews, P., Enomoto, H., Milbrandt, J., Pachnis, V., Coles, M. C., Kioussis, D., and Veiga-Fernandes, H. (2012) Differential RET Signaling Pathways Drive Development of the Enteric Lymphoid and Nervous Systems. *Science Signaling*. **5**, ra55–ra55

435. Pandey, S., Kawai, T., and Akira, S. (2015) Microbial Sensing by Toll-Like Receptors and Intracellular Nucleic Acid Sensors. *Cold Spring Harbor Perspectives in Biology*. **7**, a016246

436. Rangel-Moreno, J., Carragher, D. M., de la Luz Garcia-Hernandez, M., Hwang, J. Y., Kusser, K., Hartson, L., Kolls, J. K., Khader, S. A., and Randall, T. D. (2011) The development of inducible bronchus-associated lymphoid tissue depends on IL-17. *Nature Immunology*. **12**, 639–646

437. Fleige, H., Ravens, S., Moschovakis, G. L., Bölter, J., Willenzon, S., Sutter, G., Häussler, S., Kalinke, U., Prinz, I., and Förster, R. (2014) IL-17–induced CXCL12 recruits B cells and induces follicle formation in BALT in the absence of differentiated FDCs. *The Journal of Experimental Medicine*.

211, 643–651

438. Marinkovic, T., Garin, A., Yokota, Y., Fu, Y.-X., Ruddle, N. H., Furtado, G. C., and Lira, S. A. (2006) Interaction of mature CD3+CD4+ T cells with dendritic cells triggers the development of tertiary lymphoid structures in the thyroid. *The Journal of Clinical Investigation*. **116**, 2622–32

439. Burke, D. L., Frid, M. G., Kunrath, C. L., Karoor, V., Anwar, A., Wagner, B. D., Strassheim, D., and Stenmark, K. R. (2009) Sustained hypoxia promotes the development of a pulmonary artery-specific chronic inflammatory microenvironment. *American Journal of Physiology. Lung Cellular and Molecular Physiology*. **297**, L238-50

440. Colvin, K. L., Cripe, P. J., Ivy, D. D., Stenmark, K. R., and Yeager, M. E. (2013) Bronchus-associated lymphoid tissue in pulmonary hypertension produces pathologic autoantibodies. *American Journal of Respiratory and Critical Care Medicine*. **188**, 1126–36

441. Tieu, B. C., Lee, C., Sun, H., LeJeune, W., Recinos, A., Ju, X., Spratt, H., Guo, D.-C., Milewicz, D., Tilton, R. G., and Brasier, A. R. (2009) An adventitial IL-6/MCP1 amplification loop accelerates macrophage-mediated vascular inflammation leading to aortic dissection in mice. *Journal of Clinical Investigation*. **119**, 3637–3651

442. Jabs, A., Okamoto, E., Vinten-Johansen, J., Bauriedel, G., and Wilcox, J. N. (2007) Sequential patterns of chemokine- and chemokine receptor-synthesis following vessel wall injury in porcine coronary arteries. *Atherosclerosis*. **192**, 75–84

443. El Kasmi, K. C., Pugliese, S. C., Riddle, S. R., Poth, J. M., Anderson, A. L., Frid, M. G., Li, M., Pullamsetti, S. S., Savai, R., Nagel, M. A., Fini, M. A., Graham, B. B., Tuder, R. M., Friedman, J. E., Eltzschig, H. K., Sokol, R. J., and Stenmark, K. R. (2014) Adventitial fibroblasts induce a distinct proinflammatory/profibrotic macrophage phenotype in pulmonary hypertension. *Journal of Immunology (Baltimore, Md. : 1950)*. **193**, 597–609

444. Wu, Q., Salomon, B., Chen, M., Wang, Y., Hoffman, L. M., Bluestone, J. A., and Fu, Y.-X. (2001) Reversal of Spontaneous Autoimmune Insulitis in Nonobese Diabetic Mice by Soluble Lymphotoxin Receptor. *The Journal of Experimental Medicine*. **193**, 1327–1332

445. Lee, Y., Chin, R. K., Christiansen, P., Sun, Y., Tumanov, A. V., Wang, J., Chervonsky, A. V., and Fu, Y.-X. (2006) Recruitment and activation of naive T cells in the islets by lymphotoxin beta receptor-dependent tertiary

lymphoid structure. *Immunity*. **25**, 499–509

446. Houtkamp, M. A., de Boer, O. J., van der Loos, C. M., van der Wal, A. C., and Becker, A. E. (2001) Adventitial infiltrates associated with advanced atherosclerotic plaques: structural organization suggests generation of local humoral immune responses. *The Journal of Pathology*. **193**, 263–9

447. Lukacs-Kornek, V., Malhotra, D., Fletcher, A. L., Acton, S. E., Elpek, K. G., Tayalia, P., Collier, A., and Turley, S. J. (2011) Regulated release of nitric oxide by nonhematopoietic stroma controls expansion of the activated T cell pool in lymph nodes. *Nature Immunology*. **12**, 1096–1104

448. Siegert, S., Huang, H.-Y., Yang, C.-Y., Scarpellino, L., Carrie, L., Essex, S., Nelson, P. J., Heikenwalder, M., Acha-Orbea, H., Buckley, C. D., Marsland, B. J., Zehn, D., and Luther, S. A. (2011) Fibroblastic reticular cells from lymph nodes attenuate T cell expansion by producing nitric oxide. *PLoS ONE*. **6**, e27618

449. Dakin, S. G., Buckley, C. D., Al-Mossawi, M. H., Hedley, R., Martinez, F. O., Wheway, K., Watkins, B., and Carr, A. J. (2017) Persistent stromal fibroblast activation is present in chronic tendinopathy. *Arthritis Research & Therapy*. **19**, 16

450. Buechler, M. B., and Turley, S. J. (2018) A short field guide to fibroblast function in immunity. *Seminars in Immunology*. **35**, 48–58

451. Tang, H., Zhu, M., Qiao, J., and Fu, Y.-X. (2017) Lymphotoxin signalling in tertiary lymphoid structures and immunotherapy. *Cellular & Molecular Immunology*. **14**, 809–818

452. Naylor, A. J., Filer, A., and Buckley, C. D. (2013) The role of stromal cells in the persistence of chronic inflammation. *Clinical & Experimental Immunology*. **171**, 30–35

453. Crisan, M., Yap, S., Casteilla, L., Chen, C.-W., Corselli, M., Park, T. S., Andriolo, G., Sun, B., Zheng, B., Zhang, L., Norotte, C., Teng, P.-N., Traas, J., Schugar, R., Deasy, B. M., Badylak, S., Buhring, H.-J., Giacobino, J.-P., Lazzari, L., Huard, J., and Péault, B. (2008) A perivascular origin for mesenchymal stem cells in multiple human organs. *Cell Stem Cell*. **3**, 301–13

454. Majesky, M. W., Horita, H., Ostriker, A., Lu, S., Regan, J. N., Bagchi, A., Dong, X. R., Poczobutt, J., Nemenoff, R. A., and Weiser-Evans, M. C. M. (2017) Differentiated Smooth Muscle Cells Generate a Subpopulation of Resident Vascular Progenitor Cells in the Adventitia Regulated by Klf4.

Circulation Research. **120**, 296–311

455. Guimarães-Camboa, N., Cattaneo, P., Sun, Y., Moore-Morris, T., Gu, Y., Dalton, N. D., Rockenstein, E., Masliah, E., Peterson, K. L., Stallcup, W. B., Chen, J., and Evans, S. M. (2017) Pericytes of Multiple Organs Do Not Behave as Mesenchymal Stem Cells In Vivo. *Cell Stem Cell*. **20**, 345-359.e5

456. Cano, E., Gebala, V., and Gerhardt, H. (2017) Pericytes or Mesenchymal Stem Cells: Is That the Question? *Cell Stem Cell*. **20**, 296–297

457. Vishvanath, L., Long, J. Z., Spiegelman, B. M., and Gupta, R. K. (2017) Do Adipocytes Emerge from Mural Progenitors? *Cell Stem Cell*. **20**, 585–586

458. Hsu, Y.-C., Li, L., and Fuchs, E. (2014) Transit-amplifying cells orchestrate stem cell activity and tissue regeneration. *Cell*. **157**, 935–49

459. Botchkareva, N. V, Botchkarev, V. A., Chen, L.-H., Lindner, G., and Paus, R. (1999) A Role for p75 Neurotrophin Receptor in the Control of Hair Follicle Morphogenesis. *Developmental Biology*. **216**, 135–153

460. Ho, Y. Y., Lagares, D., Tager, A. M., and Kapoor, M. (2014) Fibrosis--a lethal component of systemic sclerosis. *Nature Reviews. Rheumatology*. **10**, 390–402

461. Rajkumar, V. S., Howell, K., Csiszar, K., Denton, C. P., Black, C. M., and Abraham, D. J. (2005) Shared expression of phenotypic markers in systemic sclerosis indicates a convergence of pericytes and fibroblasts to a myofibroblast lineage in fibrosis. *Arthritis Research & Therapy*. **7**, R1113-23

462. Helmbold, P., Fiedler, E., Fischer, M., and Marsch, W. C. (2004) Hyperplasia of dermal microvascular pericytes in scleroderma. *Journal of Cutaneous Pathology*. **31**, 431–440

463. Svegliati Baroni, S., Santillo, M., Bevilacqua, F., Luchetti, M., Spadoni, T., Mancini, M., Fraticelli, P., Sambo, P., Funaro, A., Kazlauskas, A., Avvedimento, E. V, and Gabrielli, A. (2006) Stimulatory Autoantibodies to the PDGF Receptor in Systemic Sclerosis. *New England Journal of Medicine*. **354**, 2667–2676

464. Makino, K., Makino, T., Stawski, L., Mantero, J. C., Lafyatis, R., Simms, R., and Trojanowska, M. (2017) Blockade of PDGF Receptors by Crenolanib Has Therapeutic Effect in Patient Fibroblasts and in Preclinical Models of Systemic Sclerosis. *The Journal of Investigative Dermatology*. **137**, 1671–

1681

465. Cipriani, P., Di Benedetto, P., Ruscitti, P., Liakouli, V., Berardicurti, O., Carubbi, F., Ciccia, F., Guggino, G., Zazzeroni, F., Alesse, E., Triolo, G., and Giacomelli, R. (2016) Perivascular cells in diffuse cutaneous systemic sclerosis overexpress activated ADAM12 and are involved in myofibroblast transdifferentiation and development of fibrosis. *Journal of Rheumatology*. **43**, 1340–1349

466. Ceni, C., Kommaddi, R. P., Thomas, R., Vereker, E., Liu, X., McPherson, P. S., Ritter, B., and Barker, P. A. (2010) The p75NTR intracellular domain generated by neurotrophin-induced receptor cleavage potentiates Trk signaling. *Journal of Cell Science*. **123**, 2299–2307

467. Barcelona, P. F., Sitaras, N., Galan, A., Esquiva, G., Jmaeff, S., Jian, Y., Sarunic, M. V, Cuenca, N., Sapieha, P., and Saragovi, H. U. (2016) p75 NTR and Its Ligand ProNGF Activate Paracrine Mechanisms Etiological to the Vascular, Inflammatory, and Neurodegenerative Pathologies of Diabetic Retinopathy. *The Journal of Neuroscience*. **36**, 8826–8841

468. Mohamed, R., Shanab, A. Y., and El Remessy, A. B. (2017) Deletion of the Neurotrophin Receptor p75NTR Prevents Diabetes-Induced Retinal Acellular Capillaries in Streptozotocin-Induced Mouse Diabetic Model. *Journal of Diabetes, Metabolic Disorders & Control*. **4**, 163–169

469. Elshaer, S. L., and El-Remessy, A. B. (2017) Implication of the neurotrophin receptor p75 NTR in vascular diseases: beyond the eye. *Expert Review of Ophthalmology*. **12**, 149–158

470. Nguyen, N. M., Song, K. M., Choi, M. J., Ghatak, K., Kwon, M. H., Ock, J., Yin, G. N., Ryu, J. K., and Suh, J. K. (2019) Inhibition of proNGF and p75 NTR Pathway Restores Erectile Function Through Dual Angiogenic and Neurotrophic Effects in the Diabetic Mouse. *Journal of Sexual Medicine*. **16**, 351–364

471. Siao, C.-J., Lorentz, C. U., Kermani, P., Marinic, T., Carter, J., McGrath, K., Padow, V. A., Mark, W., Falcone, D. J., Cohen-Gould, L., Parrish, D. C., Habecker, B. A., Nykjaer, A., Ellenson, L. H., Tessarollo, L., and Hempstead, B. L. (2012) ProNGF, a cytokine induced after myocardial infarction in humans, targets pericytes to promote microvascular damage and activation. *The Journal of Experimental Medicine*. **209**, 2291–2305

472. Kanik, A. B., Yaar, M., and Bhawan, J. (1996) p75 nerve growth factor receptor staining helps identify desmoplastic and neurotropic melanoma. *Journal of Cutaneous Pathology*. **23**, 205–10

473. Perosio, P. M., and Brooks, J. J. (1988) Expression of nerve growth factor receptor in paraffin-embedded soft tissue tumors. *The American Journal of Pathology*. **132**, 152–60

474. Hoshi, N., Hiraki, H., Yamaki, T., Natsume, T., Watanabe, K., and Suzuki, T. (1994) Frequent expression of 75 kDa nerve growth factor receptor and phosphotyrosine in human peripheral nerve tumours: an immunohistochemical study on paraffin-embedded tissues. *Virchows Archiv*. **424**, 563–568

475. Nowak, D., Stewart, D., and Koeffler, H. P. (2009) Differentiation therapy of leukemia: 3 decades of development. *Blood*. **113**, 3655–65

476. Friedrich, R. E., Holstein, A.-F., Middendorff, R., and Davidoff, M. S. (2012) Vascular wall cells contribute to tumourigenesis in cutaneous neurofibromas of patients with neurofibromatosis type 1. A comparative histological, ultrastructural and immunohistochemical study. *Anticancer Research*. **32**, 2139–58

477. Scandella, E., Bolinger, B., Lattmann, E., Miller, S., Favre, S., Littman, D. R., Finke, D., Luther, S. A., Junt, T., and Ludewig, B. (2008) Restoration of lymphoid organ integrity through the interaction of lymphoid tissue-inducer cells with stroma of the T cell zone. *Nature Immunology*. **9**, 667–75

478. Junt, T., Scandella, E., and Ludewig, B. (2008) Form follows function: lymphoid tissue microarchitecture in antimicrobial immune defence. *Nature Reviews. Immunology*. **8**, 764–775

479. Fletcher, A. L., Acton, S. E., and Knoblich, K. (2015) Lymph node fibroblastic reticular cells in health and disease. *Nature Reviews. Immunology*. **15**, 350–361

480. Le Moan, N., Houslay, D. M., Christian, F., Houslay, M. D., and Akassoglou, K. (2011) Oxygen-Dependent Cleavage of the p75 Neurotrophin Receptor Triggers Stabilization of HIF-1α. *Molecular Cell*. **44**, 476–490

CURRICULUM VITAE